https://doi.org/10.35662/unine-thesis-2999

Combining experiments and modelling to study microbial coexistence in heterogeneous environments

PhD candidate: Thierry Kuhn
Institute of Biology
23.11.2022

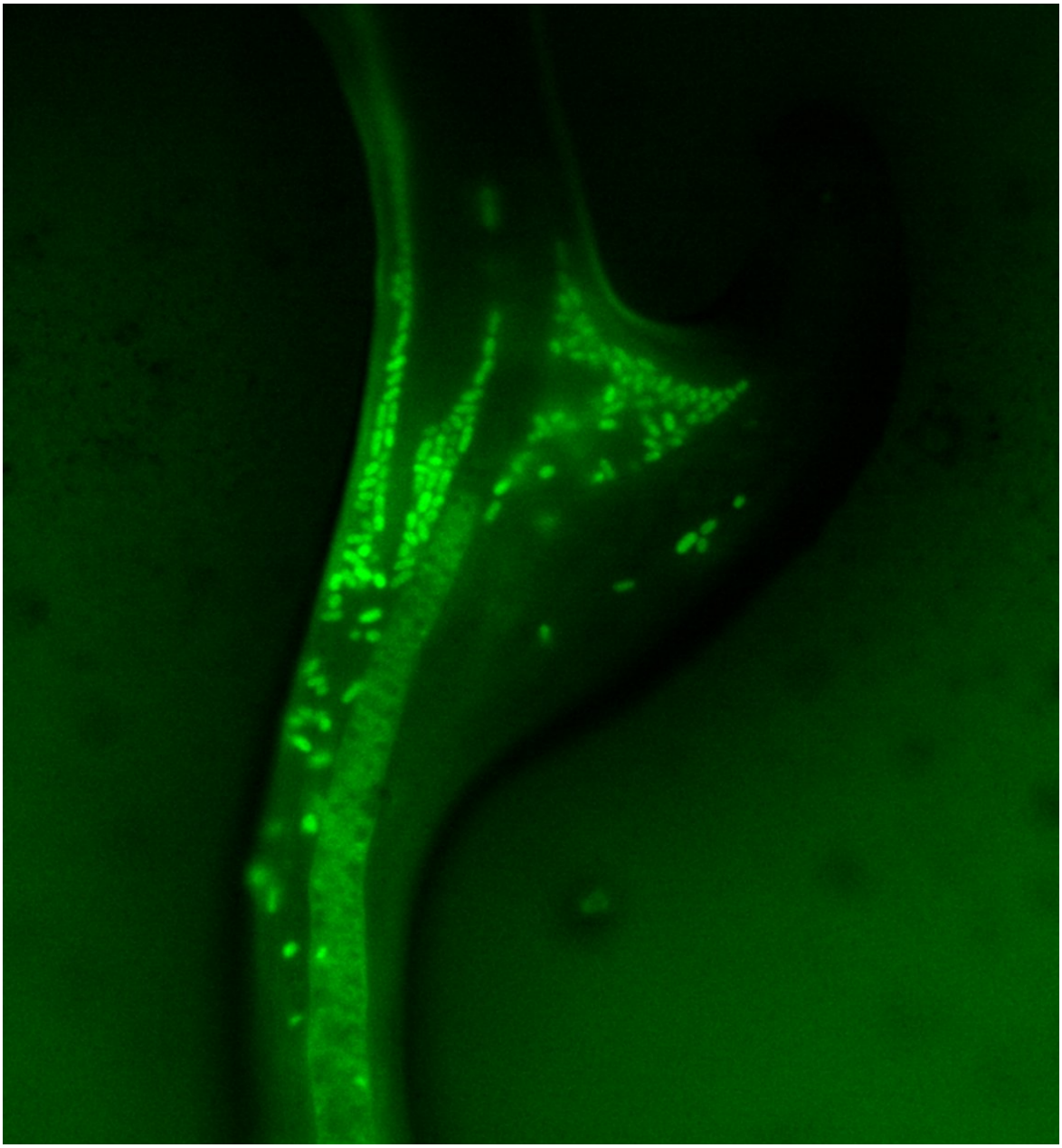

Supervisor: Dr. Xiang-Yi Li Richter
Co-supervisor: Prof. Pilar Junier
Internal examiners: Prof. Redouan Bshary and Dr. Diego Gonzalez
External examiners: Dr. Claire Stanley, Dr. Andrey Morozov, Dr. Lukas Wick

unine
Université de Neuchâtel
Faculté des sciences

Rue Emile-Argand 11
CH-2000 Neuchâtel
doctorat.sciences@unine.ch

IMPRIMATUR POUR THESE DE DOCTORAT

La Faculté des sciences de l'Université de Neuchâtel autorise l'impression de la présente thèse soutenue par

Monsieur Thierry KUHN

Titre :

"Combining experiments and modelling to study microbial coexistence in heterogeneous environments"

sur le rapport des membres du jury composé comme suit :

- Dr Xiang-Yi Richter, directrice de thèse, Université de Neuchâtel, Suisse
- Prof. Pilar Junier, co-directrice de thèse, Université de Neuchâtel, Suisse
- Prof. Redouan Bshary, Université de Neuchâtel, Suisse
- Dr Diego Gonzalez, Université de Neuchâtel, Suisse
- Dr Claire Stanley, Imperial College London, United Kingdom
- Dr Andrey Morozov, University of Leicester, United Kingdom
- Dr Lukas Wick, Helmholtz Centre for Environmental Research, Allemagne

Neuchâtel, le 22 décembre 2022 Le Doyen, Prof. R. Bshary

Summary

In nature we find a high amount of diversity which is hard to explain, if we only consider Darwin's naturalization hypothesis. There must be multiple different mechanisms which allow the coexistence of the species and thereby work against the naturalize hypothesis.

In my thesis, I focused on two mechanisms that have been proposed to positively impact the coexistence of closely related species with overlapping niches. The first mechanism investigated in the first two chapters was spatial avoidance. To be more precise, I focused on the exploration-exploitation trade-off, in which a motile strain with higher motility uses dispersal to avoid competition with a more competitive strain on a local scale. To allow spatial avoidance, fungal highways were used in the experiments. I used two closely related *Pseudomonas putida* strains to investigate whether fungal highways support the maintenance of biodiversity of closely related strains sharing a similar niche. My experimental results show that competition on the local scale led to competitive exclusion while regional competition promoted coexistence. The exploration-exploitation trade-off promoted coexistence if the two strains were inoculated in separated droplets on the dispersal networks. It has been previously shown that intermediate competition conditions in exploration-exploitation trade-off experiments allow for coexistence, similar to my findings.

To investigate the exploration-exploitation trade-off in a more controlled environment, I developed two devices mimicking different states of water saturation in soil using 3D-printing technology. The trail device mimics fully-saturated soil and allows for the passive dispersal of microbes. The bridge device mimics semi-saturated soil and only allows for active dispersal and hitchhiking. I did not just create two devices which enable studying bacterial dispersal, hitchhiking and population dynamics along controllable abiotic network but also proved the potential of 3D-printing in microbiology.

In my third chapter, I investigated the second mechanism, which was non-transitive competition. I used three *Escherichia coli* strains to study the population dynamics using a system based on the classic childrens´ rock-paper-scissors (RPS) game. To investigate the population dynamics and cycles based on the RPS game in three *Escherichia coli strains*, I developed a mini bioreactor for the experiment. We used the bioreactors and an individual-based-model (IBM) to investigate the effects of the nutrient composition, toxin production, diffusion and removal. The different nutrient compositions in the bioreactors changed the dynamics dramatically, favouring a single dominant *E. coli* strain in all but one treatment. The toxin removal had minor effects on the population dynamics, but I showed that the amount of released toxin retained in the system predicts possible coexistence across broad parameter space. Furthermore, we highlighted the importance of toxin diffusion on the population dynamics and showed its correlation to dispersal patterns. By creating the bioreactor, we created the opportunity to study the non-transitive competition in a spatial background and combine the two mechanisms.

Key words

Biodiversity, coexistence, spatial avoidance, exploration-exploitation trade off, 3D-printing, bacterial hitchhiking, non-transitive competition, rock-paper-scissors dynamics, computer modelling

Zusammenfassung

Die überwältigende Diversität in natürlichen Systemen ist schwer zu erklären, wenn man nur Darwins Theorien zurate zieht. Es muss noch andere Mechanismen geben, die es gegen das Aussterben und für die Koexistenz von Arten wirken. In meiner Doktorarbeit untersuchte ich zwei Mechanismen, welche die Koexistenz von nahe verwandten Spezien mit überlappenden Nischen positiv beeinflussen.

Den ersten Mechanismus, welche in den ersten beiden Kapiteln meiner Doktorarbeit untersuchte, war der Kompromiss zwischen Erkundung und Ausbeutung von neuen Ressourcen. Dieser besteht, wenn ein mobiler Bakerienstamm seine Mobilität nutzt, um sich der lokalen Konkurrenz eines kompetitiveren Stamms zu entziehen. Um die räumliche Meidung zu ermöglichen, wurden ein Netzwerk aus Pilzhyphen verwendet («fungal highways»), welches die Verbreitung von Bakterien erlaubt. In diesen Experimenten verwendete ich zwei verwandte *Pseudomonas putida* Stämme. Diese Bakterien verwendete ich, um den Einfluss des Pilznetzwerks auf die Biodiversität von nah verwandten Arten zu untersuchen. Meine Resultate zeigen, dass die Konkurrenz auf der lokalen Ebene zum Ausschluss einer der beiden Bakterienstämmen führt, während auf der regionalen Ebene die Koexistenz gefördert wird. Da die Bakterien entweder gut im Erschliessen oder im Ausbeuten sind aber nicht beides, erlauben diese unterschiedlichen Fähigkeiten, dass die beiden Bakterienstämme koexistieren, wenn sie getrennt inokuliert wurden. Es ist ein weit verbreitetes Phänomen, dass intermediäre Bedingungen, wie bei uns in der getrennten Inokulation, die Koexistenz zwischen verschiedenen Organismen fördern.

In unseren Experimenten mit dem Pilznetzwerk fehlte uns die Möglichkeit, die Experimente in einem kontrollierten abiotischen Umfeld durchzuführen. Deswegen verwendete ich 3D-Drucker um zwei Kontrollen zu entwickeln, die das Habitat einmal gesättigt und einmal teils gesättigt simulieren.

Das Trail-Device simuliert das komplett gesättigte Habitat und erlaubt dadurch die passive Migration von Mikroben. Das Brückensystem wiederum erlaubt die Simulation von teils gesättigtem Habitat, in diesem können sich Mikroben nur unter Einsatz von Energie aktiv fortbewegen. Mit diesen beiden Gerätschaften habe ich nicht nur den Grundstein gelegt, um die Verteilung von Mikroben zu untersuchen, sondern auch eine Möglichkeit, um Populationsdynamiken zu erforschen. Durch die Verwendung von 3D-Druckern konnte ich deren Potential in der Mikrobiologie aufzeigen.

Im dritten Kapitel meiner Doktorarbeit untersuchte ich wie non-transitive Konkurrenz die Koexistenz von unterschiedlichen Spezien oder Bakterienstämme erlaubt. Hierzu verwendete ich drei unterschiedliche *Escherichia coli* Stämme. Die Populationsdynamiken zwischen den drei *E.coli* Stämmen erinnert and das Kinderspiel Schere-Stein-Papier, in welchem es keinen zuvor definierten Gewinner gibt. Um diese Dynamiken experimentell genauer unter die Lupe zunehmen entwickelte ich einen Mini-Bioreaktor, welchen ich wiederum mit 3D-Drucken herstellte. Zusätzlich zu den Experimenten, verwendeten wir Computersimulationen um den Effekt von Nährstoffen, Giftproduktion, -diffusion und -entfernung auf die Populationsdynamiken zu untersuchen. Unsere Forschung zeigte, dass die Nährstoff Zusammensetzung einen grossen Einfluss auf den Ausgang der Experimente hatte. In fünf von sechs Zusammensetzungen war einer der drei Bakterienstämme dominant. Im Vergleich zu den Nährstoffen hatten die Giftentfernung

einen kleineren Einfluss auf die Populationsdynamiken. Unsere Simulationen zeigten jedoch, die Diffusionsgeschwindigkeit einen grossen Einfluss auf den Ausgang der Simulationen hatte. Dabei unterstützten mittlere Geschwindigkeiten die Koexistenz und die beiden extremen Polen verhinderten diese. Ein weiteres Resultat war, dass die maximal erreichbare Giftkonzentration ein guter Indikator für Koexistenz ist. So erlauben nur mittlere Konzentrationen Koexistenz.

Mit den in dieser Doktorarbeit entwickelten Gerätschaften können in der Zukunft, die Verteilung von Mikroben untersucht werden oder durch eine Verknüpfung der Bioreaktoren zu einem Netzwerk die nicht transitive Kompetition in einem räumlichen Kontext untersucht werden.

Schlüsselwörter

Biodiversität, Koexistenz, räumliche Meidung, Erkundungs-Ausbeutung Kompromiss, 3D Drucken, bakterieller Autostopp, nichttransitive Kompetition, Schere-Stein-Papier Dynamiken, Computermodelle

Résumé

Dans la nature, nous observons une grande diversité qu'il est difficile d'expliquer en considérant uniquement l'hypothèse de naturalisation de Darwin. Il doit donc y avoir une multitude de mécanismes différents qui permettent la coexistence des espèces, ce qui vaà l'encontre de l'hypothèse de naturalisation.

Dans ma thèse, je me suis concentré sur deux mécanismes qui ont été proposés pour avoir un impact positif sur la coexistence d'espèces étroitement liées dont les niches se chevauchent. Le premier mécanisme,étudié dans les deux premiers chapitres, est « l'évitement spatial » et plus précisément, le compromis exploration-exploitation : à échelle locale, une souche à forte motilité utilise la dispersion pour éviter la compétition avec une souche plus compétitive.. Dans le cadre expérimental, j'ai utilisé un système d'autoroutes fongiques pour permettre « l'évitement spatial » et deux souches de *Pseudomonas putida* génétiquement proches partageant une niche similaire. Mes résultats expérimentaux montrent que la compétition à l'échelle locale conduit à l'exclusion compétitive tandis que la compétition régionale favorise la coexistence. Le compromis exploration-exploitation favorise la coexistence si les deux souches sont inoculées dans des gouttelettes séparées sur les réseaux de dispersion. Il a été démontré précédemment que les conditions de compétition intermédiaires dans les expériences de compromis exploration-exploitation permettent la coexistence, ce qui est similaire à mes résultats.

Pour étudier le compromis exploration-exploitation dans un environnement plus contrôlé, j'ai utilisé la technologie d'impression 3D pour développer deux dispositifs imitant différents états de saturation en eau du sol.. Le dispositif de « sentier » imite un sol entièrement saturé et permet la dispersion passive des microbes. Le dispositif de « pont » imite un sol semi-saturé et permet uniquement une dispersion active et l'auto-stop. En plus de la création de cesdeux dispositifs permettant d'étudier la dispersion des bactéries, l'auto-stop et la dynamique des populations le long d'un réseau abiotique contrôlable, j'ai également prouvé le potentiel de l'impression 3D en microbiologie.

Dans mon troisième chapitre, j'ai étudié le deuxième mécanisme, à savoir la « compétition non-transitive ». J'ai utilisé trois souches d'*Escherichia coli* pour étudier la dynamique des populations à l'aide d'un système basé sur le jeu classique des enfants "pierre-papier-ciseaux" (PPC) et ai développé un mini-bioréacteur pour la réalisation des expériences. Nous avons utilisé les bioréacteurs et un modèle basé sur l'individu pour étudier les effets du milieu de culture (composition en nutriments) et d'une toxine sécrétée dans l'environnement (production, diffusion et élimination). Les différentes compositions en nutriments testées dans les bioréacteurs ont changé la dynamique de façon spectaculaire, favorisant une seule souche dominante d'*E. coli* dans tous les traitements sauf un. L'élimination de la toxine n'a eu que des effets mineurs sur la dynamique de la population, mais j'ai montré que la quantité de toxine retenue dans le système pouvait prédir la coexistence possible dans une large gamme de paramètres. De plus, nous avons mis en évidence l'importance de la diffusion de la toxine sur la dynamique de la population et montré sa corrélation avec les schémas de dispersion. En générant le bioréacteur, nous avons créé l'opportunité d'étudier la compétition non-transitive dans un contexte spatial et de combiner les deux mécanismes.

Mots clés

Biodiversité, coexistence, évitement spatial, compromis exploration-exploitation, impression 3D, auto-stop bactérien, compétition non-transitive, dynamique pierre-papier-ciseaux, modélisation informatique.

Table of content

General Introduction

The astonishing number of species and, thereby, the high natural biodiversity has puzzled biologists since they began investigating biological systems. Darwin´s theory of evolution provided the first explanation for the high number of different species (Darwin, 1859). However, Darwin's naturalization hypothesis does not explain how species with overlapping niches can coexist (Daehler, 2001). Darwin concluded that due to the high selection pressure between multiple species, all but one of the species with overlapping niches would go extinct. This leads to only one species per niche and a minimal amount of niche overlap between species. However, in nature, biologists have repeatedly observed a different pattern: many species occupy similar or overlapping niches, and somehow these species manage to coexist. This has led to the constant debate about Darwin's naturalization hypothesis (Duncan & Williams, 2002; Park & Daniel, 2013; Sol et al., 2014). In this thesis, I combine experimental and theoretical approaches to investigate some of the mechanisms that help to maintain biodiversity in order to answer the question: How is biodiversity maintained under the constraint of niche overlap?

Before focusing on how biodiversity is maintained in nature, I must define the concept of biodiversity. Biodiversity is defined as the variability among living organisms. These differences can originate from different habitats and enclose the diversity within, between species, and ecosystems (Feest et al., 2010). The concept of biodiversity is such a big topic that it is hard to focus on more than one aspect of it. In my case, the focus was on the diversity of closely related bacteria species. The concept of species is one of the most fundamental ones in biology. However, it is still highly debated, especially in microbiology (Madigan et al., 2013). To avoid controversy. I will follow the textbook definition of the Brock Microbiology book. In this book, two microbes are considered as two different species if their genome differs by 30 per cent or if their 16S-rRNA gene differs by three per cent (Madigan et al., 2013).

After defining the key concepts in this thesis, I want to focus on the mechanisms studied in my thesis. Multiple mechanisms are known to contribute to the maintenance of biodiversity. Those include negative density dependence, competition avoidance, and non-transitive competition (Yamamichi et al., 2020).

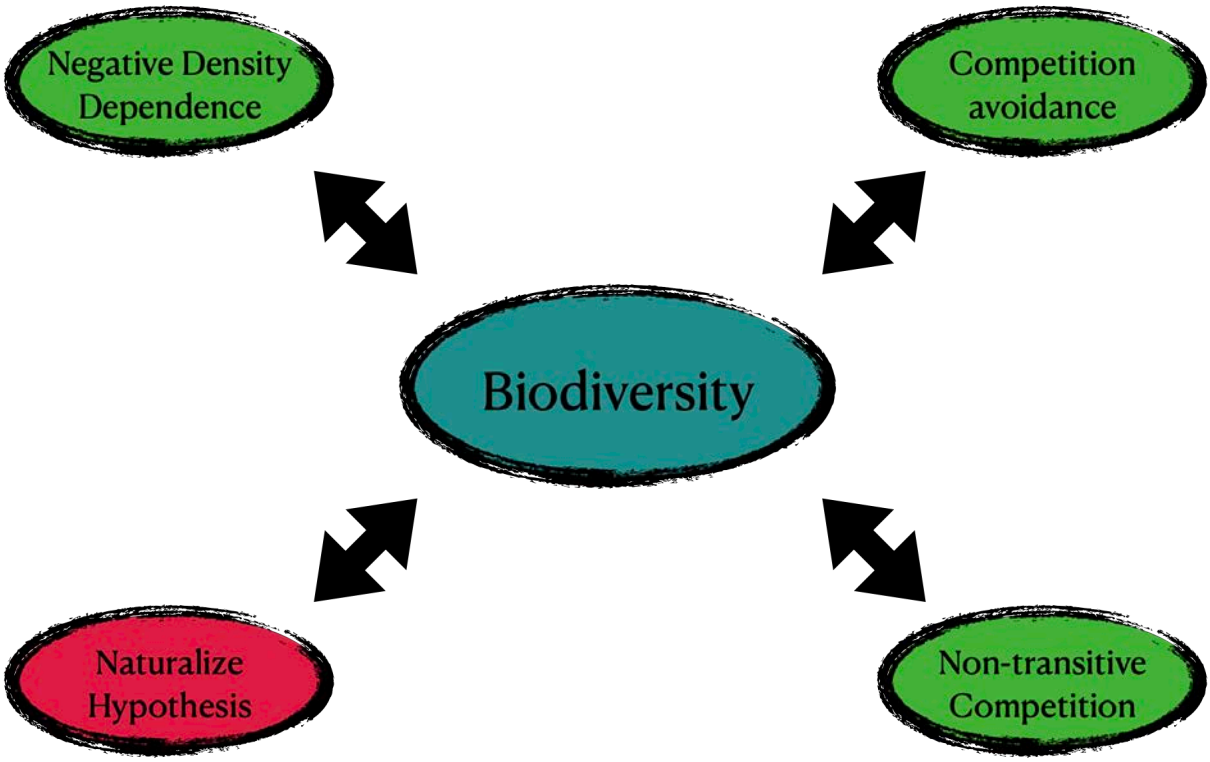

Figure 1. This graph shows some mechanisms which impact biodiversity. The ones in green support biodiversity, and the one in red decreases biodiversity.

Negative density dependence promotes biodiversity by acting at two different levels. The first one concerns predation and the second competition. Predation and competition decrease the competitiveness of the species with increasing numbers. The impact of predation is supported by an increase in predators' effectiveness with a good search image. With more training, this search image improves (Ishii & Shimada, 2010). Thereby, the more abundant a prey is, the more it will be predated as compared to less abundant prey species. The weakening effect of competition by negative density dependence is linked to Darwin's naturalization hypothesis. Darwin claimed that the closer two individuals are phylogenetically related to each other, the stronger the competition between them will be. The individuals that are most alike to one another are the ones from the same species. This means that intraspecific competition is higher than the interspecific competition (Abrams, 1983; Chesson, 2000). Thereby, an individual from a given species is often more impacted by the abundance of other members of its own species than by the abundance of competitors. The higher the density of the species, the less competitive it gets. This self-weakening effect of negative density dependence allows the weaker competitor to coexist at a lower density.

To avoid competition with other species occupying an overlapping niche and using similar resources, a species can use those resources at different temporal or spatial scales (Bunnell & Huggard, 1999; Gatti, 2016). Temporal competition avoidance happens on different time scales: on a daily scale when one species is nocturnal and the other diurnal. On an annual scale, competition avoidance occurs when species occupy an area just for a certain amount of time in the year, such as in the case of migratory birds (Bauer & Hoye, 2014; Kyba & Hölker, 2013; Stutchbury et al., 2016). Temporal competition avoidance has been found not just in vertebrates like birds or big carnivores but also in microorganisms (Dröge et al., 2017). Blagodatskaya and Kuzyakov 2013 demonstrated that bacteria are only active when the surrounding conditions are

beneficial; if the conditions are unsuitable, different bacterial species can temporally avoid competition by being inactive (Blagodatskaya & Kuzyakov, 2013).

Spatial competition avoidance requires a heterogeneous environment within which not all habitat patches are fully accessible to all species. The distance between different patches varies at different scales. For microbes in the soil, the distance between two patches is smaller than a millimeter, while for vertebrates, it can be hundreds of kilometers. The mechanism behind spatial competition avoidance is also called the exploration-exploitation tradeoff (de Martino et al., 2019). Species on the exploration side are motile and can effectively explore and invade new patches. They have the advantage of arriving at the new resource first, but their mobility entails a high energetical cost. Therefore, the strains on the exploitation side, which are strong local competitors, locally outcompete the exploratory strains in the long term. To avoid extinction, the exploratory strains evade competition by continually exploring new spatial locations.

Non-transitive competition is another mechanism that helps explain how biodiversity is maintained under the restriction of niche overlap. Non-transitive competition is also called nonhierarchical competition, in which different strategies form a loop-like dynamic. Similar to the children's rock-paper-scissor (RPS) game, strategy A beats strategy B, strategy B beats strategy C, and strategy C beats strategy A. Nontransitive competition exists in multiple different ecological systems like marine benthic systems, grasslands, the mating system of the side blotch lizards, and most famously in the bacterium *Escherichia coli* (Jackson & Buss, 1975; Kerr et al., 2002b; Sinervo & Lively, 1996b; Soliveres, Maestre, Ulrich, Manning, Boch, Bowker, Prati, Delgado-Baquerizo, Quero, Schöning, Gallardo, et al., 2015; Szolnoki et al., 2014a). What all of these systems have in common is that none of the strategies is dominant always, but they all coexist with cyclic alternations of the dominant strategy.

To investigate how biodiversity is maintained under the constraint of niche overlap, I used the closely related soil (*Pseudomonas putida*) and gut (*Escherichia coli*) bacteria. The selection of these microbial models is based on the fact that the work with microbial populations allows investigating the mechanisms of species co-existence in a relatively short timeframe due to their generation time. Furthermore, their size and relatively easy maintenance allows for testing multiple systems simultaneously. In addition, I used 3D-printing technology (additive manufacturing) to develop novel experimental devices and used them in my experiments. Experimental data was then used to run computer models, which allows for a more in-depth and mechanistic understanding of the experimental results and the development of further testable hypotheses.

Spatial competition avoidance

Soil structure

To maintain biodiversity by spatial competition avoidance, the environment must be heterogeneous and structured. An excellent example of a heterogeneous and structured environment at a microbial scale is soil. Soil is a highly heterogeneous habitat. Depending the soil type the surface can differ significantly. Sandy soil has a surface area of 10^{-1} m^2 per gram, and clay has a thousand times larger surface area with 10^2 m^2 per gram (Tecon & Or, 2017a). Therefore, depending on the soil type, there is a variable amount of available surface that bacteria can colonize. However, despite its large surface, Chenu and Stotzky 2001 calculated that only 0.1 % of

the soil surface is covered by bacteria, which indicates a high number of small non-connected patches that cannot be reached by bacteria (Chenu & Stotzky, 2001; Young et al., 2008). These patches can be separated by multiple structures like air pockets or capillaries thinner than 0.2 µm (Tecon & Or, 2017a). Despite the low bacterial surface coverage in soil, it is still the most active and biodiverse compartment of the biosphere (Hinsinger et al., 2009; Melbourne et al., 2007; Vos et al., 2013).

Matric potential

Water is a vital factor for active microbial life. However, soil is mostly water unsaturated except for capillaries and liquid films formed around structures such as rocks or gravels. In these liquid films, bacteria can be active (Tecon & Or, 2017a). Since microbial activity is linked to water availability, we must understand the water saturation state most frequently found in soil. Water saturation is measured by the matric potential (Hillel, 2003). The matric potential represents the amount of water a soil could additionally absorb. The maximum score is zero, which corresponds to fully water-saturated soil. The more negative the score is, the less water is in the system. Soil seldom reaches full saturation, and if it does, this state is only maintained for a short period of time.

Liquid films

Until a matric potential of -4 kPa is reached, the different patches in the soil are still connected by liquid films within which bacteria can disperse (Wang & Or, 2012). However, most of the time, the matric potential is lower than -4 kPa. Thus, the soil is often a patchy and heterogeneous environment (Osmond & de Mazancourt, 2013; Wang & Or, 2012). With the help of mathematical models, Wang and Or (2012) calculated the coexistence index (CI), which describes bacterial coexistence related to the connectivity of the soil. In their calculation, coexistence can only be expected at a matric potential of less than -4 kPa (Wang & Or, 2012). The same pattern was found experimentally by Zhou and colleagues (Zhou et al., 2002). Therefore, one can expect that patchiness must be maintained to promote biodiversity; otherwise, the exploration-exploitation tradeoff is biased towards the stronger competitor.

In addition to the connectivity of the habitat, the matric potential correlates with the width of the liquid layer. The bigger the liquid layer is, the smaller the swimming resistance of the bacteria. Therefore, the swimming speed of bacteria is faster in big liquid layers than in thin ones (Ebrahimi & Or, 2014).

Connecting soil microbial habitats: Fungal Highways

Even though most of the time, the liquid films do not connect the different patches in the soil, a biological system allows connectivity (Kohlmeier et al., 2005; Tuller & Or, 2005).
Leben found the first indication of this system in 1984; he described that bacteria could use fungi to spread in soil (Leben, 1984). It took 31 years until Kohlmeier and her colleagues described the mechanism of how bacteria disperse along the fungal hyphae and called this dispersal network the “fungal highway” (Kohlmeier et al., 2005).

Unlike bacteria, filamentous fungi can grow through air-filled soil gaps and even bridge air pockets up to one centimeter in diameter (Tecon & Or, 2017a). In contrast to animals, a fungus cannot overcome the water-air barrier by mechanical force, but instead, fungi have developed an alternative mechanism to cross this barrier. Fungi use small hydrophobic proteins called hydrophobins. These cysteine-rich proteins can self-assemble into amphipathic monolayers on the water-air interface, which leads to reversed surface wettability and allows the fungus to move forward (Ren et al., 2013; Wösten et al., 1999). In this way, fungi create a dense hyphal network in the soil, reaching a length from 10^2 to 10^4 meters per gram of soil (Frey et al., 1999; Osono et al., 2003; Ritz & Young, 2004). Around these fungal hyphae, a thin liquid layer is formed, thick enough for bacteria to swim in it. Therefore, the bacteria's ability to disperse along the fungal highway has been linked to their ability to move (e.g., by swimming). Non-motile bacteria have been shown not to disperse along the fungal highway (Kohlmeier et al., 2005; Pion et al., 2013). Motile bacteria can disperse relatively fast (related to their body size) along the fungal highway; for example, *Archromobacter* can swim up to 0.4 mm per hour (Kohlmeier et al., 2005).

Dispersal and motility types

The terms dispersal and motility are often used in combination with the movements of individuals from one place to another. However, the two expressions describe different things. Dispersal is "the movement of individuals or propagule with potential consequences for gene flow across space" (Ronce, 2007). In contrast, motility is the ability of an organism or a cell to move on its own with the investment of energy (Wadhwa & Berg, 2021).

The concept of dispersal is highly challenging in microbiology (Choudoir & DeAngelis, 2022). Two main factors cause the issue. Firstly, dispersal as a concept was developed for plants and animals and has not been adapted to accommodate the microbiological world yet (Prosser et al., 2007). Secondly, it is complicated to sample on a scale that would allow measuring dispersal between different habitats, as we still lack the needed resolution for precise enough investigations (Barberán et al., 2014; Shade et al., 2018). Choudoir and DeAngelis 2022 described multiple forms of dispersal, including the dispersal of vegetative cells (Choudoir & DeAngelis, 2022). Vegetative cells are active cells that either use energy-consuming active dispersal or energy-saving passive dispersal between different habitats. Depending on the motility type, the cell size and the speed, the energetic cost of active movement can vary considerably (Mitchell, 2002). Calculations with protists estimate that for flagellar motion, up to 19 per cent of the basal energy usage can be used for motility (Crawford, 1992). Another study estimated that up to 30 per cent of the ATP in flagellated *P. putida* KT2440 cells is used for the building and the use of the flagella compared to non-flagellated mutants (Martínez-García et al., 2013).

Passive dispersal

We define passive dispersal as a non-energy-consuming way to move across cellular, microhabitat, and at local spatial scales. Diverse mechanisms allow an individual cell to cover the distance. In fully water-saturated soil, organisms can move by Brownian motion (Mitchell & Kogure, 2006) or are dragged by passive water flow (Tecon & Or, 2017a); however, as mentioned before, the soil is rarely water-saturated (Or et al., 2007). In dry conditions, alternative dispersal mechanisms include attaching to a bigger organism that moves or grows through soil. For instance, bacteria

attached to roots and worms get dragged to another place (Madsen & Alexander, 1982; Vos et al., 2013).

An additional method of passive dispersal is hitchhiking (Kuhn et al., 2022; Muok & Briegel, 2021). Here, bacteria or fungal spores "hitchhike" on motile individuals to change location. A common feature of the passive dispersal mechanism is the randomness of the movement in contrast to active dispersal, which shows some directionality.

Active dispersal

Active dispersal is the bacteria's ability to move independently in space using metabolic energy sources. Different strategies exist, and they are optimized for specific conditions like on surfaces, in thin liquid films or fully immersed in liquids (Wadhwa & Berg, 2021). Independent of the motility system, building structures like flagellum or cilia consumes energy. Furthermore, these systems consume energy during their usage. The amount of energy consumed by the systems varies depending on cell size, speed and the type of motion (Mitchell, 2002). There are four major types of active dispersal that I briefly introduce below.

Twitching and gliding

The most common form of motility on a surface is called twitching. Unlike swimming and swarming, twitching does not require flagella but filaments called type IV pili (Burrows, 2012; Craig et al., 2019; Maier & Wong, 2015). Type IV pili are ubiquitous in bacteria (Mattick, 2002) and are used for multiple processes like predation, chemotaxis, phototaxis and many more (Wadhwa & Berg, 2021). Pili are similar to a kedge anchor; the pilus attaches to a particle and retracts. Thereby it pulls the bacteria over the surface.

There is another type of motility that does not require flagella or pili; it is called gliding. This motility type is enabled by adhesins that attach to the substrate and move along the bacterial cell. In this way, bacteria move like on a front tape (Mcbride, 2001).

Swarming

Bacteria have found ways to move in thin liquid and along gel-like substrates. This form of movement is called bacterial swarming. Compared to the other forms introduced here, which are performed at the individual level, swarming is a group activity in which millions of bacteria cells move together. Because swarming only happens in an extremely thin liquid layer, it requires osmolytes or surfactants near the front of the colony (Partridge & Harshey, 2013). These substances create a thicker liquid film in front of the colony, allowing them to swarm in it. This can be seen as if bacterial populations create their own wave "to surf" on it and move along. Nevertheless, bacteria still need flagella to move in this way.

Swimming

The best-studied form of active movement is flagella-propelled swimming in a liquid environment (Berg & Anderson, 1973; Nakamura & Minamino, 2019; Silverman & Simon, 1974). In general, flagella have a diameter of 20 nm and a length of micrometers (Yonekura et al., 2003). The cell moves forward by rotating the left-hand helical-shaped flagella counterclockwise. By changing the moving pattern, the bacterium can change orientation and move in a different direction. The so-called run-tumble pattern allows bacteria to detect chemical gradients and follow or avoid them depending on the nature of the chemical (Son et al., 2013; Xie et al., 2011). The ability to detect chemical gradients is one of the main advantages of active motion.

My thesis mainly focuses on active dispersal by swimming in the liquid films along the fungal highway or along abiotic surfaces. This situation happens when the soil is semi-saturated and has patchy habitats, which are still connected by liquid paths on the surface of fungi (or plant roots) or on soil particles.

Exploration-exploitation trade-off

In order to promote coexistence of multiple bacterial strains with overlapping niches in a heterogeneous patchy environment, the different strains or species can specialize and evolve towards niche separation. Some of them can have high motility and explore the space around them for new, unused patches and spatially avoid local competition with highly competitive resident bacteria. However, as indicated above, motility comes with a cost. The flagella have to be built and used; thereby, this apparatus consumes energy and minimizes the competitiveness of flagellated bacteria on a local scale. Therefore, they often cannot compete with species or strains highly effective at using local resources. The strains or species which specialize in being competitive on the local scale do explore their surrounding as effectively as those investing in exploration. Thereby, they do not manage to access all the patches of the habitat, and if they do, they will arrive later than the more exploratory strains. Thus, spatial competition avoidance by exploration-exploitation trade-off allows the competing species to coexist and can help to maintain biodiversity in species with overlapping niches.

Non-transitive competition

In addition to spatial competition avoidance, other mechanisms, such as non-transitive competition, can explain the maintenance of biodiversity under the constraint of niche overlap. Unlike hierarchical systems with a clear top to bottom ranking, in non-transitive systems, there is no linear hierarchy. The most dominant species is determined by the environment and the density of the other species. Non-transitive competition is a widespread phenomenon which can be found in many different ecological systems, such as coral reefs and grasslands. It also helps maintain the mating strategy polymorphism in the side blotch lizards. Probably the most famous example of non-transitive competition is the “rock-paper-scissors”-like competition between *E. coli* strains (Jackson & Buss, 1975; Kerr et al., 2002b; Sinervo & Lively, 1996b; Soliveres, Maestre, Ulrich, Manning, Boch, Bowker, Prati, Delgado-Baquerizo, Quero, Schöning, Gallardo, et al., 2015; Szolnoki et al., 2014a).

Given the numerous interactions on the topology of the food web, it is not surprising that there are many different examples of non-transitive competition with different amounts of entities involved in cycles (Berlow et al., 2004; Stouffer et al., 2012). To avoid over complication of the interaction between the different entities in this thesis, I focus on the simple and classic system with three different *E. coli* strains. Explaining the non-transitive competition in the *E. coli* system is easiest done by comparing it to the children's rock-paper-scissor (RPS) game. In this game, rock beats scissors, scissors cut paper and paper wraps the stone. The logic is translated into the relationships between three *E. coli* strains: a toxin producer, a toxin-susceptible strain, and a toxin-resistant strain. The toxin-sensitive strain is the fastest-growing strain, so it has a growth advantage in the absence of the toxin. The producer has the lowest growth rate but has an advantage on the toxin-susceptible sensitive strain by the production of toxin. Because the toxin kills the susceptible strain and thereby the producing strain can take over from the killed cells. The toxin-resistant strain displays a medium growth rate, so in absence of toxin, it is outcompeted by the sensitive strain but has a growth advantage over the toxin producer. In this system, there are two different types of competition: interference and exploitation.

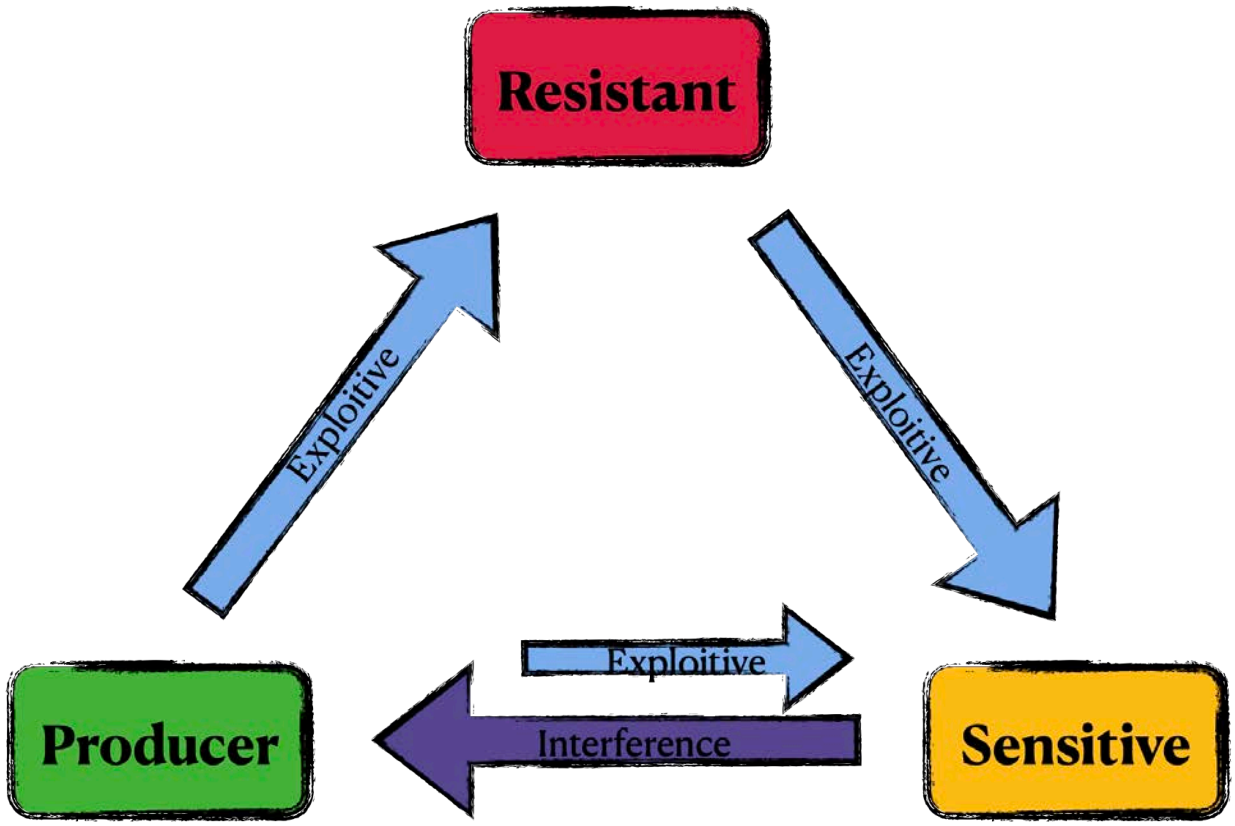

Figure 2. Cyclic dominance driven by toxin-mediated killing (i.e., interference competition, represented by the purple arrow) or higher growth rate (i.e., exploitative competition, represented by the blue arrows) between three E. coli *strains: a bacteriocidal toxin producer, a toxin-resistant, and a toxin-sensitive strain.*

Interference competition and colicin production

Interference competition between two entities happens when one or both harm each other. In animals, this can be done mechanically by hitting, beating or biting each other; in microorganisms it can be done chemically by the secretion of a toxin (Gonzalez et al., 2018b; Szabó et al., 2007). In this thesis, I use an *E. coli* strain producing the toxin colicin A. Colicin A is a pore-forming toxin binding to the ButB receptor (T. Y. Yang et al., 2010). The production costs of the toxin are set by two factors. First, it takes energy to produce the toxin molecule itself. Second, the release of the toxin happens by cell lysis, which means the releasing cell dies during the process. These two factors explain why the production and the release of the toxin are well regulated and only happen under high stress (Ghazaryan et al., 2014b). A high-stress situation can be an attack with another toxin produced by a different strain; it can also happen in response to density caused by high cell numbers or by an SOS response after a lethal error happens during DNA replication.

The resistant strain achieves immunity of Colicin A toxin by a mutation in the ButB receptor on which the colicin binds. However, this advantage comes also at the cost of a reduced growth rate because the ButB receptor allows absorbing cobalamin, which is an important for bacterial growth. This reduces the fitness of the bacteria cells and reduces their growth speed.

Exploitation competition

Exploitation competition between multiple entities happens when they use a common resource like, for instance, a common nutrient source. Each competitor exploits the resource for themself and thereby reduces the amount left for the others. The other entity does not get attacked directly, but its growth can be indirectly harmed by the reduced availability of the resource. In the example of the RPS system in *E. coli*, all three strains show exploitation competition; however, the sensitive strain is the fastest grower and competitor. Thereby, it can outcompete the others if there is only exploitation competition happening.

Non-transitive competition dynamics between *E. coli* strains

In the context of Darwinian competition, we always talk about the survival of the fittest. However, Frean and Abraham proposed the concept of the survival of the weakest (Frean & Abraham, 2001). The weakest strain is defined as the one that takes the longest to outcompete its opponent in a one-to-one assay. If the three strains get mixed (in a 1:1:1 ratio), the strain that experiences the least competition pressure starts to overgrow and outcompetes one of the two other strains. After the first strain is removed, the one-to-one competition dynamics and contestants change between the weakest competitor and the strain that overgrows in the beginning. In this one-to-one competition, the weak competitor wins and out-competes the other strain. The survival of the weakest shows that if one strain is too competitive, it has a disadvantage in the long term (Liao et al., 2020).

In 2002, Czaran, Hoekstra and Pagie included this idea of the survival of the weakest in an evolutionary model in which new resistance mechanisms and toxins can evolve (Czárán et al., 2002). Every resistance or new toxin comes with some fitness costs. The simulation system stabilizes because of the survival of the weakest effect. If the strain develops a new toxin or

resistance, it can outcompete some other strains, but because of the survival of the weakest dynamics, it gets removed by another one shortly after.

Thereby, non-transitive competition has a stabilizing effect on the biodiversity of closely related species with overlapping niches. It prevents the formation of a super competitor, which takes over and stabilizes the number of species in a system.

In simulations of the RPS games, biodiversity is maintained in most setups. However, in lab experiments, it is not so easy to keep all three strains alive for multiple days. Experiments by Kerr in 2002 showed that the combination of spatial structures and media renewal is essential to maintaining the nontransitive *E. coli* community (Kerr et al., 2002). In their experiments, they transferred the bacteria to a new plate every day by stamping and managed to maintain the species for several days. However, two of the three strains got lost in well-mixed liquid cultures with the same transfer rate. After some days, only the resistant strain was left over. This proves that spatial structure is an essential factor for the persistence of the three strains. Reichenbach showed that long-distance motility jeopardizes biodiversity because long-distance motility leads to a well-mixed culture in which all spatial structure is lost (Reichenbach et al., 2007b). Schreiber and Killingback 2013 had the same findings but formulated them differently by saying that spatial heterogeneity increases coexistence (Schreiber & Killingback, 2013b). This leads to the conclusion that the coexistence of species, even in the context of non-transitive competition, is linked to spatial distribution and dispersal.

Methodological background

In this thesis, I combined multiple approaches to investigate different facets of how biodiversity is maintained under the restriction of niche overlap in nature. Firstly, I created missing experimental tools with 3D-printing technology to be able to collect experimental data. Then, these results were implemented in computer models. This approach verifies the modelling results by comparing them to experiments and gives the experimental results more context. Relating them to a computer model allows us to test many more possibilities and factors than we could do experimentally. As microbes allow investigating mechanisms in a relatively short time due to their short generation time, the experiments were done with closely related soil or gut bacteria with an overlapping niche.

Additive manufacturing or 3D-printing

Having a tool to develop prototypes fast and independently from an external supplier was a wish for scientists for a long time. In 1981, their dream came true for the first time when Hideo Kodama developed the first 3D-printer. However, he never managed to patent his development— even though he developed a fully functional printer. Kodama's 3D-printer functions on the mechanic of stereolithography (SLA) (BCN3D, 2020). The printer creates an object by adding a layer with its own specific shape on top of the previous layers. Each layer is produced with a photosensitive resin, which hardens when it comes into contact with ultra violet (UV) light (Ahart, 2019). In the end, all the layers add up to create the final object. As this object is created from the addition of multiple layers, 3D-printing is also referred to as additive manufacturing.

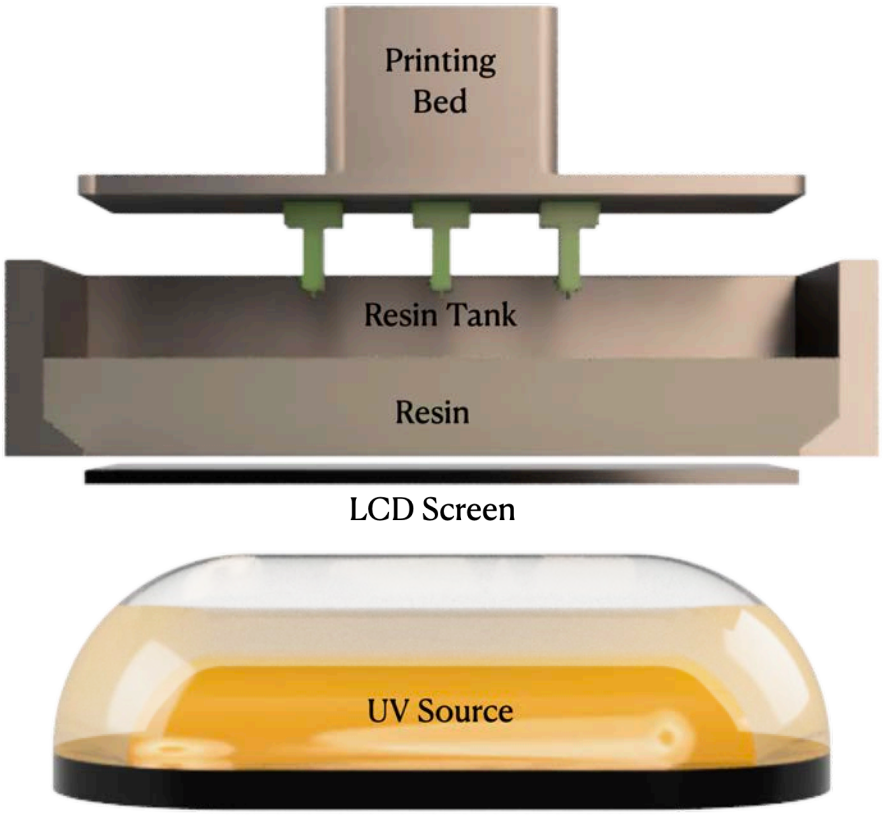

Figure 3. This graphic shows the build of an mSLA-printer. On the bottom is the UV source, then there is the LCD screen which only allows the necessary light pass, and on top, there is the resin tank. On the printing bed, there are three bridge devices, which were printed with an mSLA printer. The UV light passing the LCD screen hardens the next layer of photoactive resin. Then the printing bed moves up, and the new resin between the bottom of the bridge and the resin tank gets harden.

Five years after Kodoma's prototype, the US-American Charles Hull managed to patent his SLA printer (BCN3D, 2020). This was the start of the 3D-printing age. Even though the 3D-printing market started slowly, the use of 3D-printers has exploded in the last few years. A big game changer was the 2006 release of the first commercially usable 3D-printer. In addition to the hardware, new computer-aided design (CAD) software was developed and released. This development allowed for easier usage of 3D-printing. For example, the amount of post-printing processes (i.e., curing) was reduced, making it more user-friendly. The easier handling and reduced costs of 3D-printers increased the demand for the machines and printed goods so that in 2020 the estimated value of 3D-printed goods was around 2.6 billion us dollars (Grand View Research, 2020). Following the predictions, it will reach a market value of over 20 billion dollars in 2030 (Grand View Research, 2020). To reach this prediction, the value of the market for 3D-printed goods must increase by around 20 per cent every year, making it one of the fastest growing markets worldwide.

Multiple industries have implemented 3D-printing. One of the most spectacular examples is the printing of entire houses in China and the USA (Ahrens, 2014). However, printing on this enormous scale is not the most important for research, especially in microbiology. Nevertheless, there are other fields that impact microbiology much more. Production of medical devices, the fastest growing market in 3D-printing, is one of the most relevant for the application of 3D-printing in microbiology (Schumann & Reinhard, 2018). As materials used for medical applications must be

tested for biocompatibility, water absorption, and other essential properties, these materials are ideal for microbiological assays.

I used a 3D-printer to develop devices specifically to investigate the object of interest. To do so, we used two different types of SLA printers, which with their different properties, allowed us to develop the needed devices. Since we only used SLA printers in our work, only those printers are introduced here. Even though they are the most commonly used printer type (around 8% of all printed products come from SLA printers), there are multiple other techniques, which allow for printing in different scales and materials (metal, carbon, glass, ceramic, among many others) (Grand View Research, 2021).

To create devices that capture the essential features of the fugal highway (Chapter two), we used a masked SLA (mSLA) printer from Prusa (SL1). This type of printer works similarly to a standard SLA printer. However, instead of having a single laser beam which hardens every layer, the mSLA printer has a strong UV lamp at the bottom and a liquid crystal display (LCD) screen between the resin and the UV lamp. The LCD screen only lets the light to pass at the position needed to harden the resin. The advantage of this technique is that it is relatively fast when printing many devices simultaneously. Because every layer takes the same amount of time, independent of how many structures there are. The printing time is defined by two parameters the exposure time, which is the time needed to harden the resin, and the number of layers. Compared to other SLA printers, mSLA printers are relatively cheap: they cost a couple of hundred US dollars. The most significant disadvantage of this method is light blending. Because the light passing through the LCD screen is not always orthogonal to the screen, a minimal amount of resin gets cured on the border (Benjamin et al., 2019). The additionally hardened material may lead to less precise results.

Although the mSLA printer has many advantages, it does not satisfy the need for printing the device I needed for Chapter 3. I used instead a different type of printer — the low force stereolithography printer (LFS). One of the most significant issues associated with SLA printers is the movement from a hardened layer of resin to the next one. When the layer is hardened, there is no liquid resin between the bottom of the tank and the object. However, it is surrounded by viscous liquid resin. While moving the object upwards, the suction force between the object and the tank can damage the printed object. However, the movement is necessary to let new resin between the object and the tank and thereby creating a new layer. LFS printers reduce the risk of damage by having a flexible bottom on their tank. This technique reduces the suction forces and allows for printing more precise and smoother objects. However, the differences between an mSLA and LFS printer is still small and might be around 20 microns. The disadvantage of this technic compared to the mSLA printer is that it is slower when printing multiple objects, and the printer tends to be ten to twenty times more expensive than a simple mSLA printer.

Figure 4. This figure shows an LFS- printer. The material gets harden by a laser in the light machine, the light machine moves from left to right and the laser hardens the material at the right spots. Different to an mSLA printer the bottom of an FLS printer is soft and allows for a more precise print with smaller risk of damages.

Modelling

Even though 3D-printing allows for fast prototyping and working with microbes as a study system allows for efficient and rapid investigation of population dynamics over multiple generations, there are still limiting factors to the experiments. Those included, for instance, the number of replicates, the time in which dynamics can be recorded, or simply the costs of a large study.

Computer models have the advantage that they are less restricted to replication numbers, duration, and number different treatments. This is especially the case since computational power increased in the last centuries. Between 1956 and 2015, computational power had a one trillion-fold increase. Additionally, the cost of computer power halvens every five and a half years (Muelhauser & Rieber, 2014). The higher power and lower cost allow for more complex simulations and different treatments. Thereby, computer models allow for analyzing a broad range of parameters that are difficult to include during experiments. Besides the price and power development, computer models have additional hands-on advantages. For instance, ethical problems in computer models must be considered in the design and the analyzes of the simulation. However, the process of running a simulation is not restricted by ethical constrains, differently to experiments or invasive field work. Additionally, a computer model can be run and monitored at any time without increasing the workload for the programmer. These factors make modelling an attractive method for studying biological systems.

Like in all research fields, there are different types of models. The first one worth mentioning is the mathematical model. Mathematical modelling has its origin in the 1930s when it was first used to investigate changes in gene frequency (Servedio et al., 2014). Today, mathematical models are

often used in Evolutionary Biology (Servedio et al., 2014). Mathematical models represent the biological system in a formula, which then allows to investigate the influence of each factor as part of an equation.

The second type of model is the individual-based model (IBM). As the name of the model indicates, an IBM acts on the individual level. It allows us to track the change and development of each individuum and its ancestors. For more than four decades, IBMs have been used to investigate ecological systems (DeAngelis & Grimm, 2014). IBMs are often used in combination with empirical data (DeAngelis & Grimm, 2014a; Grimm, 1999; Volker & Railsback, 2005).

Even though computer models have advantages, it is not possible to simulate reality. A model representing reality would still be too big and complicated to write and to run. Therefore, computer models allow only for testing a hypothesis and basic concepts (Servedio et al., 2014). But these tests can be an excellent proof of concept and thereby guide the direction for experimental work or allow a more in-depth interpretation of the experimental results. Even though computer models do not represent reality, they are still helpful for investigating biological systems.

Programming languages used for the thesis projects

I used the Julia programming language (*Julia Documentation · The Julia Language*, n.d.). Julia was designed to reach a similar speed as C or C++. However, compared to C or C++, Julia is more similar to writing Python. This relatively easy style of writing code while still having the benefit of a higher speed makes Julia extremely interesting to use for our models. Like C and C++, Julia is compiled into native code via low level virtual machine (LLVM) (*Julia Documentation · The Julia Language*, n.d.). Julia is an open-source project with thousands of contributors, which makes the relatively new language fast-evolving.

Model type

In this thesis, I used an IBM to investigate the population RPS dynamics in the third Chapter. (DeAngelis & Grimm, 2014b; Volker & Railsback, 2005). The IBM allowed us to combine the empirical results of our system with modelling. The trackability of each cell and its properties were ideal for studying the population dynamics. Furthermore, the construction of a 200 x 200 grid was a perfect environment to study the effect of the toxin because it is relatively simple to change the production, removal and diffusion properties along on such a grid.

Structure of the thesis

This thesis is structured into three different research chapters. In the three chapters, I investigated how biodiversity is maintained under the restriction of overlapping niches. I used closely related soil or gut bacteria strains for lab experiments. In addition, 3D-printing technology was used to develop and produce microbiological devices to investigate the maintenance of biodiversity. The results were conceptualized by comparing them with the results from computer models.

Chapter one

Question

Does the presence of fungal highways help the exploration-exploitation tradeoff maintain the biodiversity of closely related bacteria strains with an overlapping niche?

I hypothesized that adding a spatial structure allows the more motile strain to avoid competition with the more competitive strain. Thereby, the two strains can coexist.

Method

To investigate the exploration-exploitation tradeoff´s impact on biodiversity, I compared the abundance of two closely related *Pseudomonas putida* strains. The two strains were inoculated, either mixed or separated. To control the impact of the fungus as an independent biotic system, we used glass fibers. Like the fungus, the glass fibers provide a liquid film along them within which bacteria can disperse (Pion et al., 2013). During the project, we realized that glass fibers are not perfect abiotic models for fungal hyphae because the glass fibers allow for passive dispersal. This led me to develop 3D-printed devices in the next chapter.

With the help of the newly designed devices (Chapter 2), I was able to proof the exploration-exploitation trade off. This proof allowed me to interpret the results from the experiments with the fungal highway in the framework of exploration exploitation.

Chapter two

Question

Is it possible to mimic soil in different saturated conditions to answer questions related to biodiversity maintenance using 3D printed devices?

How to design different devices that mimic different states of the matric potential in soil?

In the first chapter, I missed a novel experimental system to prove the exploration-exploitation trade-off between the two strains and to investigate bacterial dispersal in the soil further; we need two abiotic devices which mimic soil with different matric potentials. One of the two devices mimics a saturated system which allows passive dispersal. The other device represents semi-saturated soil, which only allows for dispersal associated with swimming.

Method

We designed and 3D-printed two devices establishing stable liquid films that support bacteria dispersal in the absence of biotic interactions. The thickness of the liquid film determined the presence of hydraulic flow capable of transporting non-motile cells. We performed dispersal assays using motile, non-motile and a mixture of the two cell types to test whether they can disperse in the liquid films established by each device.

These devices allow for a controlled investigation of bacterial dispersal along hydrated surfaces. To my knowledge they are the first devices, which control for passive dispersal and flow.

Chapter three

Question

How do different nutrient compositions impact the biodiversity maintenance of the three competing bacteria (*E. coli*) in a rock-paper-scissor game?

How does toxin production/diffusion impact biodiversity maintenance of the three bacteria strains (*E. coli*) in a rock-paper-scissor game?

The different nutrient composition favors or hinders the production of the toxin. Therefore, in glucose-dominated media, the sensitive strain has an advantage, and in casamino acid treatments, the toxin producer.

It has been shown that high dispersal jeopardizes biodiversity. Therefore, I hypothesized that a similar pattern is observed with the diffusion rate of the toxin. Biodiversity should be maintained at an intermediated diffusion rate.

Method

I designed and 3D-printed a bioreactor device to perform a continuous culture of the microbial community. This bioreactor allowed me to test the effects of different culturing media and different dilution rates.

The three media tested contain different casamino acid-to-glucose ratios. The different nutrient compositions impact colicin A production in the producing strain. Two different toxin removal rates are used to investigate the differences in the toxin concentration on the population dynamics.

In the second step, the experimental data is used as the baseline for the computer simulations. The Julia language was used to write an IBM, which explicitly models the toxin and the three *E. coli* strains. This allows the focus on the impact of the diffusion rate on the rock-paper-scissor dynamics.

The bioreactor allowed for the first time to study the rock-paper-scissors dynamic in the same environment over multiple days. Thereby, I was able to study the effect of the toxin on the population dynamics, because I did not remove the toxin by transferring the population.

In the simulations, the toxin was explicitly modelled. This allowed for investigating the effect of toxin diffusion. In the context of biofilms, toxin diffusion might have the higher impact on the population dynamics than bacteria dispersal. Thereby, my results allow for a better understanding of the RPS dynamics in a biofilm.

References

Abrams, P. (1983). The Theory of Limiting Similarity . *Annual Review of Ecology and Systematics*, *14*, 359–376.

Ahart, M. (2019). *Types of 3D Printing Technology*. https://www.protolabs.com/resources/blog/types-of-3d-printing/#:~:text=The primary difference between the,resulting in faster build speeds

Ahrens, K. (2014). *Chinesen drucken zehn Häuser an einem einzigen Tag - ingenieur.de*. https://www.ingenieur.de/technik/fachbereiche/bau/chinesen-drucken-zehn-haeuser-an-einzigen-tag/

Barberán, A., Casamayor, E. O., & Fierer, N. (2014). The microbial contribution to macroecology. *Frontiers in Microbiology*, *5*(MAY), 203. https://doi.org/10.3389/FMICB.2014.00203/XML/NLM

Bauer, S., & Hoye, B. J. (2014). Migratory Animals Couple Biodiversity and Ecosystem Functioning Worldwide. *Science*, *344*(6179). https://doi.org/10.1126/SCIENCE.1242552

BCN3D. (2020). *When Was 3D Printing Invented? The History of 3D Printing*. https://www.bcn3d.com/the-history-of-3d-printing-when-was-3d-printing-invented/#:~:text=The first documented iterations of,was polymerized by UV light

Benjamin, A. D., Abbasi, R., Owens, M., Olsen, R. J., Walsh, D. J., Lefevre, T. B., & Wilking, J. N. (2019). Light-based 3D printing of hydrogels with high-resolution channels. *Biomedical Physics & Engineering Express*, *5*(2), 025035. https://doi.org/10.1088/2057-1976/AAD667

Berg, H. C., & Anderson, R. A. (1973). Bacteria Swim by Rotating their Flagellar Filaments. *Nature 1973 245:5425*, *245*(5425), 380–382. https://doi.org/10.1038/245380a0

Berlow, E. L., Neutel, A.-M., Cohen, J. E., De Ruiter, P. C., Ebenman, B., Emmerson, M., Fox, J. W., Jansen, V. A. A., Jones, J. I., Kokkoris, G. D., Logofet, D. O., McKane, A. J., & Montoya Jose M. Petchey, O. (2004). Interaction Strengths in Food Webs: Issues and Opportunities. *Journal of Animal Ecology*, *73*(3), 585–598.

Blagodatskaya, E., & Kuzyakov, Y. (2013). Active microorganisms in soil: Critical review of estimation criteria and approaches. *Soil Biology and Biochemistry*, *67*, 192–211. https://doi.org/10.1016/J.SOILBIO.2013.08.024

Bunnell, F. L., & Huggard, D. J. (1999). Biodiversity across spatial and temporal scales: problems and opportunities. *Forest Ecology and Management*, *115*(2–3), 113–126. https://doi.org/10.1016/S0378-1127(98)00392-2

Burrows, L. (2012). Pseudomonas aeruginosa Twitching Motility: Type IV Pili in Action. *Article in Annual Review of Microbiology*. https://doi.org/10.1146/annurev-micro-092611-150055

Chenu, C., & Stotzky, G. (2001). Interactions between microorganisms and soil particles: an overview. *Interactions between Soil Particles and Microorganisms: Impact on the Terrestrial Ecosystem*, 3–40.

Chesson, P. (2000). Mechanisms of Maintenance of Species Diversity. *Http://Dx.Doi.Org/10.1146/Annurev.Ecolsys.31.1.343*, *31*, 343–366. https://doi.org/10.1146/ANNUREV.ECOLSYS.31.1.343

Choudoir, M. J., & DeAngelis, K. M. (2022). A framework for integrating microbial dispersal modes into soil ecosystem ecology. *IScience*, *25*(3), 103887. https://doi.org/10.1016/J.ISCI.2022.103887

Craig, L., Forest, K. T., & Maier, B. (2019). Type IV pili: dynamics, biophysics and functional consequences. *Nature Reviews Microbiology 2019 17:7*, *17*(7), 429–440. https://doi.org/10.1038/s41579-019-0195-4

Crawford, D. W. (1992). Metabolic Cost of Motility in Planktonic Protists: Theoretical Considerations on Size Scaling and Swimming Speed. *Microb Ecol*, *24*, 1–10.

Czárán, T. L., Hoekstra, R. F., & Pagie, L. (2002). Chemical warfare between microbes promotes biodiversity. *Proceedings of the National Academy of Sciences*, *99*(2), 786–790. https://doi.org/10.1073/PNAS.012399899

Daehler, C. C. (2001). Darwin's Naturalization Hypothesis Revisited. *Https://Doi.Org/10.1086/321316*, *158*(3), 324–330. https://doi.org/10.1086/321316

de Martino, A., Gueudré, T., & Miotto, M. (2019). Exploration-exploitation tradeoffs dictate the optimal distributions of phenotypes for populations subject to fitness fluctuations. *Physical Review E*, *99*(1), 012417. https://doi.org/10.1103/PHYSREVE.99.012417/FIGURES/5/MEDIUM

DeAngelis, D. L., & Grimm, V. (2014a). Individual-based models in ecology after four decades. *F1000Prime Reports*, *6*. https://doi.org/10.12703/P6-39

DeAngelis, D. L., & Grimm, V. (2014b). Individual-based models in ecology after four decades. *F1000prime Reports*, *6*. https://doi.org/10.12703/P6-39

Dröge, E., Creel, S., Becker, M. S., & Jassiel M'soka, |. (2017). Spatial and temporal avoidance of risk within a large carnivore guild. *Ecology and Evolution*, *7*, 189–199. https://doi.org/10.1002/ece3.2616

Duncan, R. P., & Williams, P. A. (2002). Darwin's naturalization hypothesis challenged. *Nature 2002 417:6889*, *417*(6889), 608–609. https://doi.org/10.1038/417608a

Ebrahimi, A. N., & Or, D. (2014). Microbial dispersal in unsaturated porous media: Characteristics of motile bacterial cell motions in unsaturated angular pore networks. *Water Resources Research*, *50*(9), 7406–7429. https://doi.org/10.1002/2014WR015897

Feest, A., Aldred, T. D., & Jedamzik, K. (2010). Biodiversity quality: A paradigm for biodiversity. *Ecological Indicators*, *10*(6), 1077–1082. https://doi.org/10.1016/J.ECOLIND.2010.04.002

Frean, M., & Abraham, E. R. (2001). Rockscissorspaper and the survival of the weakest. *Proceedings of the Royal Society of London. Series B: Biological Sciences*, *268*(1474), 1323–1327. https://doi.org/10.1098/RSPB.2001.1670

Frey, S. D., Elliott, E. T., & Paustian, K. (1999). Bacterial and fungal abundance and biomass in conventional and no-tillage agroecosystems along two climatic gradients. *Soil Biology and Biochemistry*, *31*(4), 573–585. https://doi.org/10.1016/S0038-0717(98)00161-8

Gatti, R. C. (2016). A conceptual model of new hypothesis on the evolution of biodiversity. *Biologia 2016 71:3*, *71*(3), 343–351. https://doi.org/10.1515/BIOLOG-2016-0032

Ghazaryan, L., Tonoyan, L., Ashhab, A. al, Soares, M. I. M., & Gillor, O. (2014). The role of stress in colicin regulation. *Archives of Microbiology 2014 196:11*, *196*(11), 753–764. https://doi.org/10.1007/S00203-014-1017-8

Gonzalez, D., Sabnis, A., Foster, K. R., & Mavridou, D. A. I. (2018). Costs and benefits of provocation in bacterial warfare. *Proceedings of the National Academy of Sciences of the United States of America*, *115*(29), 7593–7598. https://doi.org/10.1073/PNAS.1801028115/SUPPL_FILE/PNAS.1801028115.SD03.XLSX

Grand View Research. (2020). *3D Printing Market Worth $35.38 Billion By 2027*.

Grand View Research. (2021). *3D Printing Market Size, Share & Trends Analysis Report By Component (Hardware, Software, Services)*. https://www.forest2market.com/blog/more-rd-activities-open-up-lignins-feedstock-potential

Grimm, V. (1999). Ten years of individual-based modelling in ecology: what have we learned and what could we learn in the future? *Ecological Modelling*, *115*(2–3), 129–148. https://doi.org/10.1016/S0304-3800(98)00188-4

Hillel, D. (2003). *Introduction to Environmental Soil Physics*. Elsevier.

Hinsinger, P., Bengough, A. G., Vetterlein, D., & Young, I. M. (2009). Rhizosphere: biophysics, biogeochemistry and ecological relevance. *Plant and Soil 2009 321:1*, *321*(1), 117–152. https://doi.org/10.1007/S11104-008-9885-9

Ishii, Y., & Shimada, M. (2010). The effect of learning and search images on predator-prey interactions. *Population Ecology*, *52*(1), 27–35. https://doi.org/10.1007/S10144-009-0185-X

Jackson, J. B. C., & Buss, L. (1975). Alleopathy and spatial competition among coral reef invertebrates. *Proceedings of the National Academy of Sciences*, *72*(12), 5160–5163. https://doi.org/10.1073/PNAS.72.12.5160

Julia Documentation · The Julia Language. (n.d.). Retrieved September 5, 2022, from https://docs.julialang.org/en/v1/

Kerr, B., Riley, M. A., Feldman, M. W., & Bohannan, B. J. M. (2002). Local dispersal promotes biodiversity in a real-life game of rock–paper–scissors. *Nature 2002 418:6894*, *418*(6894), 171–174. https://doi.org/10.1038/nature00823

Kohlmeier, S., Smits, T. H. M., Ford, R. M., Keel, C., Harms, H., & Wick, L. Y. (2005). Taking the fungal highway: Mobilization of pollutant-degrading bacteria by fungi. *Environmental Science and Technology*, *39*(12), 4640–4646. https://doi.org/10.1021/es047979z

Kuhn, T., Buffi, M., Bindschedler, S., Chain, P. S., Gonzalez, D., Stanley, C., Wick, L. Y., Junier, P., & Richter, X.-Y. L. (2022). Design and construction of 3D-printed devices to investigate active and passive bacterial dispersal on hydrated surfaces. *BioRxiv*, 2022.05.16.492069. https://doi.org/10.1101/2022.05.16.492069

Kyba, C. C. M., & Hölker, F. (2013). Do artificially illuminated skies affect biodiversity in nocturnal landscapes? *Landscape Ecology*, *28*(9), 1637–1640. https://doi.org/10.1007/S10980-013-9936-3/FIGURES/1

Leben, C. (1984). Spread of plant pathogenic bacteria with fungal hyphae. *Phytopathology*, *74*(8), 983–986.

Liao, M. J., Miano, A., Nguyen, C. B., Chao, L., & Hasty, J. (2020). Survival of the weakest in non-transitive asymmetric interactions among strains of E. coli. *Nature Communications 2020 11:1*, *11*(1), 1–8. https://doi.org/10.1038/s41467-020-19963-8

Madigan, M. T., Martinko, J. M., Stahl, D. A., & Clark, D. P. (2013). *Brock Mikrobiologie* (A. Schmid & C. Schneider, Eds.; 13th ed., pp. 653–696). Pearson Deutschland GmbH.

Madsen, E. L., & Alexander, M. (1982). Transport of Rhizobium and Pseudomonas through Soil. *Soil Science Society of America Journal*, *46*(3), 557–560. https://doi.org/10.2136/SSSAJ1982.03615995004600030023X

Maier, B., & Wong, G. C. L. (2015). How Bacteria Use Type IV Pili Machinery on Surfaces. *Trends in Microbiology*, *23*(12), 775–788. https://doi.org/10.1016/J.TIM.2015.09.002

Martínez-García, E., Nikel, P. I., Chavarría, M., & de Lorenzo, V. (2013). *The metabolic cost of flagellar motion in Pseudomonas putida KT2440*. https://doi.org/10.1111/1462-2920.12309

Mattick, J. S. (2002). Type IV Pili and Twitching Motility. *Annu. Rev. Microbiol*, *56*, 289–314. https://doi.org/10.1146/annurev.micro.56.012302.160938

Mcbride, M. J. (2001). Bacterial Gliding Motility: Multiple Mechanisms for Cell Movement over Surfaces Cultivating Ecosystems: Microbial Communities in Recirculating Aquaculture Systems View project T9SS and virulence of Flavobacterium columnare View project. *Annual Review of Microbiology*, *55*, 49–75. https://doi.org/10.1146/annurev.micro.55.1.49

Melbourne, B. A., Cornell, H. V., Davies, K. F., Dugaw, C. J., Elmendorf, S., Freestone, A. L., Hall, R. J., Harrison, S., Hastings, A., Holland, M., Holyoak, M., Lambrinos, J., Moore, K., & Yokomizo, H. (2007). Invasion in a heterogeneous world: resistance, coexistence or hostile takeover? *Ecology Letters*, *10*(1), 77–94. https://doi.org/10.1111/J.1461-0248.2006.00987.X

Mitchell, J. G. (2002). The Energetics and Scaling of Search Strategies in Bacteria. *Https://Doi.Org/10.1086/343874*, *160*(6), 727–740. https://doi.org/10.1086/343874

Mitchell, J. G., & Kogure, K. (2006). Bacterial motility: links to the environment and a driving force for microbial physics. *FEMS Microbiology Ecology*, *55*(1), 3–16. https://doi.org/10.1111/J.1574-6941.2005.00003.X

Muelhauser, L., & Rieber, L. (2014). Exponential and non-exponential trends in information technology. *Machine Intelligence Research Institute*.

Muok, A. R., & Briegel, A. (2021). Intermicrobial Hitchhiking: How Nonmotile Microbes Leverage Communal Motility. *Trends in Microbiology*, *29*(6), 542–550. https://doi.org/10.1016/J.TIM.2020.10.005

Nakamura, S., & Minamino, T. (2019). Flagella-Driven Motility of Bacteria. *Biomolecules 2019, Vol. 9, Page 279*, *9*(7), 279. https://doi.org/10.3390/BIOM9070279

Or, D., Smets, B. F., Wraith, J. M., Dechesne, A., & Friedman, S. P. (2007). Physical constraints affecting bacterial habitats and activity in unsaturated porous media – a review. *Advances in Water Resources*, *30*(6–7), 1505–1527. https://doi.org/10.1016/J.ADVWATRES.2006.05.025

Osmond, M. M., & de Mazancourt, C. (2013). How competition affects evolutionary rescue. *Philosophical Transactions of the Royal Society of London. Series B, Biological Sciences*, *368*(1610), 20120085. https://doi.org/10.1098/rstb.2012.0085

Osono, T., Ono, Y., & Takeda, H. (2003). Fungal ingrowth on forest floor and decomposing needle litter of Chamaecyparis obtusa in relation to resource availability and moisture condition. *Soil Biology and Biochemistry*, *35*(11), 1423–1431. https://doi.org/10.1016/S0038-0717(03)00236-0

Park, D. S., & Daniel, P. (2013). A test of Darwin's naturalization hypothesis in the thistle tribe shows that close relatives make bad neighbors. *Proceedings of the National Academy of Sciences of the United States of America*, *110*(44), 17915–17920. https://doi.org/10.1073/PNAS.1309948110/SUPPL_FILE/ST03.DOCX

Partridge, J. D., & Harshey, R. M. (2013). Swarming: Flexible roaming plans. *Journal of Bacteriology*, *195*(5), 909–918. https://doi.org/10.1128/JB.02063-12/SUPPL_FILE/ZJB999092451SO1.PDF

Pion, M., Bshary, R., Bindschedler, S., Filippidou, S., Wick, L. Y., Job, D., & Junier, P. (2013). Gains of bacterial flagellar motility in a fungal world. *Applied and Environmental Microbiology*, *79*, 6862–6867.

Prosser, J. I., Bohannan, B. J. M., Curtis, T. P., Ellis, R. J., Firestone, M. K., Freckleton, R. P., Green, J. L., Green, L. E., Killham, K., Lennon, J. J., Osborn, A. M., Solan, M., van der Gast, C. J., & Young, J. P. W. (2007). The role of ecological theory in microbial ecology. *Nature Reviews Microbiology 2007 5:5*, *5*(5), 384–392. https://doi.org/10.1038/nrmicro1643

Reichenbach, T., Mobilia, M., & Frey, E. (2007). Mobility promotes and jeopardizes biodiversity in rock–paper–scissors games. *Nature 2007 448:7157*, *448*(7157), 1046–1049. https://doi.org/10.1038/nature06095

Ren, Q., Kwan, A. H., & Sunde, M. (2013). Invited Review Two Forms and Two Faces, Multiple States and Multiple Uses: Properties and Applications of the Self-Assembling Fungal Hydrophobins. *Biopolymers (Pept Sci)*, *100*, 601–612. https://doi.org/10.1002/bip.22259

Ritz, K., & Young, I. M. (2004). Interactions between soil structure and fungi. *Mycologist*, *18*, 52–59.

Ronce, O. (2007). How Does It Feel to Be like a Rolling Stone? Ten Questions about Dispersal Evolution. *Annual Review of Ecology, Evolution, and Systematics*, *38*, 231–253.

Schreiber, S. J., & Killingback, T. P. (2013). Spatial heterogeneity promotes coexistence of rock–paper–scissors metacommunities. *Theoretical Population Biology*, *86*, 1–11. https://doi.org/10.1016/J.TPB.2013.02.004

Schumann, R., & Reinhard, P. (2018, December 5). *3D-Druck in der Medizin: Definitionen, Anwendungen, Materialien und Maschinen*. https://www.devicemed.de/3d-druck-in-der-medizin-definitionen-anwendungen-materialien-und-maschinen-a-782881/

Servedio, M. R., Brandvain, Y., Dhole, S., Fitzpatrick, C. L., Goldberg, E. E., Stern, C. A., van Cleve, J., & Yeh, D. J. (2014). Not Just a Theory—The Utility of Mathematical Models in Evolutionary Biology. *PLoS Biology*, *12*(12). https://doi.org/10.1371/JOURNAL.PBIO.1002017

Shade, A., Dunn, R. R., Blowes, S. A., Keil, P., Bohannan, B. J. M., Herrmann, M., Küsel, K., Lennon, J. T., Sanders, N. J., Storch, D., & Chase, J. (2018). Macroecology to Unite All Life, Large and Small. *Trends in Ecology & Evolution*, *33*(10), 731–744. https://doi.org/10.1016/J.TREE.2018.08.005

Silverman, M., & Simon, M. (1974). Flagellar rotation and the mechanism of bacterial motility. *Nature 1974 249:5452*, *249*(5452), 73–74. https://doi.org/10.1038/249073a0

Sinervo, B., & Lively, C. M. (1996). The rock–paper–scissors game and the evolution of alternative male strategies. *Nature 1996 380:6571*, *380*(6571), 240–243. https://doi.org/10.1038/380240a0

Sol, D., Lapiedra, O., & Vilà, M. (2014). Do close relatives make bad neighbors? *Proceedings of the National Academy of Sciences of the United States of America*, *111*(5), E534-5. https://doi.org/10.1073/PNAS.1320729111

Soliveres, S., Maestre, F. T., Ulrich, W., Manning, P., Boch, S., Bowker, M. A., Prati, D., Delgado-Baquerizo, M., Quero, J. L., Schöning, I., Gallardo, A., Weisser, W., Müller, J., Socher, S. A., García-Gómez, M., Ochoa, V., Schulze, E. D., Fischer, M., & Allan, E. (2015). Intransitive competition is widespread in plant communities and maintains their species richness. *Ecology Letters*, *18*(8), 790–798. https://doi.org/10.1111/ELE.12456

Son, K., Guasto, J. S., & Stocker, R. (2013). Bacteria can exploit a flagellar buckling instability to change direction. *Nature Physics 2013 9:8*, *9*(8), 494–498. https://doi.org/10.1038/nphys2676

Stouffer, D. B., Sales-Pardo, M., Sirer, M. I., & Bascompte, J. (2012). Evolutionary conservation of species' roles in food webs. *Science*, *335*(6075), 1489–1492. https://doi.org/10.1126/SCIENCE.1216556/SUPPL_FILE/STOUFFER.SOM.PDF

Stutchbury, B. J. M., Siddiqui, R., Applegate, K., Hvenegaard, G. T., Mammenga, P., Mickle, N., Pearman, M., Ray, J. D., Savage, A., Shaheen, T., & Fraser, K. C. (2016). Ecological Causes and Consequences of Intratropical Migration in Temperate-Breeding Migratory Birds*. *Https://Doi.Org/10.1086/687531*, *188*(S1), S28–S40. https://doi.org/10.1086/687531

Szabó, P., Czárán, T., & Szabó, G. (2007). Competing associations in bacterial warfare with two toxins. *Journal of Theoretical Biology*, *248*(4), 736–744. https://doi.org/10.1016/J.JTBI.2007.06.022

Szolnoki, A., Mobilia, M., Jiang, L. L., Szczesny, B., Rucklidge, A. M., & Perc, M. (2014). Cyclic dominance in evolutionary games: a review. *Journal of The Royal Society Interface*, *11*(100). https://doi.org/10.1098/RSIF.2014.0735

Tecon, R., & Or, D. (2017). Biophysical processes supporting the diversity of microbial life in soil. *FEMS Microbiology Reviews*, *41*, 599–623.

Tuller, M., & Or, D. (2005). Water films and scaling of soil characteristic curves at low water contents. *Water Resources Research*, *41*(9), 1–6. https://doi.org/10.1029/2005WR004142

Volker, G., & Railsback, S. F. (2005). *Individual-based Modeling and Ecology* (8th ed.). Princeton University Press. https://doi.org/https://doi.org/10.1515/9781400850624

Vos, M., Wolf, A. B., Jennings, S. J., & Kowalchuk, G. A. (2013). Micro-scale determinants of bacterial diversity in soil. *FEMS Microbiology Reviews*, *37*(6), 936–954. https://doi.org/10.1111/1574-6976.12023

Wadhwa, N., & Berg, H. C. (2021). Bacterial motility: machinery and mechanisms. *Nature Reviews Microbiology 2021 20:3*, *20*(3), 161–173. https://doi.org/10.1038/s41579-021-00626-4

Wang, G., & Or, D. (2012). A Hydration-Based Biophysical Index for the Onset of Soil Microbial Coexistence. *Scientific Reports 2012 2:1*, *2*(1), 1–5. https://doi.org/10.1038/srep00881

Wösten, H. A. B., Van Wetter, M. A., Lugones, L. G., Van der Mei, H. C., Busscher, H. J., & Wessels, J. G. H. (1999). How a fungus escapes the water to grow into the air. *Current Biology*, *9*(2), 85–88. https://doi.org/10.1016/S0960-9822(99)80019-0

Xie, L., Altindal, T., Chattopadhyay, S., & Wu, X. L. (2011). Bacterial flagellum as a propeller and as a rudder for efficient chemotaxis. *Proceedings of the National Academy of Sciences of the United States of America*, *108*(6), 2246–2251. https://doi.org/10.1073/PNAS.1011953108/SUPPL_FILE/SM03.WMV

Yamamichi, M., Kyogoku, D., Iritani, R., Kobayashi, K., Takahashi, Y., Tsurui-Sato, K., Yamawo, A., Dobata, S., Tsuji, K., & Kondoh, M. (2020). Intraspecific Adaptation Load: A Mechanism for Species Coexistence. *Trends in Ecology & Evolution*, *35*(10), 897–907. https://doi.org/10.1016/J.TREE.2020.05.011

Yang, T. Y., Sung, Y. M., Lei, G. S., Romeo, T., & Chak, K. F. (2010). Posttranscriptional repression of the cel gene of the ColE7 operon by the RNA-binding protein CsrA of Escherichia coli. *Nucleic Acids Research*, *38*(12), 3936–3951. https://doi.org/10.1093/NAR/GKQ177

Yonekura, K., Maki-Yonekura, S., & Namba, K. (2003). Complete atomic model of the bacterial flagellar filament by electron cryomicroscopy. *Nature 2003 424:6949*, *424*(6949), 643–650. https://doi.org/10.1038/nature01830

Young, I. M., Crawford, J. W., Nunan, N., Otten, W., & Spiers, A. (2008). Chapter 4 Microbial Distribution in Soils: Physics and Scaling. *Advances in Agronomy*, *100*(C), 81–121. https://doi.org/10.1016/S0065-2113(08)00604-4

Zhou, J., Xia, B., Treves, D. S., Wu, L. Y., Marsh, T. L., O'Neill, R. V., Palumbo, A. V., & Tiedje, J. M. (2002). Spatial and resource factors influencing high microbial diversity in soil. *Applied and Environmental Microbiology*, *68*(1), 326–334. https://doi.org/10.1128/AEM.68.1.326-334.2002/ASSET/9DF49E0E-9ACF-4168-B6A2-BB8CB60B8D8C/ASSETS/GRAPHIC/AM0120965005.JPEG

Chapter one

Contribution chapter one

In the first chapter, I performed the additional experiments to add additional data to a previously started experimental data set.Therfore I follwed the workflow of Marine Mamin. Furthermore, I tested for the exploration-exploitation trade-off in the system. The statistical analyzes and the plots were conducted by myself. Furthermore, Xiang-Yi Richter and I wrote the first manuscript and answered the questions from the reviewer during the publishing process. The in-revision manuscript of Kuhn and Mamin et al. 2022 appears on the next pages.

Summary Chapter one

In this chapter, we investigate how spatial avoidance along the fungal highways helps maintain the biodiversity of closely related species. Two closely related *Pseudomonas putida* strains were used to analyze the impact of fungal highways on their coexistence under the hypothesis that adding a spatial scale would allow for spatial avoidance. To test this hypothesis, we allowed let two *p. Putida* strains to compete at local and regional scales by inoculating them either in a mixed droplet or in separate droplets in the same Petri dish, respectively. We also created conditions allowing bacterial strains to disperse across abiotic or fungal hyphae networks. We found that competition at the local scale led to competitive exclusion, while regional competition promoted coexistence. When competing in the presence of dispersal networks, the growth-motility trade-off promoted coexistence only when the strains were inoculated in separate droplets. We used the bridge system (described in Chapter two) to prove the exploration-exploitation trade-off between the two *P. putida* strains. Our results provide a mechanism, which helps to explain the widespread coexistence of competing bacterial strains.

ROYAL SOCIETY OPEN SCIENCE

royalsocietypublishing.org/journal/rsos

Research

Cite this article: Kuhn T, Mamin M, Bindschedler S, Bshary R, Estoppey A, Gonzalez D, Palmieri F, Junier P, Richter X-YL. 2022 Spatial scales of competition and a growth–motility trade-off interact to determine bacterial coexistence. *R. Soc. Open Sci.* **9**: 211592. https://doi.org/10.1098/rsos.211592

Received: 8 October 2021
Accepted: 18 November 2022

Subject Category:
Ecology, Conservation, and Global Change Biology

Subject Areas:
ecology/microbiology/evolution

Keywords:
bacterial–fungal interactions, growth–motility trade-off, dispersal, coexistence, spatial structure, fungal highway

Authors for correspondence:
Pilar Junier
e-mail: pilar.junier@unine.ch
Xiang-Yi Li Richter
e-mail: li@evolbio.mpg.de

†These authors contributed equally and share the first-authorship.

Electronic supplementary material is available online at https://doi.org/10.6084/m9.figshare.c.6316842.

THE ROYAL SOCIETY PUBLISHING

Spatial scales of competition and a growth-motility tradeoff interact to determine bacterial coexistence

Thierry Kuhn[1,2,†], Marine Mamin[1,†], Saskia Bindschedler[1], Redouan Bshary[2], Aislinn Estoppey[1], Diego Gonzalez[1], Fabio Palmieri[1], Pilar Junier[1] and Xiang-Yi Li Richter[1,2]

[1]Laboratory of Microbiology, Institute of Biology, and [2]Laboratory of Eco-Ethology, Institute of Biology, University of Neuchâtel, Rue Émile-Argand 11, CH-2000 Neuchâtel, Switzerland

RB, 0000-0001-7198-8472; X-YLR, 0000-0001-8662-0865

The coexistence of competing species is a long-lasting puzzle in evolutionary ecology research. Despite abundant experimental evidence showing that the opportunity for coexistence decreases as niche overlap increases between species, bacterial species and strains competing for the same resources are commonly found across diverse spatially heterogeneous habitats. We thus hypothesized that the spatial scale of competition may play a key role in determining bacterial coexistence, and interact with other mechanisms that promote coexistence, including a growth–motility trade-off. To test this hypothesis, we let two *Pseudomonas putida* strains compete at local and regional scales by inoculating them either in a mixed droplet or in separate droplets in the same Petri dish, respectively. We also created conditions that allow the bacterial strains to disperse across abiotic or fungal hyphae networks. We found that competition at the local scale led to competitive exclusion while regional competition promoted coexistence. When competing in the presence of dispersal networks, the growth–motility trade-off promoted coexistence only when the strains were inoculated in separate droplets. Our results provide a mechanism by which existing laboratory data suggesting competitive exclusion at a local scale is reconciled with the widespread coexistence of competing bacterial strains in complex natural environments with dispersal.

1. Introduction

Bacteria are important components of the microbial community in diverse habitats, and the coexistence of different bacterial species and strains can serve important ecosystem functions, from soil nutrient cycling to providing defence against pathogens for their animal and plant hosts [1–5]. Competition experiments under controlled laboratory conditions revealed a general trend that the closer the phylogenetic distance between the competing species, the more likely that one species/strain competitively excludes the other, since niche overlap and antagonistic interactions are generally more intense between closely related species [6–8]. Nevertheless, competing species with overlapping niche use are commonly observed in natural habitats, including soils [9,10], fermented foods [11,12] and different parts of the human body [13–16]. Various mechanisms have been identified to promote the coexistence of bacteria [17], for example, metabolic niche partitioning [18–20], negative frequency-dependent selection [21–23], shared predators or parasites [24,25] and chemical warfare [26–28]. Many of these mechanisms involve trade-offs between growth rate and other traits, such as the production and/or tolerance of antibiotics, resistance to adverse environments and predator avoidance.

One understudied trade-off is the trade-off between bacterial growth and motility. This trade-off can result from the metabolic costs of expressing and using propulsion machinery (e.g. flagella) and genetic constraints that limit the simultaneous improvement of growth and motility during evolution [29–34]. The growth–motility trade-off is interesting because it may help explain and reconcile the apparently conflicting results of a strong tendency of competitive exclusion found in laboratory experiments between competing species of overlapping resource niches and the widespread coexistence of intensely competing strains in nature. In contrast with the often spatially simple and well-mixed conditions in competition assays, natural environments such as the soil, skin and fermented foods are featured by spatial heterogeneity that allows bacterial cells to interact at different spatial scales and allows motile strains to disperse. Indeed, studies in animals and plants have shown that the competition–dispersal trade-off (analogous to the growth–motility trade-off in bacteria) can contribute to the coexistence of closely related species at relatively large regional spatial scales, but not at the smaller local scales [35,36]. Recent studies with bacteria also showed that a negative correlation between growth rate and dispersal ability can promote coexistence of closely related *Pseudomonas fluorescens* [37] strains and *Escherichia coli* [32] strains. However, the experimental designs in these studies are highly simplified from biological reality. In the former study [37], the dispersal of bacteria was implemented by artificially transferring cell suspension across wells in 96-well plates at discrete time intervals, and in the later work [32], a simple and homogeneous soft agar gel was used as the substrate where bacterial growth and dispersal took place. Therefore, there is need to test the effects of spatial scales of competition and the growth–motility trade-off incorporating other relevant biological factors, for example, in spatially heterogeneous environments created naturally by fungal hyphae networks where bacterial cells have the opportunity to disperse by swimming by means of their flagella.

In this work, we study whether the spatial scale of competition can change the competition outcome between two closely related *Pseudomonas putida* strains in the presence of a growth–motility trade-off. We created heterogeneous environments by providing biotic and abiotic dispersal networks. The biotic networks were formed by living fungal mycelia [11,38,39], known as 'fungal highways', in the soil environment [38]. The abiotic networks were based on glass fibres, which have been used in previous studies as an abiotic control for fungal hyphae [39–43]. In the absence of a dispersal network, the two bacterial strains compete either at the local scale when inoculated in mixed cell suspensions, or at the regional scale when inoculated in single-strain suspensions onto the same medium in a Petri dish. In the former case, direct contact between cells of different strains can occur, while in the latter case, cells of different strains do not touch each other but compete by using a shared nutrient pool in the medium or can exchange volatile signals. In the presence of abiotic or biotic dispersal networks, the two bacterial strains compete at intermediate scales that were initially local/regional when inoculated in mixed/separate droplets, respectively. We performed experiments with a factorial design of three different spatial structures (i.e. no dispersal network, abiotic network and biotic network) and two initial scales of competition (i.e. local scale in mixed inoculation and regional scale in separate inoculation), and quantified the competition results in terms of whether the faster growing strain can competitively exclude its slower growing competitor.

2. Materials and methods

2.1. Bacterial and fungal strains

For all experiments, we used two closely related flagellated strains of *Pseudomonas putida*. The KT2440 strain is a saprotrophic soil bacterium, originally isolated from the rhizosphere [44]; the UWC1 strain

is documented as a spontaneous rifampicin-resistant mutant of the KT2440 [45]. A comparison between the genomes of the two strains showed additional differences, with a median identity of 95.8% between homologous genes (see electronic supplementary material, documents 'genome_comparison.pdf' and 'genome_comparison_table.xls'). The KT2440 and UWC1 strains were tagged with the green fluorescent protein (GFP) and mCherry, respectively, by Mini-Tn7 transposon insertions [46,47]. The different fluorescent labels enabled the two strains to be observed by epifluorescence stereomicroscopy and enumerated by flow cytometry. The fungal species used in the experiments was *Trichoderma rossicum* (NEU388) [43], a saprotrophic soil ascomycete that has been shown to allow various bacterial species (including *P. putida*) to move along its mycelial networks.

2.2. Culture conditions and inocula preparation

Bacterial cells were cryo-preserved in 30% (v/v) glycerol at −80°C. To prepare the inocula, cells were first plated on Nutrient Agar (NA, 23 g l^{-1}, Carl Roth, AE92.2) supplemented with gentamycin (10 ppm) and grown at 30°C in darkness. The strains were then subcultured once on NA through polygonal spreading and grown under the same conditions. Bacterial suspensions were prepared from overnight cultures grown in Nutrient Broth (NB, 25 g l^{-1}, Carl Roth, AE92.2) at ambient temperature under constant agitation at 120 r.p.m. Bacteria were collected from an overnight culture by centrifugation (3000*g* for 10 min), washed once and resuspended in 0.01 M phosphate-buffered saline (PBS: 1.5 g l^{-1} $Na_2HPO_3{\cdot}2H_2O$, 0.25 g l^{-1} $NaH_2PO_3{\cdot}2H_2O$, 8.5 g l^{-1} NaCl and pH adjusted to 7.4). The cell densities of the two bacterial strains in the suspensions were determined by flow cytometry (see below) and then adjusted to the same value of 10^9 cells ml^{-1}. After that, for the local competition scenario, a 1 : 1 ratio cell suspension was prepared by combining a proportion of the single-strain suspensions.

The fungus *T. rossicum* was maintained on a slanted agar tube at 4°C. It was plated on the malt-agar medium (MA: 12 g l^{-1} malt extract Pulver amber, SIOS Homebrewing; 15 g l^{-1} technical agar, BioLife Italiana) and incubated at 22°C in darkness. Before being used for inoculation, the fungus was subcultured by replating a plug cored from the active apical margin of the 2-day-old mycelial colony on a fresh medium and grown under the same conditions.

2.3. Experimental set-up

As shown in figure 1*a*, we inoculated the mCherry-labelled UWC1 strain and the GFP-labelled KT2440 strain in droplets of either single-strain or mixed cell suspensions onto plates of MA medium, under three different spatial conditions—no network, fungal mycelial network and glass fibre network—each with four to eight replicates.

In the 'no network' settings, both bacterial strains have limited capacity to disperse. The colonies (both separate or mixed) can only expand from the colony margin (electronic supplementary material, figure S1). Under the 'fungal network' and 'glass fibre network' settings, the two bacterial strains used their flagella to swim and thereby dispersed in the liquid film along the surface of fungal hyphae or glass fibres, respectively [39].

In the network settings, when the two bacterial strains were inoculated separately, each strain could grow and start to disperse before encountering each other, and therefore the scale of interaction was initially regional. In this case, although the bacterial cells of the two strains were not in direct contact, they can still compete for resources diffused in the culturing medium in the same Petri dish. When inoculated in mixed droplets, the two strains engaged in direct competition right from the start before they could disperse, and thus the competition was initially local. Overall, the competition between the two strains occurred at finer scales when inoculated in mixed droplets, and the spatial scale of competition was coarser when the two strains were inoculated in separate droplets.

The bacteria and fungi inocula and the PBS control were positioned according to the diagram in figure 1*b*. The distances between the inocula were determined based on preliminary tests. The relatively shorter distances between point A (where the fungi or PBS control were inoculated) and the other inocula ensure a quick start of bacterial–fungal interactions (the fungal mycelium network can grow past the bacteria inocula within 24 h, see electronic supplementary material, figure S2). The relatively larger distance between inocula B and D ensures that the separate colonies of the KT2440 and UWC1 strains did not get in direct contact by the end of the experiments (electronic supplementary material, figure S3). We kept the positions of inoculation in figure 1*b* fixed throughout all treatments to ensure that the fungal networks were of the same 'age' when they expand and enter into contact with the bacterial colonies, because younger and older mycelia behave differently when

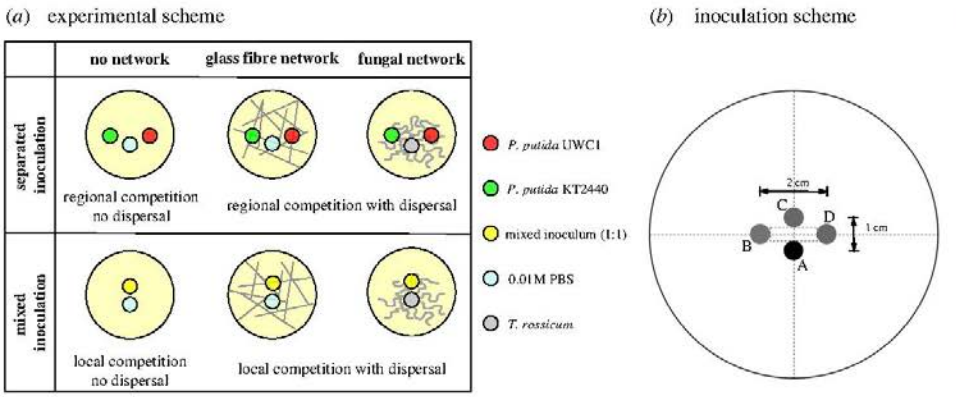

Figure 1. (*a*) Diagram of the experimental set-up under spatial settings representing different spatial scales of competition. The inocula are represented in the diagram as disproportionally large for the purpose of a clear illustration. The diameters of the bacteria/PBS inocula and the fungal inocula were 5.8 mm and 5.0 mm, respectively. See (*b*) for a diagram of the actual positions of different inoculates on a diameter 9 cm Petri dish. When applicable, the fungus or the PBS control was inoculated at position A, the KT2440 strain suspension was inoculated at position B, the mixed inoculum was inoculated at position C, and the UWC1 strain was inoculated at position D.

interacting with bacterial colonies. Younger mycelial networks tend to stay outside bacterial colonies (electronic supplementary material, figure S4a,b; fungal hyphae tips are in contact with bacterial colonies only at the colony margin) while older mycelial networks expand into the bacterial colonies (electronic supplementary material, figure S4c,d; fungal hyphae tips are accessible to bacterial cells in the interior of the colonies). Because the UWC1 strain tends to constrain the KT2440 strain to the interior of a mixed colony (electronic supplementary material, figure S1c), the KT2440 strain has a better chance to access and disperse on fungal networks (compare electronic supplementary material, figure S5b and S5d; green cells were constrained to the interior of the bacterial colony in the electronic supplementary material, figure S5b, but they were able to spread on the fungal hyphae in the electronic supplementary material, figure S5d).

2.4. Inoculation procedures and culture conditions

In the 'no network' setting, the inoculations of bacterial suspensions with separate/mixed strains and the PBS control were carried out by dropping on the medium surface 3 µl of the vortexed suspension with a microsyringe (Hamilton® 1701 N syringe 10 µl needle size 26s ga) according to the corresponding positioning scheme in figure 1. The resulting inocula were round-shaped with an area of 0.27 ± 0.011 cm^2.

In the 'glass fibre network' setting, we first placed around 30 glass fibres (8 µm diameter, 3–6 cm length, Cole-Parmer, USA) randomly on the agar plate and then performed the inoculations of bacteria as described earlier.

In the 'fungal networks' setting, we first inoculated the fungus as a diameter 5 mm plug cored with the wide-end of a Pasteur capillary pipette from the distal part of the *T. rossicum* mycelial network. Note that the mycelium was not in direct contact with the medium but laid on the top of the plug. The two bacterial strains in separate or mixed droplets were inoculated immediately afterwards according to the schemes in figure 1, following the same procedures as under the 'no network'. To prevent the fungal inoculum agar plug from impeding the expansion of bacterial colony/colonies, we removed it after 24 h, when the mycelial network had already expanded to the medium surface in the Petri dish.

After inoculation, the plates were parafilmed and incubated, in an upright position, at 22°C in constant darkness.

2.5. Collection of bacterial cells for enumeration

After 5 days of growth, the bacteria cells were collected for enumeration by flow cytometry. Under the 'no network' settings, we retrieved all bacterial cells by scraping the whole colony and resuspending the cells in 0.22 µm-filtered PBS. The suspensions were then stored on ice.

Under the 'glass fibre network' and the 'fungal network' settings, we first removed the bacterial colonies from the plates with a scalpel. We excluded cells in the bacterial colonies because we aimed to examine the relative abundance of the two bacterial strains that had already dispersed in the fungal/glass fibre networks. To collect those cells, we added 7 ml filtered PBS to the Petri dish, closed it and agitated it at 100 r.p.m. for 20 min on a rotary shaker. After that, we intensively flushed the surface of the medium with a 1000 µl micropipette, collected 5 ml of the resulting suspension and stored it on ice.

All the suspensions were then sonicated in a sonic bath at 35 kHz (Transsonic 310, Elma) twice for 30 s each and with a 30 s break in between [38]. This step was done to disaggregate bacterial clumps and/or to separate cells that might have stuck to the fungal/glass fibre fragments that might present in the suspension by chance. To remove those fragments before the flow cytometry analysis, we filtered the suspension through a polycarbonate filter with pores of 10 µm (Whatman, Nucleopore Track-Etch Membrane) pre-autoclaved in the Swinnex filters holders. All samples were kept at 4°C before performing the flow cytometry analysis the day after.

2.6. Flow cytometry

We estimated the relative abundances of the bacterial strains with a CyFlow space cytometer (Partec-System) equipped with a blue laser (480 nm/20 mV) and a green laser (532 nm/30 mV). The forward scatter (FSC) and side scatter (SSC) optical parameters are associated with the blue laser. The green fluorescence of the KT2440 strain was excited by the blue laser and detected on a photomultiplier tube with a 488 nm bandpass filter (FL1 parameter). The red fluorescence of the UWC1 strain was excited by the green laser and detected on a photomultiplier tube associated with a 590/50 nm bandpass filter (FL2 parameter). The lasers were arranged in parallel, with a delay of 50 µs between the two signals. Calibration of the instruments was verified before the analysis with calibration beads (Partec-Sysmex). The leading trigger was set on SSC, with a lower threshold of 500. Gains were set to 700 for FL1 and 750 for FL2. A four-decade logarithmic amplification was used for all parameters. The instrument was equipped with a true volumetric absolute counting facility: events were counted in a defined volume of 200 µl. A speed of 2 µl s^{-1} was used. We diluted the samples with 0.22 µm-filtered PBS to reach an event rate of approximately 1500 total events s^{-1}. This rate was determined with preliminary assays to yield an optimal signal to noise ratio. Samples were kept on ice during the whole analysis and were run in random order. Analysis of the flow cytometry data was performed with the instrument software FloMax. Events corresponding to the mCherry and GFP fluorescent signals were selected and counted with a quadrant gate set on a biplot of the FL1 and FL2 parameters.

2.7. Data preparation and statistics

We focused on the relative abundance of the UWC1 and KT2440 strains, and therefore, we calculated the cell density ratio in each replicate at the end of the experiments. We then transformed the data by taking the common log (of base 10) and confirmed the normality of the transformed data with the Shapiro–Wilk normality test. We then performed the Student's *t*-test against our null hypothesis that the relative abundance of the two strains remains identical to that at the beginning of experiments (with a log ratio of zero). The competitions between the abundances of the two strains when inoculated in mixed or separate droplets were performed by the Welch's two-sample *t*-tests. The statistical significance threshold value was chosen at $p = 0.05$. We adjusted the *p*-values to account for the false discovery rate due to multiple comparisons using the Benjamini and Hochberg method [48]. All statistical analyses were carried out within the R statistical environment [49]. The R scripts are provided in the electronic supplementary material, Information.

3. Results

Under the 'no network' treatment, when bacteria cells were inoculated in separate droplets (corresponding to regional competition), the relative abundance of the KT2440 strain and the UWC1 strain remained similar ($p = 0.569$) after 5 days of growth (figure 2*a*, tables 1 and 2). By contrast, in mixed inocula (corresponding to local competition), the UWC1 strain reached much higher cell proportions ($p < 0.01$) at the end of the experiments (the UWC1 strain was on average 5.43 times more abundant than the KT2440 strain), showing a growth advantage of the UWC1 strain in direct

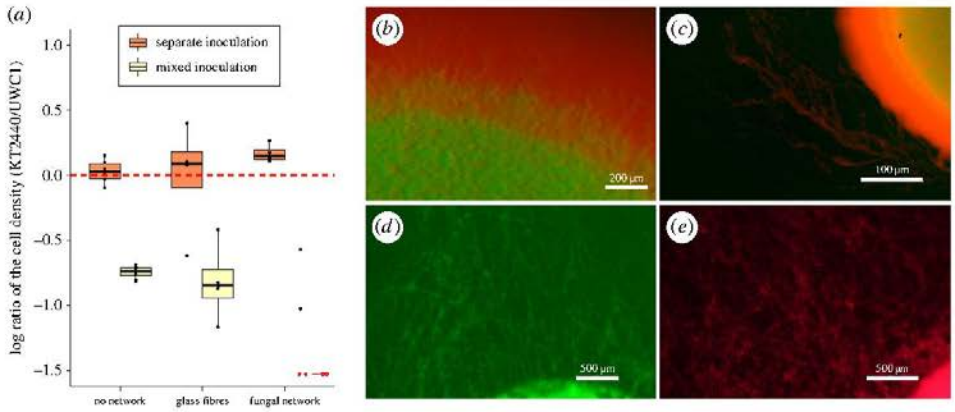

Figure 2. Box-whisker plots representing the distribution of the common logarithm (base 10) of the cell density ratio (KT2440/UWC1) under different experimental settings. The KT2440/UWC1 strain is more abundant than the other strain above/below the red horizontal line at log ratio of 0, respectively. The boxplot centre lines show the median, box limits show upper and lower quartiles, whiskers show 1.5× interquartile range, and each point corresponds to the result of an independent replicate. The red dashed line represents equal cell densities of the two bacterial strains. The numbers of replicates were 6 and 8 under the 'no network' setting for the separate and mixed inoculations, respectively. Under all other settings, the numbers of replicates were 4. Competitive exclusion of the KT2440 strain by the UWC1 strain occurred in two replicates under the fungal network treatment with mixed strain inoculates (the log density ratio was $-\infty$, marked with the two red dots). (*b*) Colony formed by bacterial strains in a mixed droplet 2 days after inoculation in the absence of a dispersal network. (*c*) Colony formed by bacterial strains in a mixed droplet in the presence of fungal hyphae networks 2 days after inoculation. Only the UWC1 strain with red fluorescence was visible along the fungal hyphae. (*d*) Dispersed KT2440 cells along fungal hyphae networks 3 days after being inoculated in a separate droplet. (*e*) Dispersed UWC1 cells along fungal hyphae networks 2 days after being inoculated in a separate droplet. The pictures were taken at magnifications of 10×, 3×, 5× and 5× with epifluorescence stereomicroscopy in (*b–e*), respectively.

Table 1. The median of the absolute density ratio (before log transformation) of the KT2440 strain relative to the UWC1 strain.

	no network	glass fibre network	fungal network
separate inoculation	1.064	1.239	1.418
mixed inoculation	0.184	0.143	N.A.[a]

[a]The KT2440 strain was competitively excluded in two of the four replicates.

Table 2. Mean and s.d. of the log density ratio between the KT2440 and the UWC1 strain, and the *p*-value of the *t*-test with a null hypothesis that the mean of the log ratio was not significantly different from zero.

		no network	glass fibre network	fungal network
separate inoculation	mean ± s.d.	0.030 ± 0.094	−0.006 ± 0.688	0.170 ± 0.111
	p-value	0.569	0.978	0.028
mixed inoculation	mean ± s.d.	−0.746 ± 0.039	−0.820 ± 0.488	N.A.[a]
	p-value	<0.01	0.028	

[a]The KT2440 strain was competitively excluded in two of the four replicates.

competition. Moreover, the spatial distribution of the two fluorescently tagged strains indicated that the UWC1 strain has expanded faster and constrained the KT2440 strain to the interior of the mixed colony, thus blocking the further growth of the KT2440 strain (figure 2*b*). The marked difference in the relative competitiveness of the two strains implies the competitive exclusion of the KT2440 strain by the UWC1 strain at the local scale in the long term.

Table 3. Comparison between the distributions of the common logarithm (base 10) of the cell density ratio (KT2440/UWC1) under separate and mixed inoculation treatments.

spatial settings	*p*-value of the Welch's two sample *t*-test
no network	<0.001
glass fibre network	0.025
fungal hyphae network	N.A., because of the two $-\infty$ values under mixed inoculation treatment

Under the 'glass fibres' treatment, the KT2440 strain was slightly more abundant (but the difference was not statistically significant, $p = 0.978$) when the two bacterial strains were inoculated separately (corresponding to an intermediate scale of competition that was initially regional, figure 2*a*, table 1), reaching 1.239 times the density of the UWC1 strain. We therefore cannot reject the null hypothesis that the relative abundance of the two strains remained identical (table 2). This result implies possible long-term coexistence of the two strains at the regional scale. In plates where the two bacterial strains were inoculated in mixed droplets (corresponding to an intermediate scale of competition that was initially local), similar to the results of local competition under the 'no network' treatment, the UWC1 strain has a substantial competitive advantage ($p = 0.028$) and reached on average 6.99 times the density of the KT2440 strain, implying that competitive exclusion was likely at the local scale (figure 2*a*, tables 1 and 2).

Under the 'fungal network' treatment, the KT2440 strain reached even larger (statistically significant, $p = 0.028$) relative abundances when inoculated in separate droplets (1.42 times the abundance of the UWC1 strain), implying a competitive advantage at the regional scale. The competitive advantage of the KT2440 strain outside the initial inocula resulted from its higher motility and faster spread in the presence of fungal hyphae networks. See electronic supplementary material, figure S7 for direct verification of the motility advantage of the KT2440 strain. The distribution of bacterial cells in the fungal network can be considered as mini-colonies with either mixed or separate strains. Since the KT2440 strain grows equally fast as the UWC1 strain in separate colonies, and it grows much slower than the UWC1 strain in mixed colonies, the overall higher densities of the KT2440 strain were likely to result from its superior motility in the presence of dispersal networks provided by fungal hyphae. In mixed inoculations, however, the KT2440 strain was competitively excluded outside the initial inocula (figure 2*c* for an example) in two of the replicates (in these cases, the cell densities of the KT2440 strain were so low that they were not distinguishable from the noise background in the flow cytometry assays), and in the other two replicates, the cell densities of the UWC1 strain were 3.72 times and 10.67 times more abundant than the KT2440 strain (figure 2*a*, tables 1 and 2). The spatial distribution of the two tagged strains indicated that when inoculated in mixed droplets in the presence of fungal networks, the slower growing KT2440 strain was constrained to the interior of the mixed colony and consequently was not able to disperse through the fungal networks (figure 2*c*; note that only red fluorescence was visible along the fungal hyphae connected to the colony). By contrast, when inoculated in separate droplets, both bacterial strains can efficiently disperse along fungal hyphae networks (figure 2*d*,*e*).

Across all spatial settings, the relative abundance of UWC1 and KT2440 strains differ greatly depending on whether they were inoculated in separate or mixed droplets (figure 2*a*, table 3), showing the importance of the spatial scale of competition in determining the competition outcome and long-term coexistence of the two bacterial strains, in the presence or absence of dispersal networks.

4. Discussion

Our experimental results showed a clear pattern: local competition between the two bacterial strains (treatments with mixed inocula) caused competitive exclusion, while competition at the regional scale (treatments with separate inocula) is more favourable for coexistence. This is consistent with the effect of the spatial scale on the competition outcome found in larger organisms [35,36]. Our results thus help to reconcile the conflicting findings that bacteria [6–8] and protists [50] species/strains that overlap in their niches of resource utilization tend to competitively exclude each other in well-mixed liquid cultures (implying local competition), and the widespread phenomenon of microbial species/strains coexisting while competing for the same resources in spatially complex environment (implying

regional competition), such as cheese rind [11,12], the human gut [13,16] and skin [14]. It is important to note that spatial complexity does not automatically promote biodiversity. The effect of spatial structure crucially depends on the type of interactions between species, and in some cases, adding spatial structure can lead to the breakdown of diversity and competitive exclusion of species that could have coexisted under a well-mixed environment [51–53].

In the current work, we showed that when the competing species are involved in a growth–motility trade-off, spatial structure provided by dispersal networks can help the competing species to coexist. In the presence of dispersal networks, the higher motility of the slower growing strain (KT2440) can confer an advantage only when the initial scale of competition was regional (the two strains were inoculated in separate droplets). Otherwise, the faster growing strain (UWC1) can quickly outgrow the slower growing strain, constraining the latter to the interior of the mixed colony and thus preventing it from dispersing. Instead of comparing the growth rates of the UWC1 and KT2440 strains in isolation, we inferred the growth advantage of the UWC1 strain in direct competition by comparing the log ratios of the cell densities under mixed and separate inoculations in the 'no network' setting, controlling that spatial arrangement was the only difference. Microbial growth rates are highly context dependent. Literature has shown that even when growing in monoculture the relative growth rates of competing species can switch in different environments (e.g. *in vivo* in the host environment and *in vitro* when cultured in microcosms [54]), and the relative growth rates in co-culture can show complex nonlinear patterns with multiple crossings at different initial frequency combinations [22]. Not only the growth rate, the motility of microorganisms is also context dependent and can be sensitive to environmental conditions [55]. Because of the strong association between microbial growth and dispersal rates and their sensitivity to biotic and abiotic environmental factors, it is important to measure them in the same competition context, as we did in the current work.

Note that the significantly higher abundance of the KT2440 strain in the presence of fungal networks when inoculated in separate droplets does not imply that it can competitively exclude the UWC1 strain for three reasons. First, due to the limitations of the experimental system (e.g. the fungal network has already covered the entire Petri dish and could not expand further by the end of 5 days), our results only showed a snapshot of the competition dynamics and therefore have limited power to predict the entire competition trajectory. In addition, we focused on quantifying the relative abundance of cells *outside* the colonies formed by the initial inocula, and thus the result of a higher abundance of the KT2440 cells was limited to cells descended from the dispersed ones, and it is possible that the UWC1 strain has nevertheless reached higher abundance *inside* the initial colony. Finally, our results have shown a consistent growth advantage of the UWC1 strain when competition occurs locally. Therefore, we expect that as soon as the cells of the two strains meet in the dispersal network and engage in direct local competition, the UWC1 strain would overgrow its competitor locally. The competitive advantage of the UWC1 strain in local competition is highly contingent on its ability to block the KT2440 strain from accessing the dispersal network. Unlike diffusible nutrients, space is a non-sharable resource. By occupying specific locations in space, such as the expansion frontiers of a mixed bacterial colony or the locations where a mixed colony meets a dispersal network, the faster growing species (the UWC1 strain in our case) not only prevents its competitor from occupying the same space *per se*, but also deprives it of the opportunity to use a section of space extending from the colony margin [56–58], and in the presence of a dispersal network, also the section of space in the network that is accessible through that location. Existing work has shown that physical interactions play essential roles in shaping the structure of microbial colonies and biofilms [59–61]. In this work, we showed that the spatial occupation of the UWC1 cells at the 'entrance points' of a dispersal network gives them an 'opportunity advantage' to explore and expand to new territories.

The competitive advantage of the KT2440 strain when dispersal is allowed suggests that the growth–motility trade-off plays a role in promoting the coexistence of the two bacterial strains, with the UWC1 strain growing faster under direct competition while the KT2440 is better at dispersing and exploring empty habitats. When competing species are regulated by a trade-off between their rate of reproduction and their ability to disperse, theory predicts that there are conditions where coexistence is possible [62,63]. A previous study with two *P. fluorescens* strains also demonstrated that regional competition in the presence of a growth–dispersal trade-off can promote coexistence [37]. In the aforementioned study, however, dispersal occurred by manually transferring bacterial cells at discrete intervals. Such experimental design, while promoting the controllability of the system and helping to reduce variation between different replicates, is highly artificial and corresponds to natural conditions that only rarely occur (e.g. occasional heavy rains that saturate the soil for a short time [47,64,65]). In this work, we allowed continuous dispersal of the two bacterial strains, either through glass fibre

networks, or fungal mycelial networks that can interact dynamically with the bacteria [66,67]. The bacterial dispersal in our experiments thus corresponds to that in environments such as the typical well-drained soil, where the movement of bacteria is restricted by the thinness and patchiness of the liquid films [68] on the surface of abiotic (e.g. rocks and soil particles) and biotic (e.g. roots and fungal hyphae) components. Despite the additional factors and variation involved, our results showed robustly that interactions at the local scale tend to cause competitive exclusion, while coexistence is more likely when competition is regional.

In this work, the abiotic network was formed by placing thin glass fibres randomly on a Petri dish, while the biotic network was formed by the actively growing fungal hyphae, which follow species-specific structural patterns. The glass fibre network was designed as an abiotic 'control' of the fungal network as in several previous studies [39–43]. However, our work showed that the glass fibre network is not an ideal abiotic substitute for the fungal network, partly because the liquid films formed around glass fibres are much thicker than those surrounding fungal hyphae (electronic supplementary material, figure S6). The thickness of liquid film determines whether cells can disperse solely actively by flagella-propelled swimming or also passively driven by hydraulic flow in the liquid film [69]. The hydraulic flow caused by inoculation may have flushed some KT2440 cells into the dispersal network, leading to a large variation in the competition outcome under the glass fibre treatment. Another factor contributing to the variation could be the randomness of dispersal network created when placing the extremely thin (8 µm in diameter) and brittle glass fibres on the Petri dish (electronic supplementary material, figure S6). Theory and experiments have shown that the network structure and connectivity can shape biodiversity patterns [70,71]. Since we were not able to precisely control the abiotic network structures in the current work, large variations persist in the relative abundance of the two bacterial strains. This also limits our ability to investigate deeper the interactions between network type and different ways of inoculation, for example, by performing a two-factor ANOVA test. Therefore, a valuable next step would be to tease apart the large variations of our current results under the abiotic and biotic network settings by manipulating their structures, for example, by using three-dimensional printed abiotic hyphae models with fixed structure and surface physico-chemical properties, or microfluidic platforms that constrain the growth of fungal hyphae networks into predefined topology [72,73].

5. Conclusion

To conclude, using experiments with two closely related strains of the bacteria *Pseudomonas putida*, we found that spatial scales of competition and the growth–motility trade-off interact to determine the competition outcome. We showed that local competition caused competitive exclusion while regional competition is more favourable for coexistence. The results are consistent with previous findings in animals and plants. Furthermore, we showed that in the presence of dispersal networks, the growth–motility trade-off can promote coexistence only when the scale of competition was regional initially. Only in this case, the slower growing but faster dispersing strain has the opportunity to use the dispersal networks to escape from direct local competition with its faster growing competitor. It is interesting to ask whether the phenomenon we observed in this study may generalize to microbial competition dynamics in other spatially complex environments, where interactions occur at different spatial scales and in the presence of dispersal networks provided by diverse fungi and fungi-like organisms. Therefore, we encourage future work to systematically study the interactions between spatial scales of competition and the growth–motility trade-off between pairs of microorganisms with different phylogenetic relatedness. The current work identified new factors that affect microbial competition dynamics in spatially complex environments—in particular, along dispersal networks provided by fungal hyphae, and raised new questions regarding the roles of network topology and the biotic interactions between fungi and different bacterial strains that disperse along them. Future investigations along these lines would help us delve deeper into the mechanisms that govern microbial competition dynamics and coexistence in spatially complex environments.

Data accessibility. All data supporting the reported results can be found in the data tables in the manuscript and the electronic supplementary materials.

The data are provided in the electronic supplementary material [74].

Authors' contributions. T.K.: data curation, formal analysis, investigation, methodology and visualization; M.M.: data curation, formal analysis, investigation, methodology and visualization; S.B.: conceptualization and writing—review and editing; R.B.: conceptualization and writing—review and editing; A.E.: methodology and writing—review and editing; D.G.:

conceptualization, supervision and writing—review and editing; F.P.: methodology and writing—review and editing; P.J.: conceptualization, funding acquisition, supervision and writing—review and editing; X.-Y.L.R.: conceptualization, funding acquisition, project administration, supervision, writing—original draft and writing—review and editing.

All authors gave final approval for publication and agreed to be held accountable for the work performed therein.

Conflict of interest declaration. We have no competing interests.

Funding. This research was funded by a U.S. Department of Energy Biological and Environmental Research Science Focus Area grant to P.J. (grant no. DE-AC52-06NA25396) and a Swiss National Science Foundation Ambizione grant to X.-Y.L.R. (grant no. PZ00P3_180145).

Acknowledgements. The authors would like to thank Arnaud Dechesne and Jan van der Meer for providing the two bacteria strains. We also thank the associate editor Nicole Hynson and the three anonymous reviewers for their constructive comments and suggestions.

References

1. Van Der Heijden MGA, Bardgett RD, Van Straalen NM. 2008 The unseen majority: soil microbes as drivers of plant diversity and productivity in terrestrial ecosystems. *Ecol. Lett.* **11**, 296–310. (doi:10.1111/j.1461-0248.2007.01139.x)
2. Awasthi A, Singh M, Soni SK, Singh R, Kalra A. 2014 Biodiversity acts as insurance of productivity of bacterial communities under abiotic perturbations. *ISME J.* **8**, 2445–2452. (doi:10.1038/ismej.2014.91)
3. Vandenkoornhuyse P, Quaiser A, Duhamel M, Le Van A, Dufresne A. 2015 The importance of the microbiome of the plant holobiont. *New Phytol.* **206**, 1196–1206. (doi:10.1111/nph.13312)
4. Lozupone CA, Stombaugh JI, Gordon JI, Jansson JK, Knight R. 2012 Diversity, stability and resilience of the human gut microbiota. *Nature* **489**, 220–230. (doi:10.1038/nature11550)
5. Rosshart SP *et al.* 2017 Wild mouse gut microbiota promotes host fitness and improves disease resistance. *Cell* **171**, 1015–1028. (doi:10.1016/j.cell.2017.09.016)
6. Tan J, Pu Z, Ryberg WA, Jiang L. 2015 Resident-invader phylogenetic relatedness, not resident phylogenetic diversity, controls community invasibility. *Am. Nat.* **186**, 59–71. (doi:10.1086/681584)
7. Jiang L, Tan J, Pu Z. 2010 An experimental test of Darwin's naturalization hypothesis. *Am. Nat.* **175**, 415–423. (doi:10.1086/650720)
8. Russel J, Røder HL, Madsen JS, Burmølle M, Sørensen SJ. 2017 Antagonism correlates with metabolic similarity in diverse bacteria. *Proc. Natl Acad. Sci. USA* **114**, 10 684–10 688. (doi:10.1073/pnas.1706016114)
9. Goberna M, Montesinos-Navarro A, Valiente-Banuet A, Colin Y, Gómez-Fernández A, Donat S, Navarro-Cano JA, Verdú M. 2019 Incorporating phylogenetic metrics to microbial co-occurrence networks based on amplicon sequences to discern community assembly processes. *Mol. Ecol. Res.* **9**, 1552–1564. (doi:10.1111/1755-0998.13079)
10. Lentendu G, Dunthorn M. 2021 Phylogenetic relatedness drives protist assembly in marine and terrestrial environments. *Glob. Ecol. Biogeogr.* **30**, 1532–1544. (doi:10.1111/geb.13317)
11. Zhang Y, Kastman EK, Guasto JS, Wolfe BE. 2018 Fungal networks shape dynamics of bacterial dispersal and community assembly in cheese rind microbiomes. *Nat. Commun.* **9**, 336. (doi:10.1038/s41467-017-02522-z)
12. Kastman EK, Kamelamela N, Norville JW, Cosetta CM, Dutton RJ, Wolfe BE. 2016 Biotic interactions shape the ecological distributions of *Staphylococcus* species. *MBio* **7**, e01157-16. (doi:10.1128/mBio.01157-16)
13. Li SS *et al.* 2016 Durable coexistence of donor and recipient strains after fecal microbiota transplantation. *Science (1979)* **352**, 586–589.
14. Oh J, Byrd AL, Deming C, Conlan S, Kong HH, Segre JA. 2014 Biogeography and individuality shape function in the human skin metagenome. *Nature* **514**, 59–64. (doi:10.1038/nature13786)
15. Kreth J, Merritt J, Shi W, Qi F. 2005 Competition and coexistence between *Streptococcus mutans* and *Streptococcus sanguinis* in the dental biofilm. *J. Bacteriol.* **187**, 7193–7203. (doi:10.1128/JB.187.21.7193-7203.2005)
16. Darcy JL, Washburne AD, Robeson MS, Prest T, Schmidt SK, Lozupone CA. 2020 A phylogenetic model for the recruitment of species into microbial communities and application to studies of the human microbiome. *ISME J.* **14**, 1359–1368. (doi:10.1038/s41396-020-0613-7)
17. Hibbing ME, Fuqua C, Parsek MR, Peterson SB. 2010 Bacterial competition: surviving and thriving in the microbial jungle. *Nat. Rev. Microbiol.* **8**, 15–25. (doi:10.1038/nrmicro2259)
18. Wilson M, Lindow SE. 1994 Coexistence among epiphytic bacterial populations mediated through nutritional resource partitioning. *Appl. Environ. Microbiol.* **60**, 4468. (doi:10.1128/aem.60.12.4468-4477.1994)
19. Song W, Kim M, Tripathi BM, Kim H, Adams JM. 2016 Predictable communities of soil bacteria in relation to nutrient concentration and successional stage in a laboratory culture experiment. *Environ. Microbiol.* **18**, 1740–1753. (doi:10.1111/1462-2920.12879)
20. Nuccio EE *et al.* 2020 Niche differentiation is spatially and temporally regulated in the rhizosphere. *ISME J.* **14**, 999–1014. (doi:10.1038/s41396-019-0582-x)
21. Kerr B, Riley MA, Feldman MW, Bohannan BJM. 2002 Local dispersal promotes biodiversity in a real-life game of rock–paper–scissors. *Nature* **418**, 171–174. (doi:10.1038/nature00823)
22. Li XY, Pietschke C, Fraune S, Altrock PM, Bosch TCG, Traulsen A. 2015 Which games are growing bacterial populations playing? *J. R. Soc. Interface* **12**, 20150121. (doi:10.1098/rsif.2015.0121)
23. Harmand N, Federico V, Hindré T, Lenormand T. 2019 Nonlinear frequency-dependent selection promotes long-term coexistence between bacteria species. *Ecol. Lett.* **22**, 1192–1202.
24. Hiltunen T, Kaitala V, Laakso J, Becks L. 2017 Evolutionary contribution to coexistence of competitors in microbial food webs. *Proc. R. Soc. B* **284**, 20170415. (doi:10.1098/rspb.2017.0415)
25. Li XY, Lachnit T, Fraune S, Bosch TCG, Traulsen A, Sieber M. 2017 Temperate phages as self-replicating weapons in bacterial competition. *J. R. Soc. Interface* **14**, 20170563. (doi:10.1098/rsif.2017.0563)
26. Brown SP, Fredrik Inglis R, Taddei F. 2009 SYNTHESIS: evolutionary ecology of microbial wars: within-host competition and (incidental) virulence. *Evol. Appl.* **2**, 32–39. (doi:10.1111/j.1752-4571.2008.00059.x)
27. García-Bayona L, Comstock LE. 2018 Bacterial antagonism in host-associated microbial communities. *Science (1979)* **361**, eaat2456.
28. Granato ET, Meiller-Legrand TA, Foster KR. 2019 The evolution and ecology of bacterial warfare. *Curr. Biol.* **29**, R521–R537. (doi:10.1016/j.cub.2019.04.024)
29. Yi X, Dean AM. 2016 Phenotypic plasticity as an adaptation to a functional trade-off. *Elife* **5**, e19307. (doi:10.7554/eLife.19307)
30. Ni B, Ghosh B, Paldy FS, Colin R, Heimerl T, Sourjik V. 2017 Evolutionary remodeling of bacterial motility checkpoint control. *Cell Rep.* **18**, 866–877. (doi:10.1016/j.celrep.2016.12.088)
31. Fraebel DT, Mickalide H, Schnitkey D, Merritt J, Kuhlman TE, Kuehn S. 2017 Environment determines evolutionary trajectory in a constrained phenotypic space. *Elife* **6**, e24669. (doi:10.7554/eLife.24669)
32. Gude S, Pinçe E, Taute KM, Seinen AB, Shimizu TS, Tans SJ. 2020 Bacterial coexistence driven by motility and spatial competition. *Nature* **578**, 588–592. (doi:10.1038/s41586-020-2033-2)
33. Nadell CD, Bassler BL. 2011 A fitness trade-off between local competition and dispersal in *Vibrio cholerae* biofilms. *Proc. Natl Acad. Sci. USA* **108**, 14 181–14 185. (doi:10.1073/pnas.1111147108)
34. Yawata Y, Cordero OX, Menolascina F, Hehemann JH, Polz MF, Stocker R. 2014

Competition-dispersal tradeoff ecologically differentiates recently speciated marine bacterioplankton populations. *Proc. Natl Acad. Sci. USA* **111**, 5622–5627. (doi:10.1073/pnas.1318943111)

35. Ma C, Li S, Pu Z, Tan J, Liu M, Zhou J, Li H, Jiang L. 2016 Different effects of invader-native phylogenetic relatedness on invasion success and impact: a meta-analysis of Darwin's naturalization hypothesis. *Proc. R. Soc. B* **283**, 20160663. (doi:10.1098/rspb.2016.0663)
36. Park DS, Feng X, Maitner BS, Ernst KC, Enquist BJ. 2020 Darwin's naturalization conundrum can be explained by spatial scale. *Proc. Natl Acad. Sci. USA* **117**, 10 904–10 910. (doi:10.1073/pnas.1918100117)
37. Livingston G, Matias M, Calcagno V, Barbera C, Combe M, Leibold MA, Mouquet N. 2012 Competition-colonization dynamics in experimental bacterial metacommunities. *Nat. Commun.* **3**, 1234. (doi:10.1038/ncomms2239)
38. Kohlmeier S, Smits THM, Ford RM, Keel C, Harms H, Wick LY. 2005 Taking the fungal highway: mobilization of pollutant-degrading bacteria by fungi. *Environ. Sci. Technol.* **39**, 4640–4646. (doi:10.1021/es047979z)
39. Pion M, Bshary R, Bindschedler S, Filippidou S, Wick LY, Job D, Junier P. 2013 Gains of bacterial flagellar motility in a fungal world. *Appl. Environ. Microbiol.* **79**, 6862–6867. (doi:10.1128/AEM.01393-13)
40. Schamfuß S, Neu TR, van der Meer JR, Tecon R, Harms H, Wick LY. 2013 Impact of mycelia on the accessibility of fluorene to PAH-degrading bacteria. *Environ. Sci. Technol.* **47**, 6908–6915. (doi:10.1021/es304378d)
41. Otto S, Banitz T, Thullner M, Harms H, Wick LY. 2016 Effects of facilitated bacterial dispersal on the degradation and emission of a desorbing contaminant. *Environ. Sci. Technol.* **50**, 6320–6326. (doi:10.1021/acs.est.6b00567)
42. Worrich A *et al.* 2016 Bacterial dispersal promotes biodegradation in heterogeneous systems exposed to osmotic stress. *Front. Microbiol.* **7**, 1214. (doi:10.3389/fmicb.2016.01214)
43. Bravo D, Cailleau G, Bindschedler S, Simon A, Job D, Verrecchia E, Junier P. 2013 Isolation of oxalotrophic bacteria able to disperse on fungal mycelium. *FEMS Microbiol. Lett.* **348**, 157–166. (doi:10.1111/1574-6968.12287)
44. Regenhardt D, Heuer H, Heim S, Fernandez DU, Strömpl C, Moore ERB, Timmis KN. 2002 Pedigree and taxonomic credentials of *Pseudomonas putida* strain KT2440. *Environ. Microbiol.* **4**, 912–915. (doi:10.1046/j.1462-2920.2002.00368.x)
45. McClure NC, Weightman AJ, Fry JC. 1989 Survival of *Pseudomonas putida* UWC1 containing cloned catabolic genes in a model activated-sludge unit. *Appl. Environ. Microbiol.* **55**, 2627–2634. (doi:10.1128/aem.55.10.2627-2634.1989)
46. Rochat L, Péchy-Tarr M, Baehler E, Maurhofer M, Keel C. 2010 Combination of fluorescent reporters for simultaneous monitoring of root colonization and antifungal gene expression by a biocontrol pseudomonad on cereals with flow cytometry. *Mol. Plant Microbe Interact.* **23**, 949–961. (doi:10.1094/MPMI-23-7-0949)
47. Dechesne A, Wang G, Gülez G, Or D, Smets BF. 2010 Hydration-controlled bacterial motility and dispersal on surfaces. *Proc. Natl Acad. Sci. USA* **107**, 14 369–14 372. (doi:10.1073/pnas.1008392107)
48. Benjamini Y, Hochberg Y. 1995 Controlling the false discovery rate: a practical and powerful approach to multiple testing. *J. R. Stat. Soc.* **57**, 289–300. (doi:10.1111/j.2517-6161.1995.tb02031.x)
49. R Core Team. 2021 *R: a language and environment for statistical computing*. Vienna, Austria: R Foundation for Statistical Computing. See https://www.R-project.org/.
50. Violle C, Nemergut DR, Pu Z, Jiang L. 2011 Phylogenetic limiting similarity and competitive exclusion. *Ecol. Lett.* **14**, 782–787. (doi:10.1111/j.1461-0248.2011.01644.x)
51. Saxer G, Doebeli M, Travisano M. 2009 Spatial structure leads to ecological breakdown and loss of diversity. *Proc. R. Soc. B* **276**, 2065–2070. (doi:10.1098/rspb.2008.1827)
52. Weiner BG, Posfai A, Wingreen NS. 2019 Spatial ecology of territorial populations. *Proc. Natl Acad. Sci. USA* **116**, 17 874–17 879. (doi:10.1073/pnas.1911570116)
53. Lowery NV, Ursell T. 2019 Structured environments fundamentally alter dynamics and stability of ecological communities. *Proc. Natl Acad. Sci. USA* **116**, 379–388. (doi:10.1073/pnas.1811887116)
54. Deines P, Hammerschmidt K, Bosch TCG. 2020 Microbial species coexistence depends on the host environment. *MBio* **11**, e00807-20. (doi:10.1128/mBio.00807-20)
55. Ni B, Colin R, Link H, Endres RG, Sourjik V. 2020 Growth-rate dependent resource investment in bacterial motile behavior quantitatively follows potential benefit of chemotaxis. *Proc. Natl Acad. Sci. USA* **117**, 595–601. (doi:10.1073/pnas.1910849117)
56. Hallatschek O, Hersen P, Ramanathan S, Nelson DR. 2007 Genetic drift at expanding frontiers promotes gene segregation. *Proc. Natl Acad. Sci. USA* **104**, 19 926–19 930. (doi:10.1073/pnas.0710150104)
57. Hallatschek O, Nelson DR. 2010 Life at the front of an expanding population. *Evolution (N Y)* **64**, 193–206.
58. Farrell FD, Gralka M, Hallatschek O, Waclaw B. 2017 Mechanical interactions in bacterial colonies and the surfing probability of beneficial mutations. *J. R. Soc. Interface* **4**, 20170073. (doi:10.1098/rsif.2017.0073)
59. Doumic M, Hecht S, Peurichard D. 2020 A purely mechanical model with asymmetric features for early morphogenesis of rod-shaped bacteria micro-colony. *Math. Biosci. Eng.* **17**, 6873–6908. (doi:10.3934/mbe.2020356)
60. Maier B. 2021 How physical interactions shape bacterial biofilms. *Annu. Rev. Biophys.* **50**, 401–417. (doi:10.1146/annurev-biophys-062920-063646)
61. Warren MR, Sun H, Yan Y, Cremer J, Li B, Hwa T. 2019 Spatiotemporal establishment of dense bacterial colonies growing on hard agar. *Elife* **8**, e41093. (doi:10.7554/eLife.41093)
62. Levins R, Culver D. 1971 Regional coexistence of species and competition between rare species. *Proc. Natl Acad. Sci. USA* **68**, 1246–1248. (doi:10.1073/pnas.68.6.1246)
63. Yu DW, Wilson HB. 2001 The competition-colonization trade-off is dead; long live the competition-colonization trade-off. *Am. Nat.* **158**, 49–63. (doi:10.1086/320865)
64. Šťovíček A, Azatyan A, Soares MIM, Gillor O. 2017 The impact of hydration and temperature on bacterial diversity in arid soil mesocosms. *Front. Microbiol.* **8**, 1078. (doi:10.3389/fmicb.2017.01078)
65. Šťovíček A, Kim M, Or D, Gillor O. 2017 Microbial community response to hydration-desiccation cycles in desert soil. *Sci. Rep.* **7**, 45735. (doi:10.1038/srep45735)
66. Deveau A *et al.* 2018 Bacterial–fungal interactions: ecology, mechanisms and challenges. *FEMS Microbiol. Rev.* **42**, 335–352. (doi:10.1093/femsre/fuy008)
67. Pion M, Spangenberg JE, Simon A, Bindschedler S, Flury C, Chatelain A, Bshary R, Job D, Junier P. 2013 Bacterial farming by the fungus *Morchella crassipes*. *Proc. R. Soc. B* **280**, 20132242. (doi:10.1098/rspb.2013.2242)
68. Or D, Smets BF, Wraith JM, Dechesne A, Friedman SP. 2007 Physical constraints affecting bacterial habitats and activity in unsaturated porous media – a review. *Adv. Water Res.* **30**, 1505–1527. (doi:10.1016/j.advwatres.2006.05.025)
69. Kuhn T, Buffi M, Bindschedler S, Chain P, Gonzalez D, Stanley C, Wick L, Junier P, Richter XYL. 2022 Design and construction of 3D printed devices to investigate active and passive bacterial dispersal on hydrated surfaces. *BMC Biol.* **20**, 203. (doi:10.1186/s12915-022-01406-z)
70. Altermatt F, Fronhofer EA. 2018 Dispersal in dendritic networks: ecological consequences on the spatial distribution of population densities. *Freshw. Biol.* **63**, 22–32. (doi:10.1111/fwb.12951)
71. Carrara F, Altermatt F, Rodriguez-Iturbe I, Rinaldo A. 2012 Dendritic connectivity controls biodiversity patterns in experimental metacommunities. *Proc. Natl Acad. Sci. USA* **109**, 5761–5766. (doi:10.1073/pnas.1119651109)
72. Aleklett K, Ohlsson P, Bengtsson M, Hammer EC. 2021 Fungal foraging behaviour and hyphal space exploration in micro-structured Soil Chips. *ISME J.* **15**, 1782–1793.(doi:10.1038/s41396-020-00886-7)
73. Gimeno A *et al.* 2021 A versatile microfluidic platform measures hyphal interactions between *Fusarium graminearum* and *Clonostachys rosea* in real-time. *Commun. Biol.* **4**, 262. (doi:10.1038/s42003-021-01767-1)
74. Kuhn T, Mamin M, Bindschedler S, Bshary R, Estoppey A, Gonzalez D, Palmieri F, Junier P, Richter XYL. 2022 Spatial scales of competition and a growth–motility trade-off interact to determine bacterial coexistence. Figshare. (doi:10.6084/m9.figshare.c.6316842)

Chapter one supplementary materials

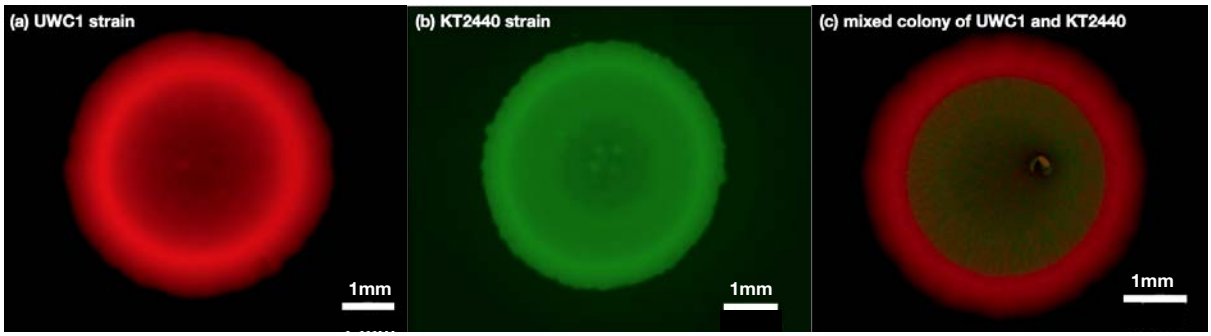

Figure S1. The UWC1 and KT2440 strains in separate or mixed colonies in the absence of a dispersal network. The pictures were taken with an epifluorescence microscope 2 days after inoculation.

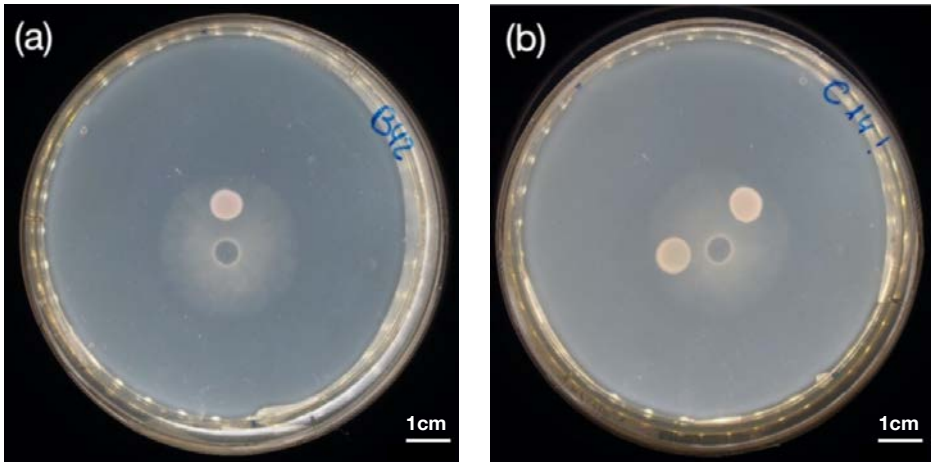

Figure S2. Two examples of Petri dishes with bacteria and the fungus *Trichoderma rossicum* showing that the latter has already grown passed the bacterial inocula after 24h of growth, either in the case of a single bacterial inoculum (panel a, bacterial strain was UWC1) or two separated inocula (panel b, bacterial strains were UWC1 and KT2440). The pictures were taken after having removed the fungal inoculum plug.

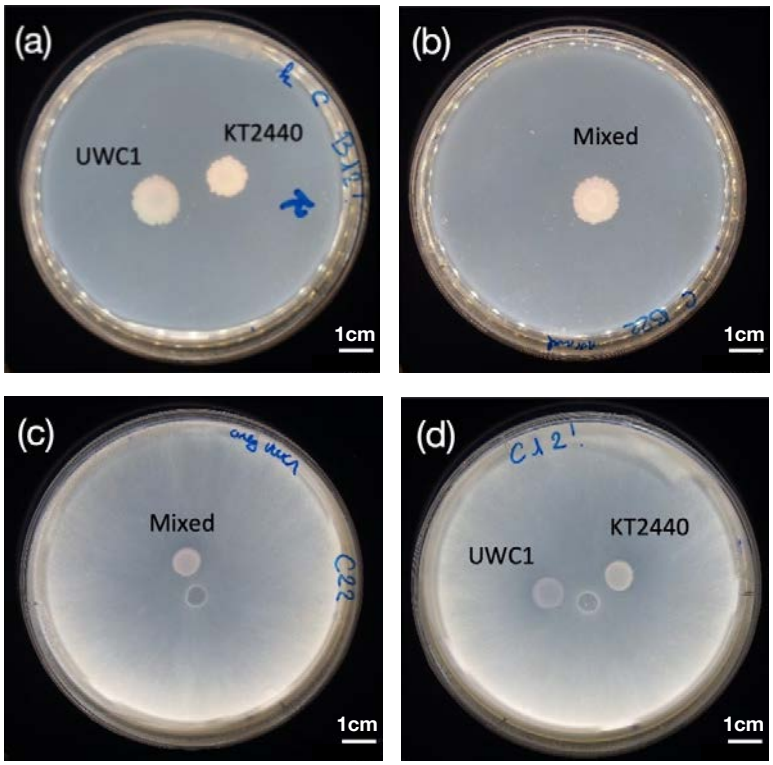

Figure S3. Examples of Petri dishes after 5 days of growth showing that the margins of the bacterial colonies remain separate at the end of the experiments. Dispersal networks formed by the fungus *Trichoderma rossicum* were absent in panels (a) and (b), and present in panels (c) and (d).

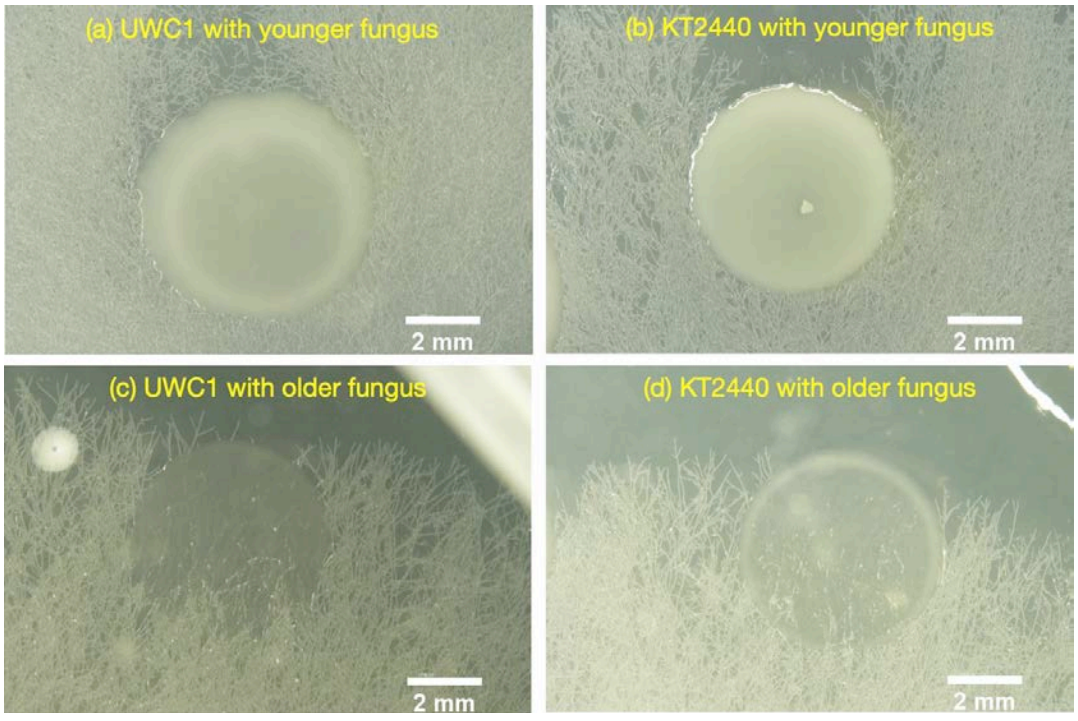

Figure S4. Bright field photos of the colonies of the UWC1 and KT2440 strains in the presence of younger (2 days) and older (5 days) fungal networks. The younger fungus does not invade the bacterial colonies, while the older fungus penetrated the colonies of both bacterial strains.

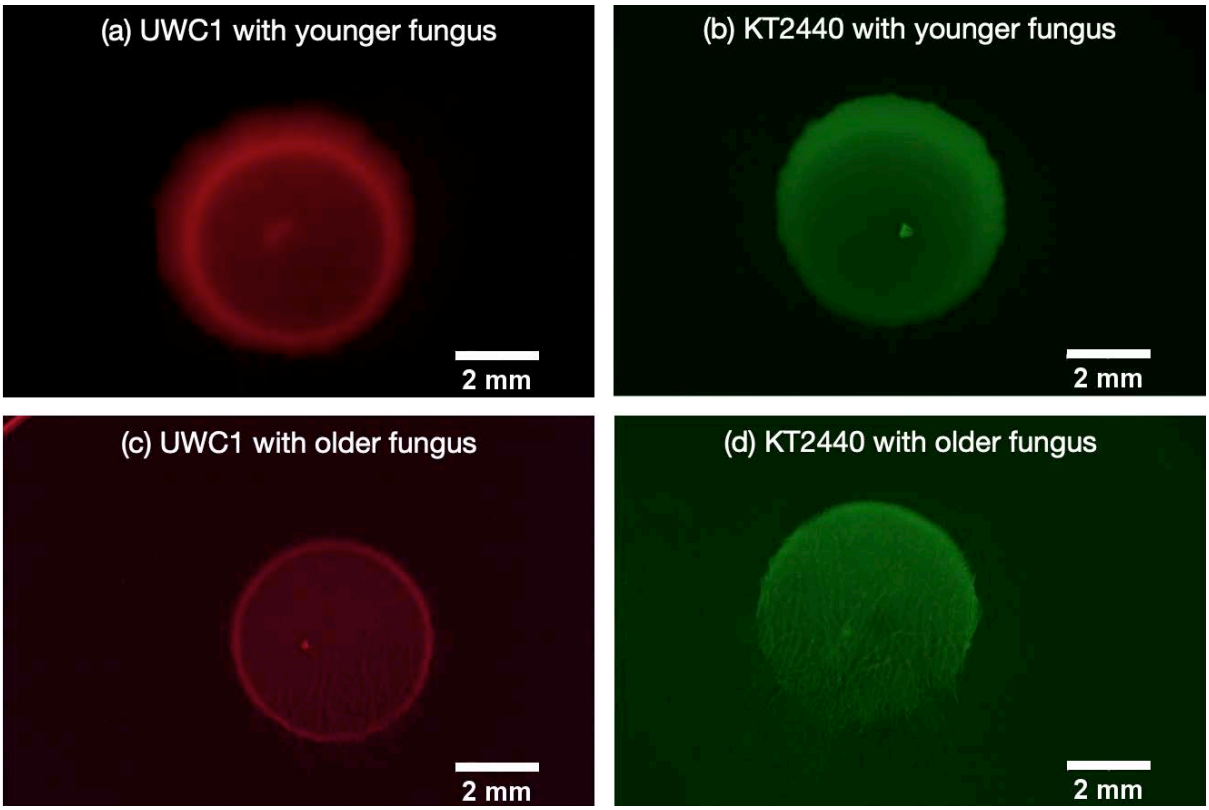

Figure S5. Pictures of the same plates as in Figure S3 taken with epifluorescence microscopy, showing the spatial distribution of bacterial cells along fungal hyphae networks. The UWC1 strain can spread efficiently on younger fungal networks, without the fungal hyphae penetrating the colony (panel a), but it spread less well on older fungal networks (panel c), despite that the fungal network has penetrated the colony. The effects of younger and older fungus were the opposite for the KT2440 strain – bacterial cells did not spread on the networks of younger fungus (panel b), but dispersed efficiently along the networks of older fungus that penetrated the bacterial colony (panel d).

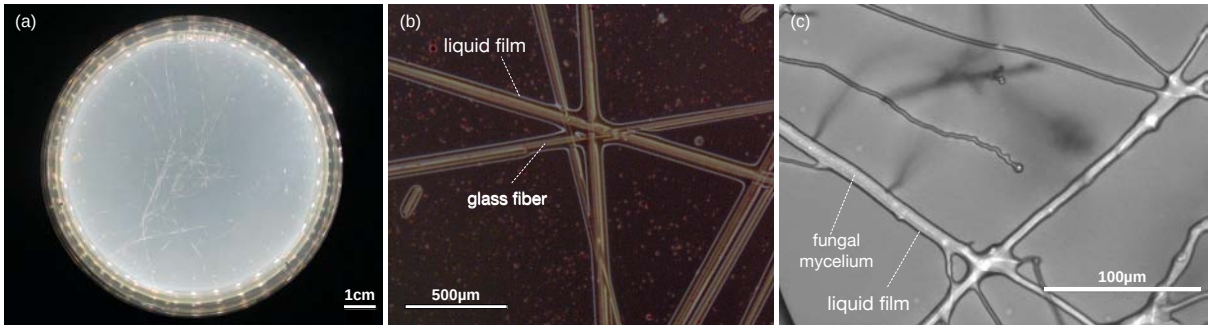

Figure S6. (a) Picture of a glass fiber network placed on the culturing medium in a Petri dish. Around 30 pieces of fine (8 μm diameter) glass fibers were distributed randomly to form the network. (b) Relatively thick liquid films form along the surface of glass fibers. (c) Thin liquid films form along the surface of fungal mycelia.

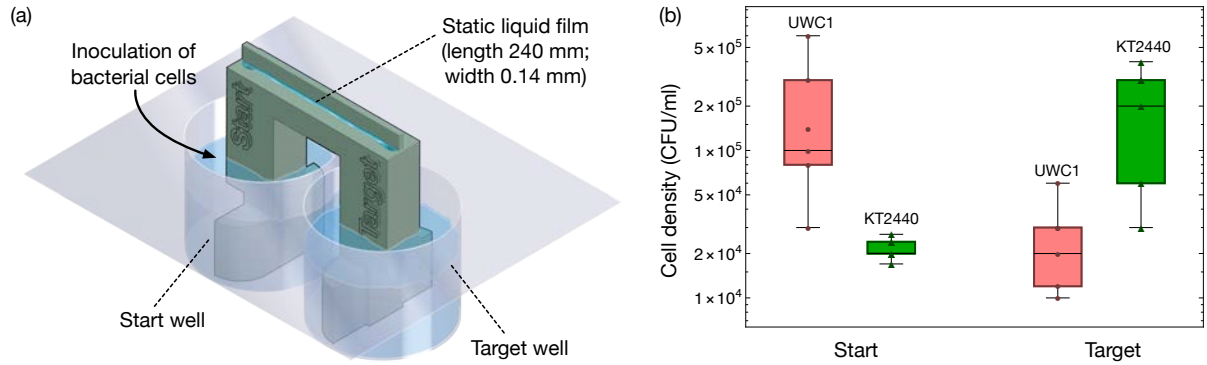

Figure S7. (a) Illustration of the design of bacterial motility assay. 5 μl cell suspension of the UWC1 or KT2440 strain (adjusted to an optical density of one) were added to the start well of the "bacterial bridge" device (described in detail in Kuhn *et al*, 2022), where two medium reservoirs were connected by a static liquid film through two vertical capillaries. The culture medium contained 0.01 M PBS with 1% of NB and 1% of Ficoll (10g/L, Sigma-Aldrich). Due to a lack of hydraulic flow in the liquid film, bacterial cells can move from the start well to the target well only by active flagella-propelled swimming. Cell densities in the start and target wells were measured 72 hours after inoculation. Experiments for each strain have six independent replicates. (b) Box-Whisker charts showing the cell densities in the start and target wells at the end of experiments. More cells of the KT2440 strain dispersed from the start well to the target well than cells of the UWC1 strain (p = 0.025, Student t-test).

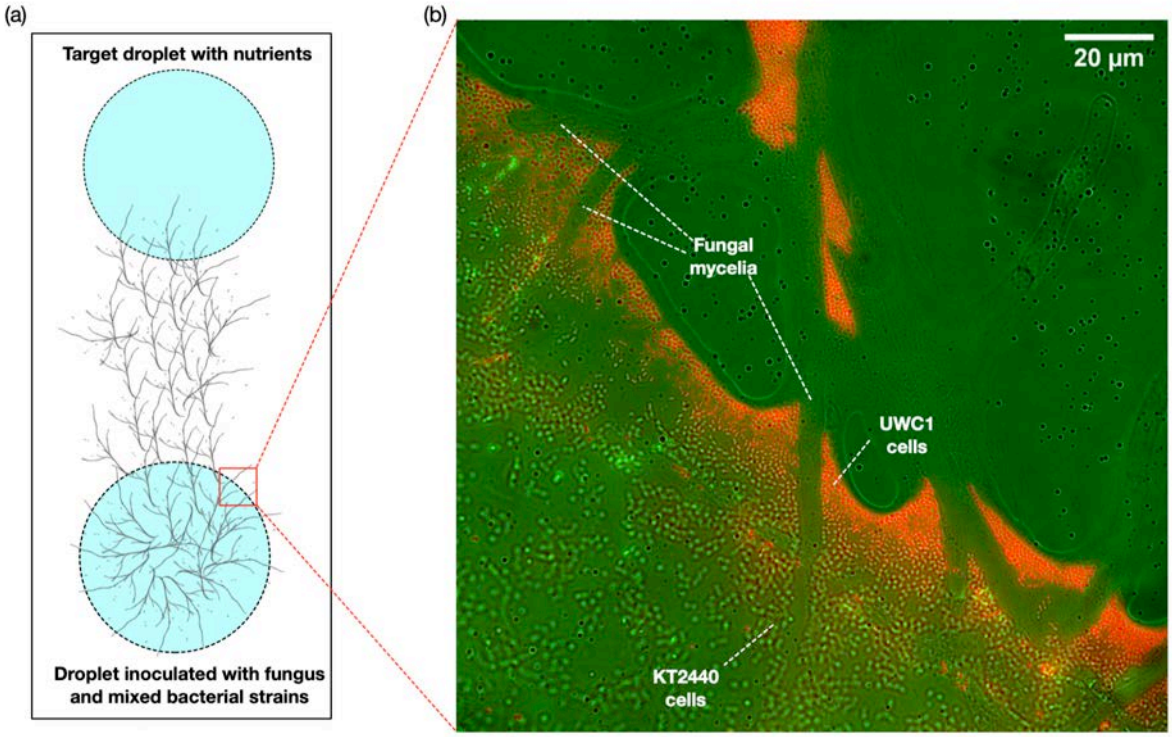

Figure S8. (a) Illustration of bacterial dispersal in the fungal network on a glass slide. The oomycete *Pythium ultimum* and a 1:1 mixture of *Pseudomonas putida* KT2440 and UWC1 cells were inoculated in a droplet of NB medium. Within 72 hours, the hyphal network has reached a separate target droplet. (b)Epifluorescence microscopic picture showing the advantage of the UWC1 strain (red cells) in accessing the fungal mycelial network on the glass slide. The upper left — lower right diagonal of the figure corresponds to the margin of the source droplet where the fungus and bacterial strains were inoculated. The picture was taken 72 hours after inoculation.

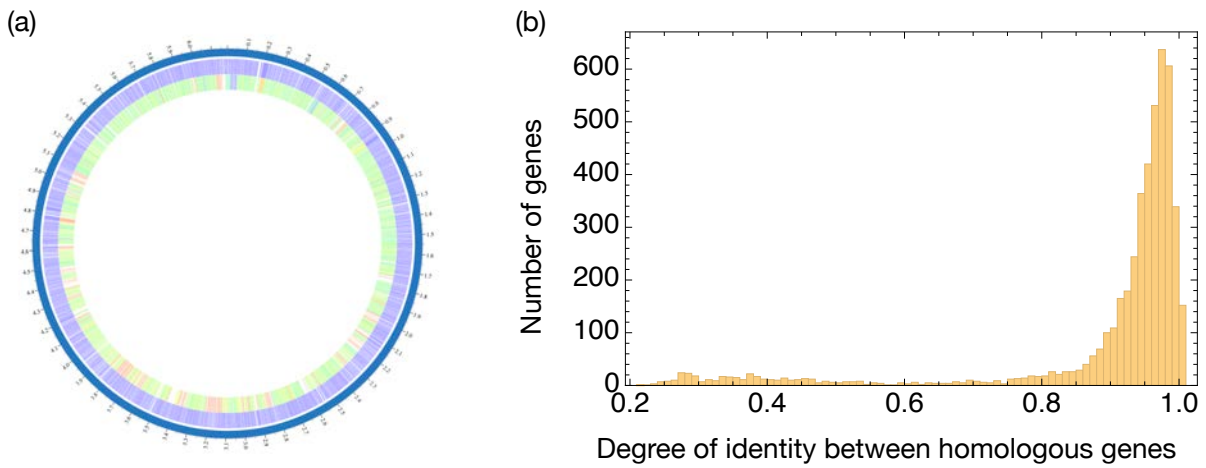

Figure S9. (a) A snapshot of the genome comparison between the KT2440 and UWC1 strains. Annotated reference genome *P. putida* KT2440 (Taxonomy ID: 160488) was compared to annotated representative genome *P. putida* NBRC 14164 (synonymous to strain UWC1; Taxonomy ID: 1407054) using the proteome comparison tool provided by (https://patricbrc.org; Davis et al, 2020). Both genomes have annotated versions already available on the NCBI genome database website. The color scale from purple to red represents genome identity from high to low. The tracks from outside to inside are the KT2440 and UWC1 strains, respectively. See supplementary file "genome_comparison.pdf" and supplementary table "genome_comparison_table.xls" for detailed information. (b) Histogram of the identity levels between homologous genes. The chart represents a total of 4691 genes.

References

Kuhn, Thierry, et al. "Design and construction of 3D-printed devices to investigate active and passive bacterial dispersal on hydrated surfaces." bioRxiv (2022). DOI: https://doi.org/10.1101/2022.05.16.492069

Davis JJ et al. 2020 The PATRIC Bioinformatics Resource Center: expanding data and analysis capabilities. Nucleic Acids Research 48, D606–D612.

Chapter two

Contribution to Chapter two

In the second chapter, I designed, developed and produced two new devices. I ran all the experiments and collected all the data in this chapter. With the support of Xiang-Yi Richter, I wrote the manuscript and answered the reviewers. The accepted author manuscript of Kuhn et al. 2022 appears on the following pages.

Summary Chapter two

In the second chapter, we create devices missing during our investigation of spatial avoidance in the first chapter. We used the 3d-printer's ability to develop and design the missing devices to be able to investigate dispersal in liquid film independently from FH.

We designed, and 3D printed two devices establishing stable liquid films that support bacteria dispersal without biotic interactions. The trail device has a thick liquid layer, while the bridge device has a small one. The thick liquid layer of the trail device enables hydraulic flow capable of transporting non-motile cells. The absence of flow in the bridge device only enables motile cells to disperse in the presence of an energy source. Non-motile cells could not disperse autonomously without flow but dispersed as "hitchhikers" when co-inoculated with motile cells. Our results show the potential of 3D printing in microbiology. Furthermore, the two devices allow for studying dispersal in a liquid layer in a controlled abiotic system.

Design and Construction of 3D printed devices to investigate active and passive bacterial dispersal on hydrated surfaces

Thierry Kuhn[1], Matteo Buffi[1], Saskia Bindschedler[1], Patrick S. Chain[2], Diego Gonzalez[1], Claire E. Stanley[3], Lukas Y. Wick[4], Pilar Junier[1*] and Xiang-Yi Li Richter[1*]

Abstract

Background: To disperse in water-unsaturated environments, such as the soil, bacteria rely on the availability and structure of water films forming on biotic and abiotic surfaces, and, especially, along fungal mycelia. Dispersal along such "fungal highways" may be driven both by mycelial physical properties and by interactions between bacteria and fungi. However, we still do not have a way to disentangle the biotic and abiotic elements.

Results: We designed and 3D printed two devices establishing stable liquid films that support bacteria dispersal in the absence of biotic interactions. The thickness of the liquid film determined the presence of hydraulic flow capable of transporting non-motile cells. In the absence of flow, only motile cells can disperse in the presence of an energy source. Non-motile cells could not disperse autonomously without flow but dispersed as "hitchhikers" when co-inoculated with motile cells.

Conclusions: The 3D printed devices can be used as an abiotic control to study bacterial dispersal on hydrated surfaces, such as plant roots and fungal hyphae networks in the soil. By teasing apart the abiotic and biotic dimensions, these 3D printed devices will stimulate further research on microbial dispersal in soil and other water-unsaturated environments.

Keywords: 3D printing, Bacterial motility, Bacterial-fungal interactions, Fungal highways, Bacterial dispersal, Hitchhiking dispersal

Background

Spatial structure and physicochemical properties of microbial habitats strongly influence the composition and the ecological functions of microbial communities [1]. This is evident in water-unsaturated environments such as soils, where the combination of an unequal distribution of resources and the restricted movement of bacteria are often factors limiting their activity, as exemplified by the poor degradation of organic pollutants in soil ecosystems [2, 3]. Limited dispersal is particularly significant in the case of bacteria, as most types of active dispersal require liquid films at the interface of biotic and abiotic surfaces [4, 5]. Due to a lack of dispersal pathways in the form of continuous liquid films in water-unsaturated environments, the colonization and redistribution of bacteria to suitable habitats are restricted by their effective motility. In contrast to bacteria, dispersal limitation in water-unsaturated habitats is less of a problem for filamentous fungi [6]. Fungal mycelia extend readily in soils, colonizing also larger, air-filled pores that hinder bacterial dispersal most severely [7, 8]. Fungal mycelia can reach up to a total length of 10^2 m/g, 10^3 m/g, and

*Correspondence: pilar.junier@unine.ch; li@evolbio.mpg.de

[1] Institute of Biology, University of Neuchâtel, CH-2000 Neuchâtel, Switzerland
Full list of author information is available at the end of the article

10^4 m/g in arable, pasture, and forest soils, respectively [9, 10], providing a highly efficient and ubiquitous three-dimensional connective scaffold.

In recent years, several studies have shown that motile bacteria can utilize the continuous liquid films on the surface of likely hydrophilic and semi-hydrophobic hyphal networks to disperse, using so-called "fungal highways" [11–15]. Fungal networks are, however, not only a physical support resembling the highway system built by humans. Instead, hyphal networks continuously grow, reshape, and interact dynamically with the biotic and abiotic environment, including bacteria that disperse across them [16, 17]. The diverse interactions between bacteria and fungi on these fungal highways remain difficult to study, partly due to the intertwining roles of fungi as both providers of a dispersal network and active biological players. For instance, one important aspect of fungal highways is that it requires bacteria to actively disperse on the network. This may occur using one of the motility types described so far: swimming and swarming, which rely on extracellular filamentous appendages, or other forms of dispersal such as crawling, gliding, or twitching [18]. However, to date, the relative importance of these different motility types in navigating on the fungal highway is still unknown. Also, several mechanisms occurring as a result of or triggered by fungal highways dispersal could be better studied if the physical and biological properties of the dispersal network could be teased apart. This includes investigating the role of chemotaxis [19], cell-to-cell signaling [14, 19, 20], germination of dormant cells [21], gene transfer [22], or co-metabolism [3, 11, 12, 23], all of which have been observed in previous studies involving fungal highways. While glass fiber networks have been previously used to study such interactions [8, 12, 24], the rapid development of 3D printing technologies, including miniaturization, provides us with the opportunity to make customized devices to study the physical component of fungal networks. By studying bacterial dispersal on 3D printed models of fungal highways that provide a water film of defined properties (thickness, presence or absence of hydraulic flow), we can separate the part fungal mycelia play as a dispersal scaffold from the potential biotic interactions they exert on dispersing bacteria.

In this work, we designed two devices that reproduce a liquid-surface interface in the form of a meniscus, of varying thickness, as it may be found in hydrophilic soil surfaces or along fungal hyphae. The first device, which we term the "bacterial trail" can establish a relatively wide liquid film of 1.35 mm in lateral depth. The second device, which we term the "bacterial bridge" can establish much narrower liquid films of 0.14 mm in lateral depth. Motile bacterial cells dispersed in the liquid films in both devices. Non-motile cells were unable to disperse alone in the liquid film on the bacterial bridge device, but they could disperse (probably as "hitchhikers" [14, 18, 25, 26]) in the presence of motile cells. Our devices lay a cornerstone for future investigations concerning microbial dispersal in natural unsaturated environments such as the soil and can be used to investigate the diverse and dynamic interactions between soil microorganisms occurring on fungal highways [18, 27]. They also serve as a proof of principle of the vast potential of applying 3D printing technologies to rapidly design, prototype, and produce customized tools in modern biology labs and their particular application in microbial ecology [28].

Results

Design and 3D printing of the devices

We designed two devices in an attempt to represent fungal hyphae under different water-saturation conditions. Printed parts can nowadays reach a resolution of 50 µm on the *x*- and *y*-axes and a resolution between 25 µm to 100 µm on the *z*-axis [29]; this is however still far from the real dimensions of a fungal hypha (typically hyphae are reported to have diameters on the order of 1–30 µm [30]). To replicate the liquid film formed by surface tension next to a hypha, we relied on a bar-shaped structure printed with a hydrophilic resin capable of maintaining a continuous liquid meniscus when connected to liquid reservoirs. In the first device, the "bacterial trail" (hereafter "trail" for brevity), the bar is placed on top of eight discrete liquid reservoirs (Fig. 1a); the "trail" device corresponds to wet conditions, where the liquid films forming on hydrophilic surfaces would be relatively thick (see below). The inoculation and end sampling wells were located directly below the bar along the longitudinal axis of the device. The other sampling wells (numbered from 1 to 6) were positioned to the sides of the bar, served to maintain a uniform thickness of the liquid film, and can also be used for sampling. In the liquid film on the "trail" device, small volume changes during inoculation or sampling can generate flow caused by pressure differences between the sampling wells, which may be able to transport non-motile particles such as bacterial cells and virus particles that do not have the ability to disperse actively. In the second device, the "bacterial bridge" (hereafter "bridge" for brevity), the bar mimicking fungal hyphae is placed at the top of two capillaries of 1 mm in diameter and 15 mm in height connected to two liquid reservoirs (interchangeable start and end sampling wells) (Fig. 1b); this device corresponds to water-limiting conditions where the liquid films are thinner and less susceptible to disturbance by volumetric changes in the reservoir, despite being continuous along the hydrophilic surface [31, 32]. In this way, the water film was also created and

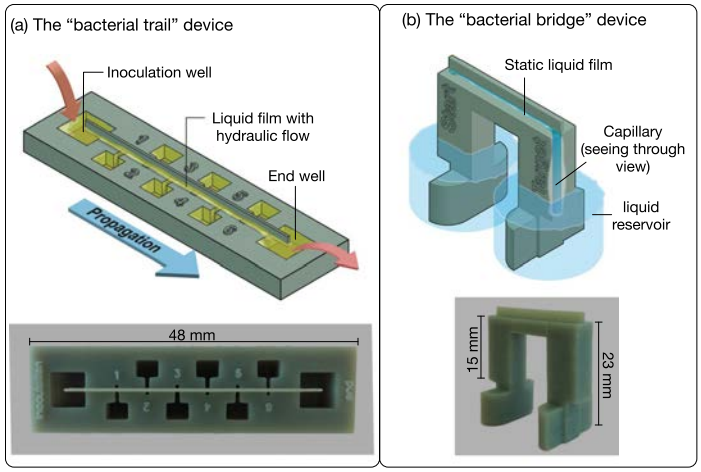

Fig. 1 Cartoon illustrations and photos of the "bacterial trail" and "bacterial bridge" devices. The dimensions of different parts of the two devices are provided in the detailed CAD illustrations in Additional file 1: Fig. S1. In the "trail" device (**a**), a bar-shaped support structure connects eight liquid reservoirs, including an inoculation well, an end sampling well, and six intermediate sampling wells. In the "bridge" device (**b**), the support structure to form liquid films is located on the top of two capillaries of 1 mm in diameter and 15 mm in length

maintained by surface tension, but in contrast to the "trail" device, sampling or changes in the volume of the liquid in the reservoirs did not generate flow. The dimensions of different parts of the two devices are provided in the detailed computer-aided design (CAD) illustrations in Additional file 1: Fig. S1. The two devices were 3D printed using a masked stereolithography (MSLA) printer. Corresponding Standard Tessellation Language—STL—files are provided in Additional files 2 and 3. The printing material has the desirable properties of being hydrophilic (with a contact angle of 52.8°, measured using a snake-based approach [33]), autoclavable, and biocompatible (Additional file 1: Table S1 and Fig. S2). Detailed printing and subsequent preparation procedures are provided in the Methods.

Characterization of the liquid films formed on the 3D printed devices

We generated liquid films on the "trail" and "bridge" devices (Fig. 2) following the procedures shown in the videos in Additional files 4 and 5 and described in the Methods. To control for the consistency of liquid film thickness (lateral depth), we measured the liquid films on four independently printed devices of each type at nine different locations on each device (Fig. 2, Box-Whisker charts). The liquid film lateral depth did not differ significantly between devices of the same type by pairwise *Z*-tests with a threshold *p*-value of 0.0083 (six pairwise comparisons for each device) adjusted using the Bonferroni correction (Additional file 1: Table S2). Across the "trail" devices, the liquid film had a lateral depth of 1.35 ± 0.32 mm ($n = 4$). Across "bridge" devices, the liquid film had a lateral depth of 0.14 ± 0.04 mm ($n = 4$), approximately one tenth of the liquid film lateral depth on the "trail" devices. The liquid film width on the "bridge" device can be adjusted by varying the length of liquid columns in the capillaries, which can be achieved by adding different volumes of liquid to the reservoirs (Additional file 1: Fig. S3). However, attention must be paid as the thinner the liquid film is, the more likely it will break during the duration of bacterial dispersal experiments if those last several days. The broader liquid film on the "trail" device allows flow caused by hydraulic pressure differences between the sampling wells. Using fluorescein as a marker, we measured the flow rate as the mean speed of marker transportation in the flow (1.19 mm/h, Additional file 1: Fig. S4, Additional files 6 and 7). In contrast, the narrower liquid films on the "bridge" device and the vertical capillaries connecting the liquid films to the sampling wells effectively suppressed flow caused by disturbances to the liquid in the sampling wells. We found that the traveling speed of fluorescein from the start well to the

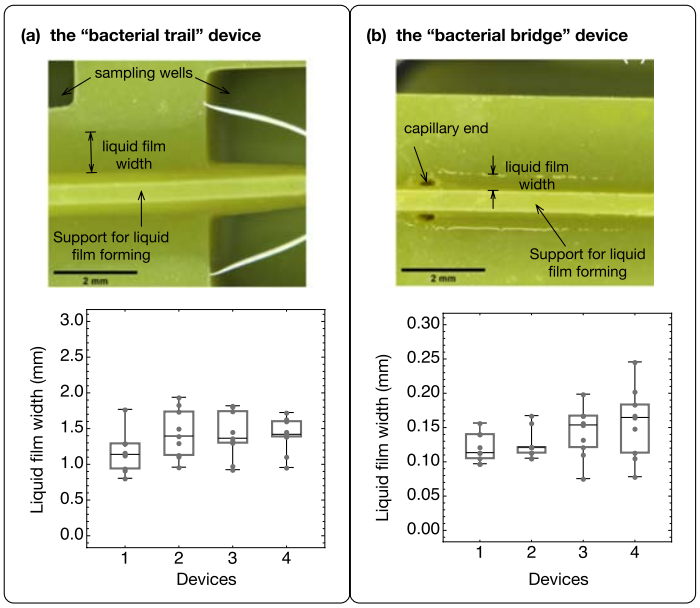

Fig. 2 Stereoscopic pictures of the liquid film on the "bacterial trail" (**a**) and "bacterial bridge" (**b**) devices and the distribution of the liquid film widths on four independently printed devices of each type. The photograph in each panel shows a typical stereoscopic image of the liquid films on the corresponding device. For each of the four devices of each type, a total of nine measurements of the liquid film width were measured and overlaid with the corresponding box-whisker chart. The middle line in each chart shows the median of the data points; the upper and lower boundaries of the boxes mark the 25% and 75% quantiles of the data. The liquid film widths do not differ significantly within a device type

end well can be explained by diffusion alone, suggesting the absence of hydraulic flow (Additional file 1: Fig. S4).

Active and passive dispersal in the liquid films on the two 3D printed devices

We used *Pseudomonas putida* KT2440 and its Δ*fliM* non-motile mutant strain to test the active and passive dispersal of cells in the liquid films on the "trail" and "bridge" devices.

Experiments with the "trail" device

Because of the presence of hydraulic flow in the liquid films on the "trail" device, we hypothesized that both strains could passively disperse from the inoculation well to other sampling wells driven by the flow. In addition, we expected the motile strains to have a dispersal advantage due to their ability to swim when sufficient energy sources are present in the environment. To test these hypotheses, we performed experiments under a full factorial design with the two bacterial strains (motile and non-motile), a culturing medium [nutrient broth (NB) that contains the required nutrients for active dispersal and cell replication, and phosphate-buffered saline (PBS) solution, which does not contain any usable energy source], and two dispersal durations (4 h and 24 h), each with four replicates. At the start of the experiments, we inoculated 5 µl cell suspension (at an optical density of one) of either strain in the inoculation well. The cell density in each sampling well was quantified at the end of the corresponding dispersal duration (Fig. 3a, b). To establish the relative contribution of growth versus dispersal, we compared the growth curves of the two strains in NB and PBS (Fig. 3c).

For both dispersal durations, there was a general trend of decreasing cell densities at larger distances to the inoculation well. Robust two-way ANOVA tests showed that the density of cells differed significantly across sampling wells after 4 h ($p = 0.002$ for in NB and $p = 0.06$ in PBS) and after 24 h ($p < 0.001$ in NB and in PBS) of dispersal. The cell densities did not differ significantly between the motile and non-motile strains in either condition ($p = 0.299$ in NB and $p = 0.585$ in PBS) after 4 h of

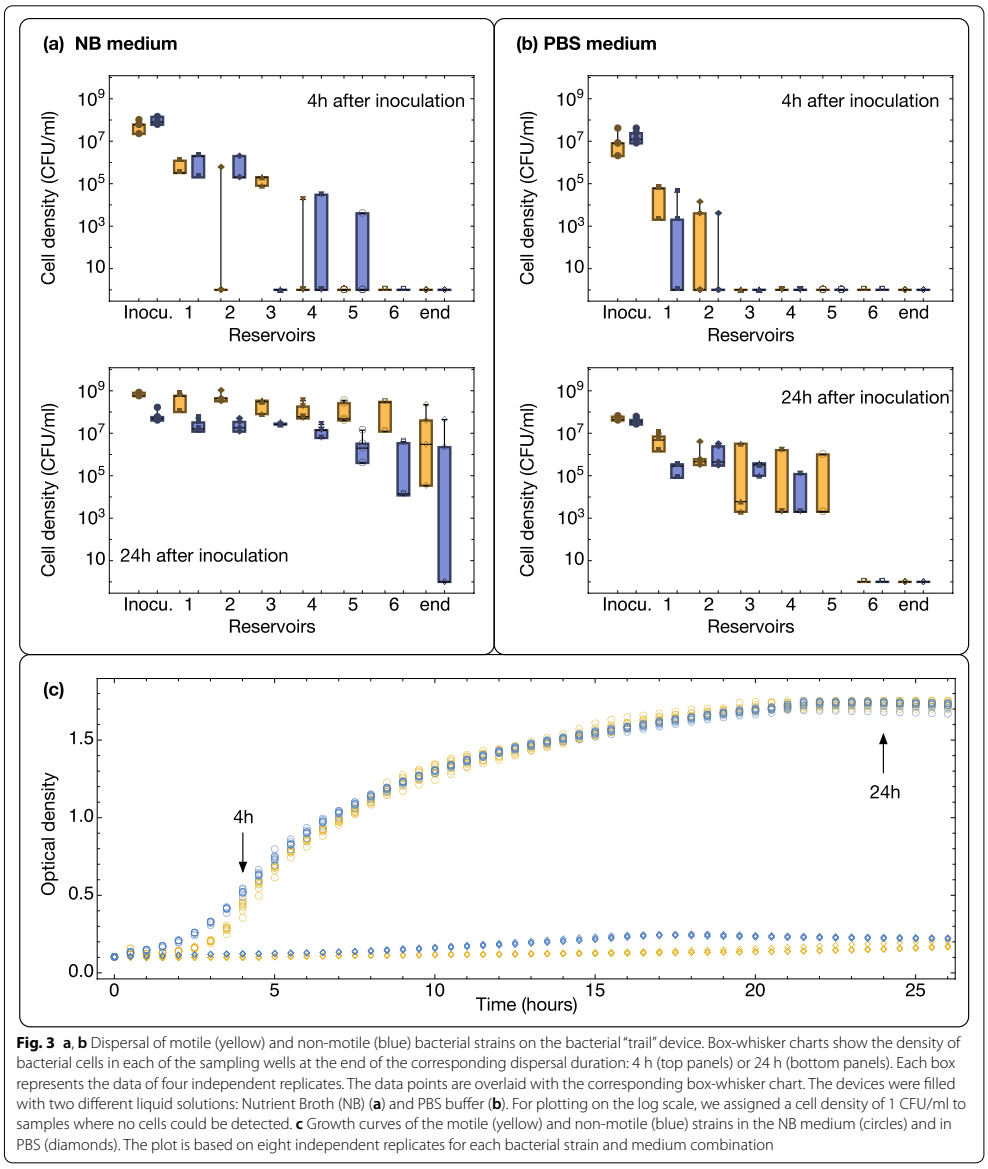

Fig. 3 **a**, **b** Dispersal of motile (yellow) and non-motile (blue) bacterial strains on the bacterial "trail" device. Box-whisker charts show the density of bacterial cells in each of the sampling wells at the end of the corresponding dispersal duration: 4 h (top panels) or 24 h (bottom panels). Each box represents the data of four independent replicates. The data points are overlaid with the corresponding box-whisker chart. The devices were filled with two different liquid solutions: Nutrient Broth (NB) (**a**) and PBS buffer (**b**). For plotting on the log scale, we assigned a cell density of 1 CFU/ml to samples where no cells could be detected. **c** Growth curves of the motile (yellow) and non-motile (blue) strains in the NB medium (circles) and in PBS (diamonds). The plot is based on eight independent replicates for each bacterial strain and medium combination

dispersal. After 24 h, the motile strain was significantly more abundant than the non-motile strain across sampling wells in NB ($p = 0.001$) but not in PBS ($p = 0.1$). In the NB medium, the growth curves of the motile and non-motile strains differed significantly ($p < 0.001$) within the first 4 h of growth, with the non-motile strain

growing significantly faster than the motile strain, but the overall growth did not differ significantly ($p = 0.3$) between the strains. In the PBS medium, both strains experienced minimal growth, with their optical densities barely doubled by 24 h, although the non-motile strain grew consistently more than the motile strain ($p < 0.001$).

Experiments with the "bridge" device

Because of the absence of hydraulic flow in the thin liquid film on the "bridge" device, we expected that only motile bacterial cells inoculated into the start well could disperse across the "bridge" and arrive at the target well. To test this hypothesis, we inoculated the motile and non-motile cells separately into the start well and tested the presence and density of cells in the target well after 72 h. Our pilot experiments showed that the motile strain already arrived at the target well within 20 h (data not shown), while the non-motile strain could not cross the "bridge" by diffusion in 72 h. The culturing medium contained nutrients (PBS+1% NB+1% Ficoll) to allow for energy-consuming bacterial swimming but sustained minimal growth and prevented the formation of a biofilm that could block the capillaries or help the non-motile strain to reach the target well through biofilm expansion (the growth curves of the two strains in the medium are provided in Additional file 1: Fig. S5). Our experiments showed that the motile cells arrived at the target well across all four replicates, while the non-motile cells did not arrive in all three replicates (Fig. 4a).

Non-motile bacteria are known to disperse along fungal hyphae by "hitchhiking" on motile bacterial cells [14]. To test whether this could happen in our system, we inoculated the motile and non-motile cells at a 1:1 ratio of cell numbers into the start well and tested the presence and cell densities of each cell type in the target well after 96 h. Both motile and non-motile cells were detected in the target well in five out of six replicates (Fig. 4b). In one replicate, the liquid film broke due to evaporation during the course of the experiments so that neither motile nor non-motile cells arrived at the target well (Fig. 4b, the failed replicate 5 is marked with an X). Because the motile and non-motile cells are tagged with green and red fluorescent proteins, respectively, we could distinguish them upon plating (Fig. 4c; corresponding color-blind-friendly pictures are provided in the Additional file 1: Fig. S4).

Discussion

3D printed devices as models to investigate bacterial dispersal

The dispersal capacity of bacteria in water unsaturated environments plays a crucial role in determining the spatial and temporal dynamics of microbial communities and in turn their ecological functions [5]. In this work, we use 3D printing to produce two devices that generate continuous liquid films in which bacteria can disperse. The variable thickness of the films produced mimic typical liquid films formed on hydrophilic biological (i.e., plant roots or fungal hyphae [12, 14, 15, 34]) or abiotic surfaces. Thus, the devices can be used in control experiments involving bacterial dispersal on natural supports to help disentangle abiotic processes and biotic interactions. Due to the properties of the resin used, the devices have a hydrophilic surface for continuous liquid films to form, and are heat resistant up to 140 °C, enabling the devices to be autoclaved for sterilization and repeated use. The material cost for producing the devices is also low (0.35 USD per "bridge" device and 0.5 USD per "trail" device), allowing for affordability and widespread use.

The new experimental systems we developed allow for the study of bacterial dispersal under different water saturation conditions. Under some natural conditions, bacterial cells can be transported passively by flowing streams of water, such as percolation after rainfall or concentrated flow in cracks and macropores formed by growing plant roots in relatively dry soils [35, 36]. The relatively thick water films formed by the "trail" device serve to model this situation. By contrast, in unsaturated soils, bacterial dispersal is restricted by cell-substrate viscous drag and capillary pinning forces imposed by the thin and fragmented water films on the surface of substrates [31, 32]. In these cases, the pore water velocity drops below the movement speed of motile bacterial cells, and the effect of passive transportation (i.e., in hydraulic flow) on cell motion is then negligible [37]. The relatively thin and stationary water films formed by our "bridge" device capture this situation. A previous soil model showed that liquid films thicker than 5 μm were rare and rapidly drained even under mild suction conditions, and the resulting patchiness of the liquid films severely limits the dispersal capacity of bacteria [5]. Our results with the "bridge device" extended the conditions where non-motile bacteria cannot disperse alone in unsaturated soil. We showed that even in continuous water films (0.14 ± 0.04 mm on the "bridge" device) that were much broader than 5 μm, the non-motile cells were still unable to disperse unassisted (in the timeframe of the experiments, 72 h), although motile cells could efficiently disperse (over 2.1 cm). Similar results were found using glass fibers to represent fungal hyphae [12]. Although an estimation of the liquid film thickness on the mycelia of soil fungi under conditions corresponding to typical unsaturated soils is currently inexistent, we expect it to be thinner than the liquid films established with the bridge device. If this is the case, the widespread fungal highways may provide a dispersal advantage exclusive to flagellated bacteria and

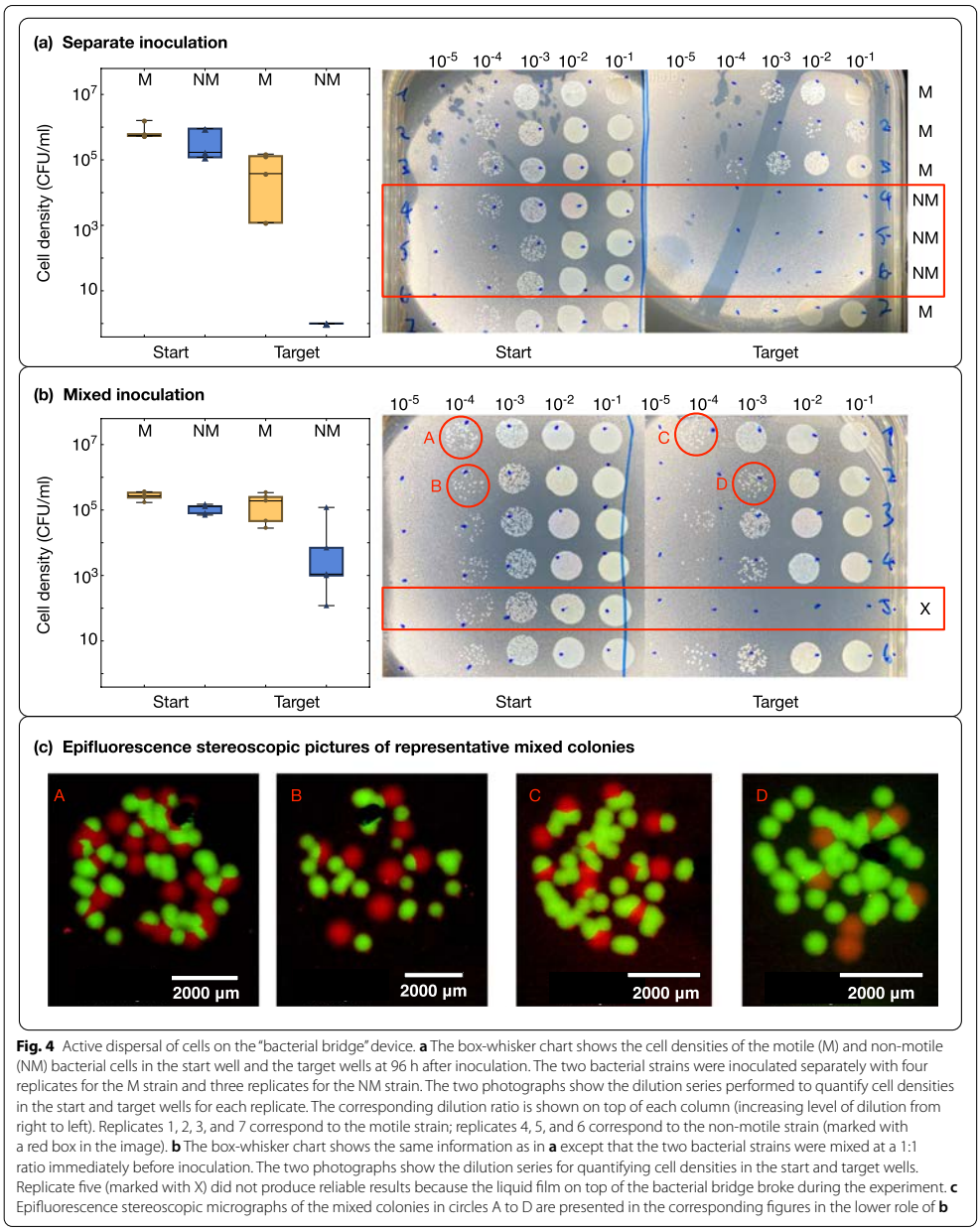

Fig. 4 Active dispersal of cells on the "bacterial bridge" device. **a** The box-whisker chart shows the cell densities of the motile (M) and non-motile (NM) bacterial cells in the start well and the target wells at 96 h after inoculation. The two bacterial strains were inoculated separately with four replicates for the M strain and three replicates for the NM strain. The two photographs show the dilution series performed to quantify cell densities in the start and target wells for each replicate. The corresponding dilution ratio is shown on top of each column (increasing level of dilution from right to left). Replicates 1, 2, 3, and 7 correspond to the motile strain; replicates 4, 5, and 6 correspond to the non-motile strain (marked with a red box in the image). **b** The box-whisker chart shows the same information as in **a** except that the two bacterial strains were mixed at a 1:1 ratio immediately before inoculation. The two photographs show the dilution series for quantifying cell densities in the start and target wells. Replicate five (marked with X) did not produce reliable results because the liquid film on top of the bacterial bridge broke during the experiment. **c** Epifluorescence stereoscopic micrographs of the mixed colonies in circles A to D are presented in the corresponding figures in the lower role of **b**

the non-motile bacteria that can hitchhike the dispersal of their associated carriers. This would be in accordance with the findings of a dispersal advantage of motile bacteria in cheese rind [38], and may contribute to explain the maintenance of costly flagella in soil bacteria [39].

Impact of liquid film lateral depth in dispersal of motile and non-motile cells

In the relatively thick liquid films established in the "trail" device (1.35 ± 0.32 mm in lateral depth), both motile and non-motile cells can disperse passively, driven by hydraulic flow. This explains why there was no significant difference in dispersal between motile and non-motile cells in the PBS solution across sampling wells (Fig. 3b). Because active dispersal by swimming with flagella requires energy [40, 41] and PBS lacks any carbon and energy sources, the motile cells can only disperse passively in a manner alike the non-motile cells. In the presence of energy sources, as in the NB medium, we expected the motile cells to have a dispersal advantage by being able to disperse actively by swimming, in addition to passive dispersal. Although the experimental results after 4 h did not support our hypothesis with statistical significance (probably due to stochastic effects on the distribution of cells within a short duration of time and the higher growth rate of the non-motile cells in the first hours after inoculation, which counterbalanced the dispersal advantage of the motile strain), the experimental results after 24 h provided clear evidence for a dispersal advantage of the motile cells over the non-motile cells, supporting our hypothesis.

In contrast to the relatively thick liquid films on the "trail" device, the liquid films on the "bridge" device are much thinner (0.14 ± 0.04 mm). The absence of hydraulic flow in these liquid films prevents non-motile cells from dispersal by drifting in the flow. This was shown in the single-strain inoculation experiments (Fig. 3a), which confirmed the importance of the flagellum for dispersal on hydrated surfaces such as in the case of fungal highways [34, 38, 39]. Interestingly, non-flagellated bacteria were still able to disperse in the presence of actively swimming motile cells, as shown in the co-inoculation experiments (Fig. 3b). Since the device does not introduce any biotic interaction between the dispersal network and the dispersing bacteria, we infer that the dispersal of non-motile bacteria facilitated by fungal highways [14, 20] may not require an active role of the fungus other than providing a continuous liquid pathway and a source of nutrients [21]. Although we do not know the exact mechanism explaining how the non-motile bacterial cells "hitchhike" to disperse in this particular case, existing literature provides some hypotheses that could be tested using our 3D printed devices. For instance, an aspect that could be investigated in the future is whether physical attachment of the non-motile to the motile cells is required for transport or if the non-motile bacteria are dragged by the flow generated by motile bacteria. In previous studies, several non-motile bacterial species were found to attach to the cell body of the motile carrier bacterium *Capnocytophaga gingivalis* [42]; similarly, non-motile bacterial and fungal spores were found to attach to the flagella of their corresponding carriers [15, 25]. Based on these observations, different combinations of carriers and hitchhikers can be considered to test the possible release of chemicals to attract motile cells for attachment and dispersal [26], as well as the transport of non-motile cells as useful "cargo" to degrade antibiotics [43], or to invade an occupied niche [44]. These functional components of hitchhiking could be investigated in future experiments using our devices in combination with parallel experiments performed using fungal hyphae or other biological surfaces (e.g., plant roots).

Limitations and opportunities of 3D printed devices

Despite the advantages of the 3D printed devices (i.e., fast prototyping, low cost, and reusability), there are still technological limitations that are relevant to mention. The most important limitation is the relatively low printing resolution, which leads to roughness with staircase-like patterns on the printed surfaces that are not parallel or perpendicular to the printing bed. This limitation prevented us from generating a highly obtuse angle between support structures with smooth surfaces to reduce the thickness of the liquid film on the devices, which may be achievable by other (often more expensive) microfabrication technologies such as photolithography, which has been used in producing microfluidic devices. In the case of the "bridge" device, the liquid columns in the vertical capillaries suppress hydraulic flow that can transport non-motile cells [37]. In principle, the thinner the capillaries, the better the effect of suppressing flow. However, the printing resolution set a lower limit on the diameter of the capillaries (0.5 to 1 mm in our case). Because the capillaries are perpendicular to the plane where the liquid films form (and we need to prioritize the smoothness of printing on that surface), it was not possible to further reduce the diameter of the capillaries (e.g., by reorienting the devices on the printing bed). The limit on capillary diameter may have contributed to the breakage of the liquid film in one of the six replicates in the bacterial hitchhiking experiment (Fig. 4b). Despite this limitation, the bridge device is shown to be able to establish and maintain a thin water film of consistent width (Fig. 2b) for experiments over long durations (96 h in the hitchhiking dispersal experiments) with satisfying reliability. Moreover, the 3D printed devices offer the possibility of

investigating the effect of two different boundaries (i.e., a surface-water and a water-air boundary) that complements other approaches such as microfluidic devices in which the water-air boundary is often not considered. In the last years, the cost of 3D printers has been decreasing rapidly to a few hundred USD. The expanding applications in the medical (especially dental) industry have promoted the development of a spectrum of hydrophilic biocompatible resins with diverse properties. In light of the increasing accessibility to 3D printing and affordable material costs, we view the two devices we developed in this work as early examples of much broader future applications of 3D printing in modern biology labs.

Conclusions

We designed and 3D printed two devices that can establish a thin liquid film to allow active or passive dispersal of bacteria, resembling the "fungal highway" mechanism of bacterial dispersal in the soil, but without introducing biotic interactions between the bacteria and fungi. By helping to tease apart the abiotic and biotic aspects of the interactions between bacteria and fungal mycelial networks, the devices we developed in this study open the door to many interesting future studies. For example, they can be used to identify and characterize fungi-secreted bioactive substances such as chemo-attractants, chemo-repellents, toxins, and signaling molecules. Furthermore, our work showcases the vast possibility and advantages of applying low-cost 3D printing technology to modern biology labs. We believe that the accessibility to fast prototyping and producing customized devices at affordable prices will play an increasingly important role in democratizing science and advancing education and research with more rational use of limited resources, such as in areas with disturbed production and supply chains.

Methods

3D printing and subsequent preparation of the devices

We designed the devices using the Autodesk Fusion 360 software, exported the design as STL files (provided in the Additional files 2 and 3), prepared the files for printing with the PrusaSlicer v2.2.0 software, and printed them using the HTR-140 green resin (3DM) with a masked stereolithographic 3D printer (Prusa SL1). The devices were printed directly on the printing bed with a layer height of 0.05 mm at 17 °C. The exposure time for each layer was 40 s for the first layer and 15 s for the rest layers. After printing, the devices were washed, blown with compressed air, and then dried overnight at room temperature. Finally, the devices were UV cured in a Prusa CW1 curing and washing machine for 4 min.

Building the liquid films on the devices and measuring their widths

To build a liquid film on the canal device, we first distributed 850 µl liquid (NB medium or PBS) in the eight sampling wells. Because of the hydrophilic property of the resin, water molecules can be attracted to the surface of the artificial hypha from the wells and spread along it automatically to form a liquid film. To make sure that the liquid film is continuous and is connected to each sampling well, we followed the artificial hyphae with the tip of a 1 ml pipette from one end to the other, going through all 8 wells. To build a liquid film on the bridge device, we first added 2.75 ml liquid each in two adjacent wells on a 24 well plate (Costar). We then placed the "start" and "target" ends of the bridge into the two wells. After that, we took 100 µl of liquid from the "start" well and ejected the liquid first at the openings of the two capillaries and then along the printed hypha. After a few seconds, most of the liquid flowed down along the two capillaries connecting the two sides of the "bridge" and the liquid surfaces in the two wells leveled off. The remaining liquid on top of the "bridge" device formed a continuous thin liquid film along the artificial hypha. Videos illustrating these procedures are provided in Additional files 4 and 5.

The widths of the liquid film on each of the devices were measured by taking pictures with a stereoscope (Nikon SMZ18) with a scale bar as reference. We measured the liquid films on four independently printed devices of each type and took three pictures at different locations (one in the middle and two in proximity to either end of the artificial hypha) on each device. We then measured the width of the liquid film at three randomly selected positions in each picture. This resulted in nine independent measurements of the liquid film width for each piece of the devices. The pictures were analyzed using the Fiji software (version 1.8.0). Using the burned-in scale as a reference, we could measure the width of the liquid film. For each picture, we performed three measurements at different randomly selected positions, leading to a total of nine independent measurements of the liquid film width for each piece of the devices.

Bacterial strains and the preparation for dispersal assays

We used an isogenic pair of motile and non-motile *P. putida* bacterial strains to test the active and passive transportation of cells in the liquid films formed on the devices. The motile KT2440 strain was isolated from the rhizosphere and is flagellated [45]. The non-motile strain is a non-flagellated (Δ*fliM*) mutant of the KT2440 strain, obtained by allelic exchange with a truncated version of *fliM* [31]. The motile strain is tagged with the green fluorescent protein, and the non-motile strain is tagged with

a red fluorescent protein (DsRed) marker. The two bacterial strains were cryo-preserved in 30% (v/v) glycerol at −80 °C. To reactivate the bacteria, cells were first plated on the Nutrient Agar (NA, 23 g/L, Carl Roth) through polygonal spreading and grown overnight at 30 °C in darkness. We then prepared bacterial suspensions from the overnight cultures by growing the cells in Nutrient Broth (NB, 23 g/L, Carl Roth) at ambient temperature under constant rotation at 120 rpm for 14 h. The bacterial suspension was adjusted with NB as blank to an optical density of 1 (600 nm wavelength), and centrifugated at 5000 g for 5 min to collect cells. The collected cells were washed once and resuspended in 0.01 M phosphate-buffered saline (PBS: 1.5 g/L $Na_2HPO_4{\cdot}2H_2O$, 0.25 g/L $NaH_2PO_4{\cdot}2H_2O$, 8.5 g/L NaCl) with 1% NB as an energy source. The cell suspension of each strain was adjusted to a final OD of 1.

Bacterial dispersal assays on the canal device

To test bacterial dispersal in the liquid film on the canal device, we performed experiments under a full factorial design with two different media (NB and PBS), two bacterial strains (motile and non-motile), and two dispersal durations (4 h and 24 h), each with 4 replicates. After building the liquid films with either NB or PBS, we added 10 µl of the cell suspension of either strain to the inoculation well. To maintain the liquid film and prevent evaporation during the experiments, we placed the devices into a large glass Petri dish with four pieces of sterile filter paper with 1 ml of autoclaved deionized water added to each. We took a sample of 20 µl from each of the eight wells following the order from one to eight at the end of each assay. The cell density in each of the wells was quantified (see below).

Bacterial dispersal assay on the bridge device

To test bacterial dispersal in the liquid film on the bridge device, we used a culture medium containing 0.01 M PBS with 1% of NB and 1% of Ficoll (10g/L, Sigma-Aldrich). We added Ficoll to the medium to increase its viscosity for suppressing flow [46]. As a thickening agent, Ficoll has the desirable properties of causing little osmotic stress and cannot be consumed or degraded by bacterial cells [47]. For the experiments, we first built liquid films on the devices and inoculated 5 µl of bacterial cell suspension (either the motile/non-motile strain alone or mixed with 1:1 ratio) to the start well. The devices were kept in a closed Petri dish to keep humidity high in darkness for 72 h for experiments where the inoculation contains only motile or non-motile cells. The experiments with inoculations that contain both motile and non-motile cells were run for 96 h under the same condition. At the end of the experiments, we took a sample of 20 µl first from the target well and then from the start well of each device, and quantified the cell density in each sample.

Cell density quantification

We performed a dilution series to quantify the cell density in each sample taken at the end of the dispersal assays. Each of the 20 µl samples were diluted five times by adding 180 µl NB (10x dilution by volume). We then inoculated 5 µl of each of the five dilutions on a rectangular NA plate with a multichannel pipette. The plates were sealed with parafilm and incubated at 30 °C in darkness for 24 h. Afterwards, the lowest dilution that enabled counting of bacterial colonies formed by a single cell was chosen to determine the initial cell density in the corresponding sample.

Supplementary Information

The online version contains supplementary material available at https://doi.org/10.1186/s12915-022-01406-z.

Additional file 1: Fig. S1. Design details and photographs of the "bacterial trail" and "bacterial bridge" devices. **Fig. S2.** Growth curves of *P. putida* in Falcon tubes and the printed tubes. **Fig. S3.** Adjusting the liquid film width on the "bacterial bridge" device. **Fig. S4.** Transport of fluorescein in the liquid films on the devices. **Fig. S5.** Growth curves of the bacteria in different media. **Fig. S6.** Adjusted Fig. 4c for colorblind readers. **Table S1.** Biocompatibility control of the resin. **Table S2.** *p*-values of pairwise Z-tests of liquid film width.

Additional file 2. STL file of the "bacterial trail" device.

Additional file 3. STL file of the "bacterial bridge" device.

Additional file 4. Video of building the liquid film on the "bacterial trail" device.

Additional file 5. Video of building the liquid film on the "bacterial bridge" device.

Additional file 6. Video of fluorescein diffusion in the liquid film on the "bacterial trail" device.

Additional file 7. Video of fluorescein diffusion in the liquid film on the "bacterial bridge" device.

Acknowledgments

We would like to thank Guillaume Cailleau for drawing the cartoon illustrations of the devices in Fig. 1 and two anonymous reviewers for their constructive comments that helped us improve the paper.

Authors' contributions

X-YLR and PJ designed the study, TK carried out the research, MB, SB, PSC, DG, CES, and LYW contributed to the research methods. X-YLR wrote the manuscript with inputs from all authors. All authors read and approved the final manuscript.

Funding

We thank the Swiss National Science Foundation (grant PZ00P3_180145) and the U.S. Department of Energy (grant LANLF59T) for financial support.

Availability of data and materials

The datasets supporting the conclusions of this article are included within the article and its additional files.

Declarations

Ethics approval and consent to participate
Not applicable.

Consent for publication
Not applicable.

Competing interests
The authors declare that they have no competing interests.

Author details
[1]Institute of Biology, University of Neuchâtel, CH-2000 Neuchâtel, Switzerland. [2]Bioscience Division, Los Alamos National Laboratory, Los Alamos, NM 87545, USA. [3]Department of Bioengineering, Imperial College, South Kensington, London SW7 2AZ, UK. [4]Department of Environmental Microbiology, Helmholtz Centre for Environmental Research, 04318 Leipzig, Germany.

Received: 13 June 2022 Accepted: 8 September 2022
Published online: 14 September 2022

References

1. Andersson MGI, Berga M, Lindström ES, Langenheder S. The spatial structure of bacterial communities is influenced by historical environmental conditions. Ecology. 2014;95:1134–40.
2. Johnsen AR, Wick LY, Harms H. Principles of microbial PAH-degradation in soil. Environ Pollut. 2005;133:71–84.
3. Banitz T, Johst K, Wick LY, Schamfuß S, Harms H, Frank K. Highways versus pipelines: contributions of two fungal transport mechanisms to efficient bioremediation. Environ Microbiol Rep. 2013;5:211–8.
4. Tecon R, Or D. Biophysical processes supporting the diversity of microbial life in soil. FEMS Microbiol Rev. 2017;41:599–623.
5. Tecon R, Or D. Bacterial flagellar motility on hydrated rough surfaces controlled by aqueous film thickness and connectedness. Sci Rep. 2016;6:1–11.
6. Xiao X, Liang Y, Zhou S, Zhuang S, Sun B. Fungal community reveals less dispersal limitation and potentially more connected network than that of bacteria in bamboo forest soils. Mol Ecol. 2018;27:550–63.
7. Falconer RE, Houston AN, Otten W, Baveye PC. Emergent behavior of soil fungal dynamics: Influence of soil architecture and water distribution. Soil Sci. 2012;177:111–9.
8. Worrich A, König S, Miltner A, Banitz T, Centler F, Frank K, et al. Mycelium-like networks increase bacterial dispersal, growth, and biodegradation in a model ecosystem at various water potentials. Appl Environ Microbiol. 2016;82:2902–8.
9. Ritz K, Young IM. Interactions between soil structure and fungi. Mycologist. 2004;18:52–9.
10. Joergensen RG, Wichern F. Alive and kicking: why dormant soil microorganisms matter. Soil Biol Biochem. 2018;116:419–30.
11. Wick LY, Remer R, Würz B, Reichenbach J, Braun S, Schäfer F, et al. Effect of fungal hyphae on the access of bacteria to phenanthrene in soil. Environ Sci Technol. 2007;41:500–5.
12. Kohlmeier S, Smits THM, Ford RM, Keel C, Harms H, Wick LY. Taking the fungal highway: mobilization of pollutant-degrading bacteria by fungi. Environ Sci Technol. 2005;39:4640–6.
13. Bravo D, Cailleau G, Bindschedler S, Simon A, Job D, Verrecchia E, et al. Isolation of oxalotrophic bacteria able to disperse on fungal mycelium. FEMS Microbiol Lett. 2013;348:157–66.
14. Warmink JA, Nazir R, Corten B, van Elsas JD. Hitchhikers on the fungal highway: the helper effect for bacterial migration via fungal hyphae. Soil Biol Biochem. 2011;43:760–5.
15. Ingham CJ, Kalisman O, Finkelshtein A, Ben-Jacob E. Mutually facilitated dispersal between the nonmotile fungus *Aspergillus fumigatus* and the swarming bacterium *Paenibacillus vortex*. Proc Natl Acad Sci U S A. 2011;108:19731–6.
16. Deveau A, Bonito G, Uehling J, Paoletti M, Becker M, Bindschedler S, et al. Bacterial–fungal interactions: ecology, mechanisms and challenges. FEMS Microbiol Rev. 2018;42:335–52.
17. de Boer W. Upscaling of fungal–bacterial interactions: from the lab to the field. Curr Opin Microbiol. 2017;37:35–41.
18. Muok AR, Briegel A. Intermicrobial hitchhiking: how nonmotile microbes leverage communal motility. Trends Microbiol. 2021;29:542–50.
19. Furuno S, Päzolt K, Rabe C, Neu TR, Harms H, Wick LY. Fungal mycelia allow chemotactic dispersal of polycyclic aromatic hydrocarbon-degrading bacteria in water-unsaturated systems. Environ Microbiol. 2010;12:1391–8.
20. Warmink JA, van Elsas JD. Migratory response of soil bacteria to *Lyophyllum sp.* strain Karsten in soil microcosms. Appl Environ Microbiol. 2009;75:2820–30.
21. Worrich A, Stryhanyuk H, Musat N, König S, Banitz T, Centler F, et al. Mycelium-mediated transfer of water and nutrients stimulates bacterial activity in dry and oligotrophic environments. Nat Commun. 2017;8:1–9.
22. Berthold T, Centler F, Hübschmann T, Remer R, Thullner M, Harms H, et al. Mycelia as a focal point for horizontal gene transfer among soil bacteria. Sci Rep. 2016;6:36390.
23. Espinosa-Ortiz EJ, Rene ER, Gerlach R. Potential use of fungal-bacterial co-cultures for the removal of organic pollutants. Crit Rev Biotechnol. 2021;42:361–83.
24. Worrich A, König S, Banitz T, Centler F, Frank K, Thullner M, et al. Bacterial dispersal promotes biodegradation in heterogeneous systems exposed to osmotic stress. Front Microbiol. 2016;7:1214.
25. Muok AR, Claessen D, Briegel A. Microbial hitchhiking: how Streptomyces spores are transported by motile soil bacteria. ISME J. 2021;15:2591–600.
26. Hagai E, Dvora R, Havkin-Blank T, Zelinger E, Porat Z, Schulz S, et al. Surface-motility induction, attraction and hitchhiking between bacterial species promote dispersal on solid surfaces. ISME J. 2014;8:1147–51.
27. Yang P, van Elsas JD. Mechanisms and ecological implications of the movement of bacteria in soil. Appl Soil Ecol. 2018;129:112–20.
28. Nai C, Meyer V. From axenic to mixed cultures: technological advances accelerating a paradigm shift in microbiology. Trends Microbiol. 2018;26:538–54.
29. Gaikwad SR, Pawar NH, Sapkal SU. Comparative evaluation of 3D printed components for deviations in dimensional and geometrical features. Mater Today Proc. 2021. https://doi.org/10.1016/j.matpr.2021.11.157.
30. Islam MR, Tudryn G, Bucinell R, Schadler L, Picu RC. Morphology and mechanics of fungal mycelium. Sci Rep. 2017;7:13070.
31. Dechesne A, Wang G, Gülez G, Or D, Smets BF. Hydration-controlled bacterial motility and dispersal on surfaces. Proc Natl Acad Sci U S A. 2010;107:14369–72.
32. Wang G, Or D. Aqueous films limit bacterial cell motility and colony expansion on partially saturated rough surfaces. Environ Microbiol. 2010;12:1363–73.
33. Stalder AF, Kulik G, Sage D, Barbieri L, Hoffmann P. A snake-based approach to accurate determination of both contact points and contact angles. Colloids Surf A Physicochem Eng Asp. 2006;286:92–103.
34. Simon A, Bindschedler S, Job D, Wick LY, Filippidou S, Kooli WM, et al. Exploiting the fungal highway: development of a novel tool for the in situ isolation of bacteria migrating along fungal mycelium. FEMS Microbiol Ecol. 2015;91:fiv116.
35. Breitenbeck GA, Yang H, Dunigan EP. Water-facilitated dispersal of inoculant *Bradyrhizobium japonicum* in soils. Biol Fertil Soils. 1988;7:58–62.
36. Hekman WE, Heijnen CE, Burgers S, van Veen JA, van Elsas JD. Transport of bacterial inoculants through intact cores of two different soils as affected by water percolation and the presence of wheat plants. FEMS Microbiol Ecol. 1995;16:143–57.
37. Ebrahimi AN, Or D. Microbial dispersal in unsaturated porous media: characteristics of motile bacterial cell motions in unsaturated angular pore networks. Water Resour Res. 2014;50:7406–29.
38. Zhang Y, Kastman EK, Guasto JS, Wolfe BE. Fungal networks shape dynamics of bacterial dispersal and community assembly in cheese rind microbiomes. Nat Commun. 2018;9:336.
39. Pion M, Bshary R, Bindschedler S, Filippidou S, Wick LY, Job D, et al. Gains of bacterial flagellar motility in a fungal world. Appl Environ Microbiol. 2013;79:6862–7.
40. Schavemaker PE, Lynch M. Flagellar energy costs across the Tree of Life. BioRxiv 2022. https://doi.org/https://doi.org/10.1101/2022.01.31.478446.
41. Morowitz HJ. The energy requirements for bacterial motility. Science. 1979;1954(119):286.

42. Shrivastava A, Patel VK, Tang Y, Yost SC, Dewhirst FE, Berg HC. Cargo transport shapes the spatial organization of a microbial community. Proc Natl Acad Sci U S A. 2018;115:8633–8.
43. Finkelshtein A, Roth D, Ben Jacob E, Ingham CJ. Bacterial swarms recruit cargo bacteria to pave the way in toxic environments. MBio. 2015;6:e00074–15.
44. You X, Kallies R, Kühn I, Schmidt M, Harms H, Chatzinotas A, et al. Phage co-transport with hyphal-riding bacteria fuels bacterial invasion in a water-unsaturated microbial model system. ISME J. 2021. https://doi.org/10.1038/s41396-021-01155-x.
45. Regenhardt D, Heuer H, Heim S, Fernandez DU, Strömpl C, Moore ERB, et al. Pedigree and taxonomic credentials of Pseudomonas putida strain KT2440. Environ Microbiol. 2002;4:912–5.
46. Qu Z, Temel FZ, Henderikx R, Breuer KS. Changes in the flagellar bundling time account for variations in swimming behavior of flagellated bacteria in viscous media. Proc Natl Acad Sci U S A. 2018;115:1707–12.
47. Bremer E, Krämer R. Responses of microorganisms to osmotic stress. Annu Rev Microbiol. 2019;73:313–34.

Publisher's Note

Appendix

1. Detailed design of the "bacterial trail" and "bacterial bridge" devices

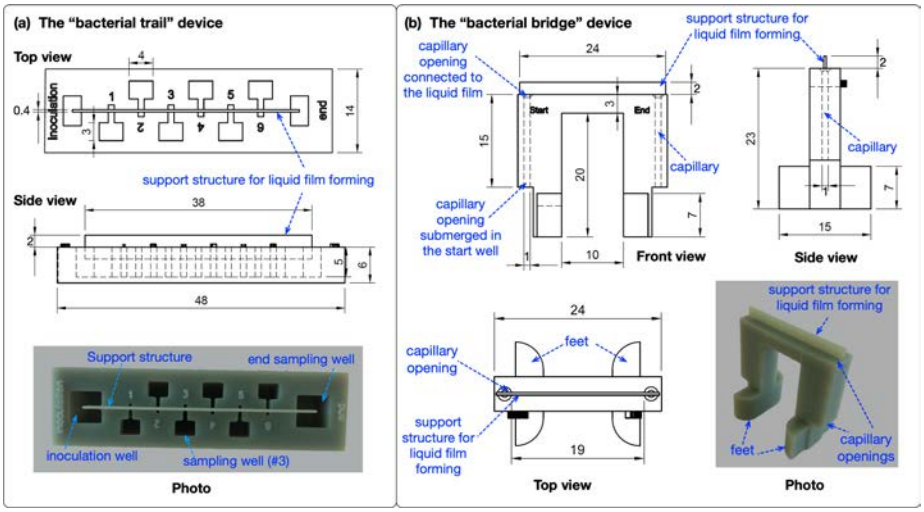

Figure S1. Design details and photographs of the "bacterial trail" and "bacterial bridge" devices. The detailed computer-aided design (CAD) illustrations indicate the dimensions of the components of the devices (corresponding Standard Tessellation Language -STL- files are provided in ESM). In the "trail" device (panel a), a bar-shaped support structure connects eight liquid reservoirs including an inoculation well, an end sampling well, and six intermediate sampling wells. In the "bridge" device (panel b), the support structure to form liquid films is located on the top of two capillaries of 1 mm in diameter and 15 mm in length. The lower openings of the capillaries next to the two feet of the device are submerged in liquid reservoirs in two wells on a 24-well plate. The upper openings of the capillaries connect to the liquid film formed along the artificial hypha on top of the device. All measurement values are in millimeters.

2. Controlling for the biocompatibility of the printing material

To control for the biocompatibility of the printing material, we printed culturing tubes using the HTR-140 green resin (3DM) and cultured the bacteria *Pseudomonas putida* in the printed tubes and standard 50 ml Falcon tubes (Sarstedt) of certified biocompatibility. We inoculated 10 µl of the bacterial suspension with an optical density equal to one into 5 ml NB medium and incubated the tubes in a thermos-shaker (Lab Gene Instruments) at 30 °C with a rotation speed of 120 r/min for 24 hours. There were three replicates for each treatment. Samples of 100 µl are taken at five time-points (immediately after inoculation, and 3, 6, 9, and 24 hours after inoculation) from each replicate. We measured the optical density of the samples to assess bacterial growth and compared the growth curves of bacteria in printed tubes and the standard Falcon tubes. Table S1 summarises the OD values at different time points. The growth curves in the printed tubes and the Falcon tubes are shown in Figure S1. We used the *compareTwoGrowthCurves*

function of the *growthcurver* package in the R environment to compare the growth curves. The growth curves in printed and Falcon tubes did not differ significantly (p=0.54).

Table S1. Optical density of the culturing medium at five different time points after inoculating *P. putida* cells either in standard Falcon tubes or in printed tubes using the HTR-140 green resin.

Treatment	Sampling time (hours after inoculation)	Mean optical density	SD of optical density
Falcon tube	0	0.002	0
Falcon tube	3	0.010	0.0015
Falcon tube	6	0.0373	0.0050
Falcon tube	9	0.1053	0.0211
Falcon tube	24	0.5837	0.0811
Printed tube	0	0.002	0
Printed tube	3	0.011	0.001
Printed tube	6	0.0323	0.0076
Printed tube	9	0.083	0.0075
Printed tube	24	0.461	0.0650

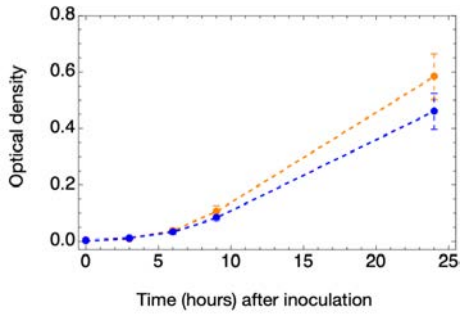

Figure S2. Growth curves of *P. putida* in biocompatible Falcon tubes (orange) and the printed tubes (blue).

3. Adjusting the liquid film width on the "bacterial bridge" device

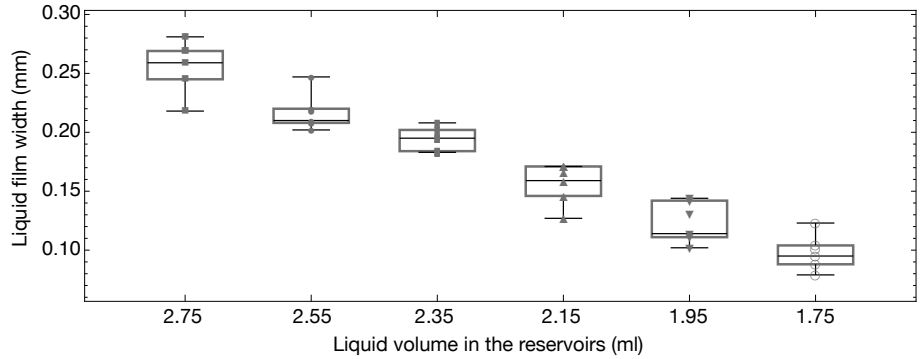

Figure S3. The liquid film width on the "bacterial bridge" device can be adjusted by varying the length of liquid columns inside the capillaries, which can be easily achieved by adjusting the volume of liquid added to the reservoirs. The results were produced using the wells on a standard 24-well plate as liquid reservoirs. However, attention must be paid as the thinner the liquid film is, the more likely it will break during the duration of bacterial dispersal experiments if those last several days.

4. Controlling for the consistency of liquid film width across devices of the same type.

To test whether different pieces of the same type of device produce liquid films of comparable width (Box-Whisker charts of the distributions are provided in Figure 2 of the main text), we performed pairwise Z-tests of the liquid film width distributions. To account for multiple comparisons (6 different pairwise comparisons for each device type), we use the Bonferroni correction to adjust the threshold *p*-value 0.05 to 0.00833. All the *p*-values of the pairwise comparisons are higher than the adjusted threshold (Table S2), and therefore, we conclude that the distributions of liquid film width are consistent across different pieces of devices of the same type.

Table S2. *P*-values of pairwise *Z*-tests of the liquid film width on four independently printed pieces of devices of each type.

Device Type	Device pairs	*p*-value of pairwise Z-test
Canal	#1 vs #2	0.066
	#1 vs #3	0.081
	#1 vs #4	0.047
	#2 vs #3	0.901
	#2 vs #4	0.859
	#3 vs #4	0.969
Bridge	#1 vs #2	0.657
	#1 vs #3	0.118
	#1 vs #4	0.054
	#2 vs #3	0.219
	#2 vs #4	0.094
	#3 vs #4	0.511

5. Transport of the fluorescein marker in the liquid films on the devices

To determine whether hydraulic flows were present in the liquid films on the "bacterial trail" and "bacterial bridge" devices, we measured the transport speed of fluorescein in the liquid films. To do so, we added 10 µl fluorescein into the inoculation well on one "bacterial trail" device (Figure S4a) and three replicates of the "bacterial bridge" devices (Figure S4b). The transport speed of fluorescein on the "bacterial trail" device was faster than that on the "bacterial bridge" devices. The temporal dynamics of

fluorescein transport on the “bacterial bridge” devices fit well to a one-dimensional diffusion model (Figure S4c, gray line), suggesting the absence of hydraulic flow in the liquid film.

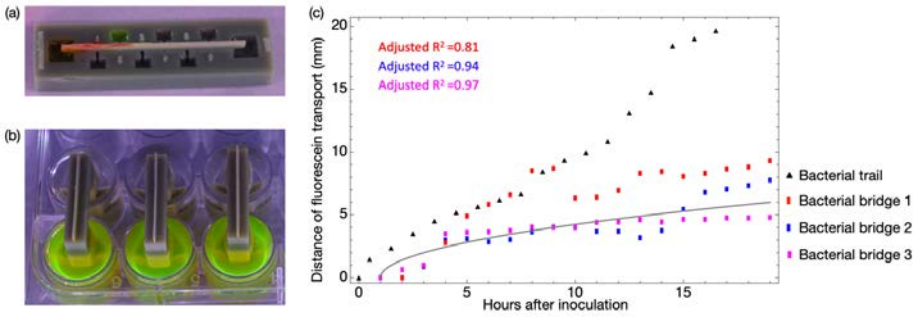

Figure S4. Transport of the fluorescein in the liquid film on the “bacterial trail” and “bacterial bridge” devices. (a) Photo of the “bacterial trail” device 10 hours after inoculating 10 µl of fluorescein into the inoculation well. (b) Photo of three replicates of the “bacterial bridge” devices immediately after inoculating 10 µl of fluorescein into the start wells. (c) Transport distance of the fluorescein over time in the liquid films on the devices. The gray solid line represents the expected diffusion speed of the fluorescein in the absence of hydraulic flow fitted from the one-dimensional diffusion model. The fluorescein did not start to diffuse in the liquid films on the “bacterial bridge” devices immediately after inoculation because we inoculated the fluorescein into the start well, and it took around one hour for the fluorescein molecules to reach the top of the capillaries that connect the liquid films to the corresponding start well.

6. Growth curves of the bacterial strains in different culturing media

To disentangle the contributions of growth and dispersal in the dispersal assays using the “trail” and “bridge” devices, we performed growth curves of the two strains in the three media we used in the experiments. In the experiments with the “trail” device, we used PBS and NB media. In the experiments with the “bridge” device, we PBS + 1% NB+ 1% Ficoll.

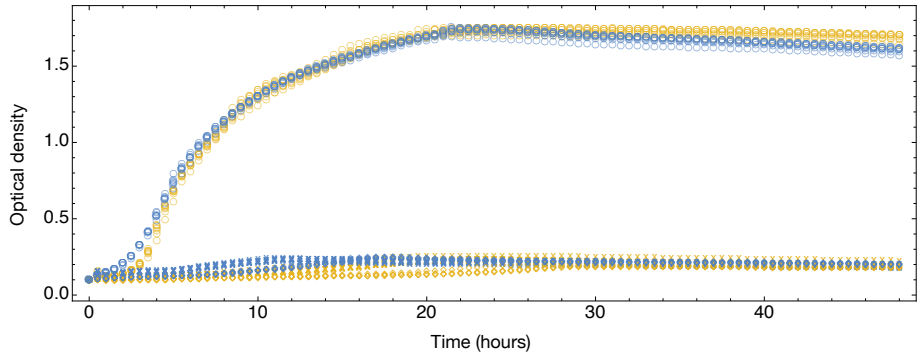

Figure S5. Growth curves of the motile (yellow) and non-motile (blue) strains in the NB medium (circles), PBS buffer (diamonds), and PBS + 1% NB + 1% Ficoll medium (crosses). The plot is based on eight independent replicates for each bacterial strain and medium combination.

7. Adjusted main text Figure 4 for readers who could not distinguish red and green colors

The motile and non-motile bacterial strains we used in the experiments were labeled with green and red fluorescent proteins, respectively. To facilitate the accessibility for readers with limited color vision, we provide below modified Figure 4c, where the red color was replaced by magenta. We further tested the result of color replacement with Fiji's colorblindness simulator (version 1.8.0).

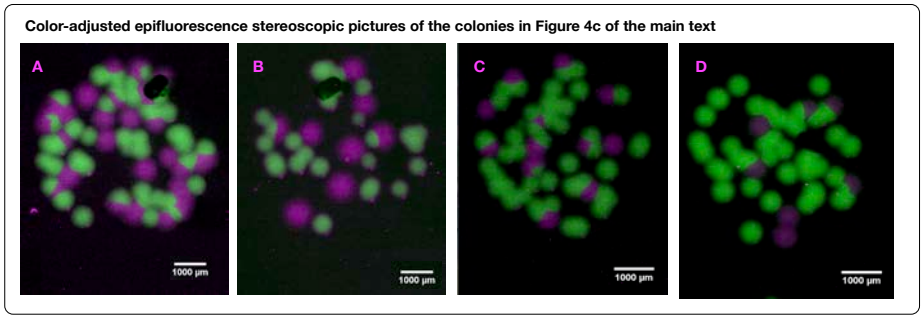

Figure S6. Color-adjusted Figure 4 panel c of the main text. The red color is replaced by magenta to distinguish it from the green fluorescence signal.

Chapter three

Contribution to Chapter three

In the third chapter, I designed, developed and produced the bioreactors and performed all the experiments. With the help of Xiang-Yi Richter, we analyzed the produced data. Xiang-Yi Richter, Diego Gonzalez and I wrote the manuscript. The in-revision manuscript of Kuhn et al. 2022 appears on the next pages.

Summary Chapter three

In the third chapter, we investigate a mechanism working on the local scale to maintain biodiversity. We develop small bioreactors to examine the impact of changing nutrient composition on the non-transitive competition dynamics in three *Escherichia coli* strains. Furthermore, we investigate the role of toxin removal by changing the flow rate of the bioreactors. We found that both nutrients and flow rates impact population dynamics. To conceptualize the toxin's impact on population dynamics, we use an IBM to simulate different diffusion, toxin production and removal rates. We show that the amount of released toxin retained in the system is a simple indicator that can predict whether the strains can coexist across broad parameter space.

Ecology shapes the cyclic dominance games between *Escherichia coli* strains

Thierry Kuhn[1], Junier Pilar[1], Redouan Bshary[1], Diego Gonzalez[1,*], Xiang-Yi Li Richter[1,*]

1. Institute of Biology, University of Neuchâtel, Rue Emile-Argand 11, 2000 Neuchâtel, Switzerland
[*]Corresponding authors: D.G. (diego.gonzalez@unine.ch); X-Y.L.R. (li@evolbio.mpg.de)

Abstract

Evolutionary game theory has provided various models to explain the coexistence of competing strategies, one of which is the rock-paper-scissors (RPS) game. A system of three *Escherichia coli* strains—a toxin-producer, a resistant, and a sensitive—has become a classic experimental model for studying RPS games. Previous experimental and theoretical studies, however, often ignored the influence of ecological factors such as nutrients and toxin dynamics on the evolutionary game between the competing strains. In this work, we combine experiments and modeling to study how these factors affect strain coexistence. Using 3D-printed mini-bioreactors, we tracked the community dynamics in different culturing media and under different flow regimes. We found that both nutrients and flow rates impact the population dynamics. In the simulations, we explicitly modeled the release, diffusion, and removal of toxin in space. We showed that the amount of released toxin that is retained in the system is a simple indicator that can predict whether the strains can coexist across broad parameter space. Using the RPS game between the *E. coli* strains as a case study, our work showed the advantage and vast potential of integrating ecology into evolutionary game models for understanding and predicting evolutionary dynamics in biologically realistic contexts.

Introduction

Cyclic dominance interactions represent an interesting type of evolutionary dynamics that have been suggested to promote species coexistence in nature (Czárán et al., 2002; Kerr et al., 2002; Kirkup & Riley, 2004; Reichenbach et al., 2007). In contrast to hierarchical competition dynamics, where stronger competitors tend to exclude weaker ones, in cyclic dominance interactions, there is no obvious best competitor. Each player can beat some competitors, but loses when confronted to others, like in the children's "rock-paper-scissors" game, where paper wraps rock, rock crushes scissors, and scissors cut paper, forming a dominance circle (Figure 1A). This type of interaction seems less common in animals (yet with famous examples, such as the mating strategy polymorphism in side-blotched lizards (Sinervo & Lively, 1996)), but it is widespread in plants (Cameron et al., 2009; Soliveres, Maestre, Ulrich, Manning, Boch, Bowker, Prati, Delgado-Baquerizo, Quero, Schöning, & others, 2015; Taylor & Aarssen, 1990) and microbial communities

where organisms engage in toxin-mediated warfare (Czárán et al., 2002; Granato et al., 2019; Liao et al., 2020; Stubbendieck & Straight, 2016).

Escherichia coli is a mammalian gut commensal and pathogen that heavily relies on bacteriocidal toxins, collectively named colicins, to exclude conspecific competitors. This bacterium has been used as a model system for studying cyclic dominance both experimentally and theoretically. In the gut, strains that produce colicins, strains that are sensitive to colicins, and strains that, at some cost, have acquired a resistance to colicins often coexist (Gordon et al., 1998; Riley & Gordon, 1999). In such a system, the toxin-producers kill sensitive individuals, the resistant individuals outgrow the toxin-producers, and the sensitive individuals outgrow the resistant ones in pair-wise competitions, which suggests that a "rock-paper-scissors" evolutionary game might underlie the coexistence between the strains (Figure 1AB). Mathematical models and experiments based on this system have identified important factors that determine the likelihood of strain coexistence, including the range of spatial interaction (Kerr et al., 2002), mobility rate (Reichenbach et al., 2007), spatial heterogeneity (Schreiber & Killingback, 2013), and community size (Müller & Gallas, 2010). The relative competitiveness between the strains has also been found to play an essential role in determining the evolutionary dynamics, for example, asymmetric competitiveness between the strains may lead to "survival of the weakest", where the least competitive strain in terms of growth or killing rates consistently dominates the community (Frean & Abraham, 2001; Liao et al., 2020; Nahum et al., 2011; Neumann & Schuster, 2007). However, previous models and experiments have often neglected the role of some key ecological factors at play in *E. coli's* natural environment, which can dramatically change the competition dynamics between the players in the "rock-paper-scissors" evolutionary game.

The mammalian gut is a complex and dynamic ecosystem in which parameters like pH, nutrient availability, spatial structure, and flow constantly vary, both locally and globally (Miller et al., 2021). Some of these parameters, especially nutrients and flow, may influence the competitive interactions between *E. coli* strains by affecting their **relative growth rates and the local concentrations of colicin. Because colicins are protein-**based toxins, their production is particularly costly and inefficient in environments where amino acids are limiting (Cascales, Buchanan, Duché, Kleanthous, Lloubes, et al., 2007). The production of colicins is therefore often directly modulated by nutrients, either at the transcriptional level, like in the case of colicin K and E1, which are induced upon starvation, or at the posttranscriptional level, like for colicin E2, whose release is inhibited by glucose (Ghazaryan et al., 2014; Götz et al., 2018; T.-Y. Yang et al., 2010). The concentration of toxins is also highly sensitive to hydrodynamic factors. Due to their high molecular weight (40 to 80 kDa (Cascales, Buchanan, Duché, Kleanthous, Lloubes, et al., 2007)), the spatial and temporal distributions of colicins can be affected by their varying diffusion rates in the heterogeneous intestinal extracellular matrix (Sandrin et al., 2016). Moreover, the rate of toxin removal, by flow or degradation, can change throughout the gut. Because colicins are potent and fast-acting (Cascales, Buchanan, Duché,

Kleanthous, Lloubes, et al., 2007), small changes in toxin concentration could dramatically impact the sensitive strain survival and threaten coexistence between the three strains. However, the effects of toxin removal have rarely been studied as such in mathematical models and are usually not controlled or accounted for in experiments (Kerr et al., 2002; Liao et al., 2020).

In this work, we combined laboratory experiments and computer simulations to study how the availability of nutrients and the rate of toxin production and removal affect the "rock-paper-scissors" evolutionary game in *E. coli.* Our experiments involved continuous cultures of communities of the three *E. coli* strains in 3D-printed mini-bioreactors with different media compositions and flow rates. To help discriminate between toxin-related and growth-related effects, we built a simulation model that independently controls toxin production, toxin diffusion, and toxin removal on the one hand, and growth parameters on the other hand. Through stepwise simulations, the model follows population dynamics and toxin levels in a spatially tractable way (Figure 1CD; see also Figure 3AB). It helps understand what the key variables can explain coexistence and competition outcomes in natural environments.

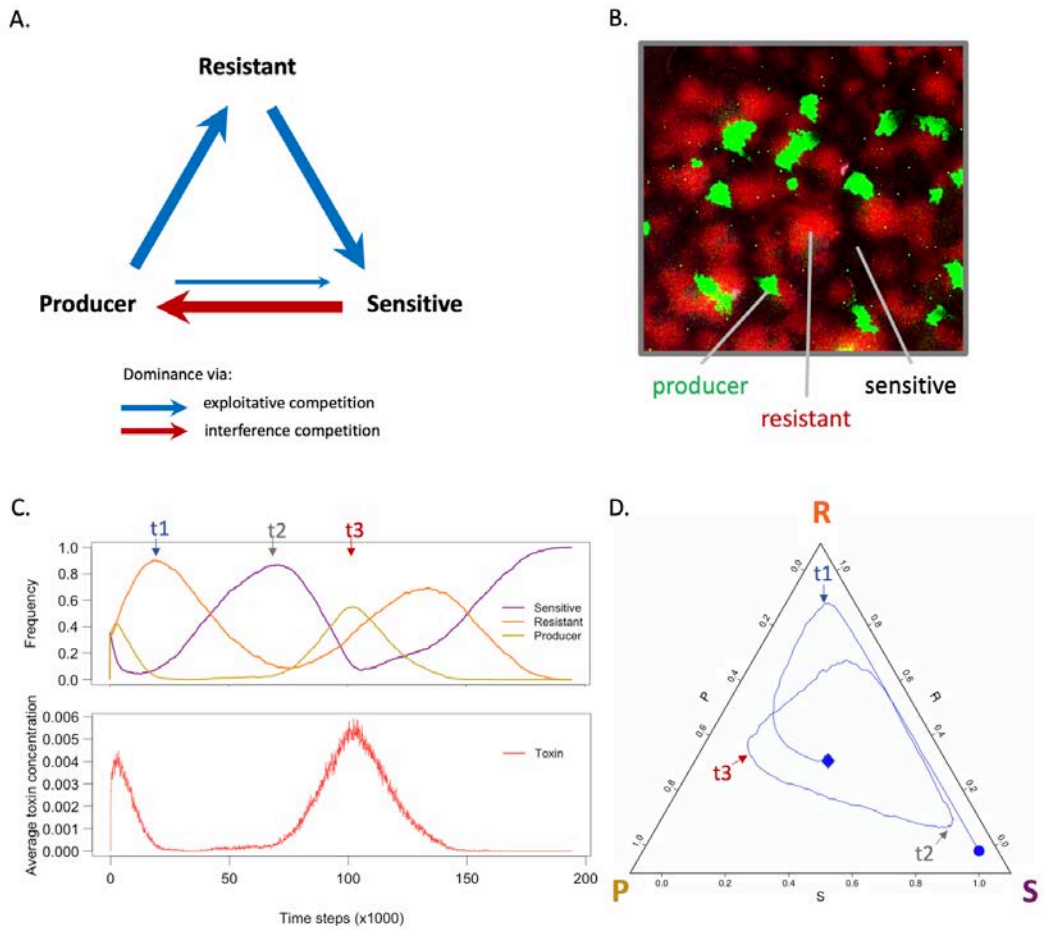

Figure 1. Basic concepts underlying the research. A. Cyclic dominance driven by toxin-mediated killing (i.e., interference competition (Cornforth & Foster, 2013; Lang & Benbow, 2013), represented by the red arrow) or higher growth rate (i.e., exploitative competition (Cornforth & Foster, 2013; Lang & Benbow, 2013), represented by the blue arrows) between three *E. coli* strains: a bacteriocidal toxin producer, a toxin-resistant, and a toxin-sensitive strain. B. Micrograph of a multi-strain biofilm on a nutrient agar plate. The producer, resistant and sensitive strains are in green (GFP), red (DsRedExpress) and black, respectively. C. Changes in strain frequency (upper part) and toxin concentration (lower part) as a function of time during a simulation run of the model. In the upper graph, yellow, orange, and purple lines represent the frequencies of the producer, the resistant, and the sensitive strains over time; in the lower graph, the red line represents the toxin concentration (which correlates, with some delay, with the frequency of the producer strain). D. Alternative representation of the strain frequencies shown in panel C as a "ternary plot." The strain frequency changes are represented as a trajectory between three vertices representing each one of the three genotypes: P for the producer, R for the resistant, and S for the sensitive strain. The three timepoints t1, t2, and t3 match between panels C and D. Ternary plot representations will be favored in the main figures of the article.

Materials and Methods

1. The experiments

1.1 3D-printed mini-bioreactor

A mini-bioreactor (Figure 2) was designed using the Autodesk Fusion 360 software and exported as an STL file (provided in the ESM). We also provide detailed CAD drawings of the design in the ESM. It was printed with the BioMed Clear (Formlabs, RS-F2-BMCL-01) resin with a layer height of 0.1 mm using a Formlabs 3b desktop 3D printer. This resin is certified to be biocompatible, water-proof, and autoclavable. The mini-bioreactor has a working volume of 1 mL. The medium is constantly renewed through an inflow connector, connected to a medium dispenser, and an outflow connector, connected to a waste container; the flow of medium is controlled by two pumps, one for the inlet, and one for the outlet. Sterile air supply is ensured by an aeration pipe connected to a 0.22 µm mesh filter. A funnel-shaped sampling chamber capped by a rubber stopper serves for inoculation and sampling purposes.

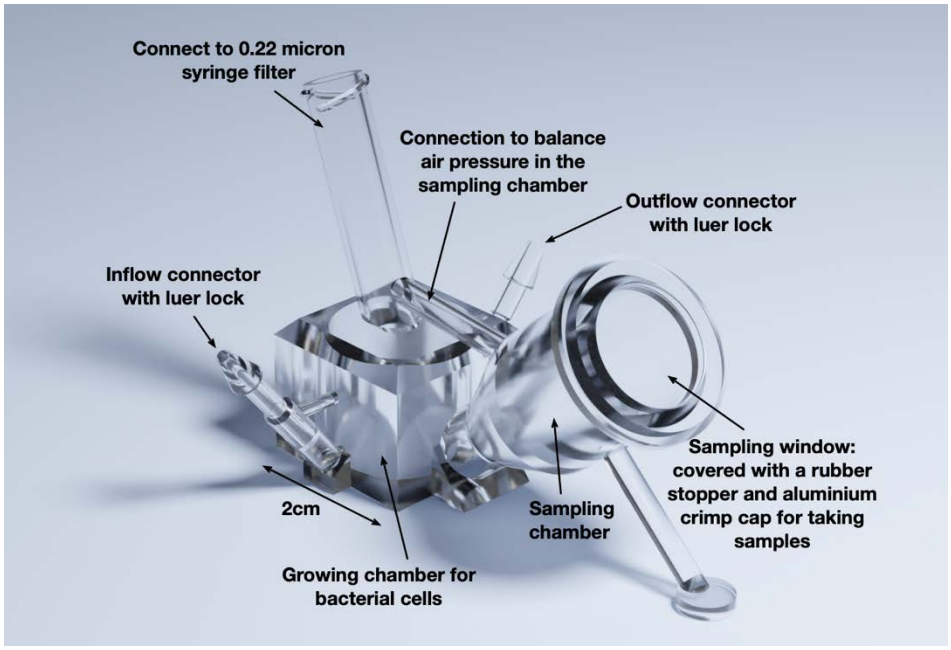

Figure 2. A 3D illustration of the mini-bioreactor used for continuous cultures of the bacterial communities in the experiments.

1.2 Bacterial strains

We use three strains of the bacterium *E. coli*: the BZB1011 pColA strain that harbors the pColA plasmid and produces colicin A (a pore-forming toxin); the BZB1011 *btuB* strain that does not produce the toxin but is resistant to it (mutation in the colicin A receptor BtuB); and the BZB1011 strain that neither produces the toxin nor is resistant to it [27]. The producer and resistant strains are chromosomally tagged with green and red fluorescence proteins, respectively; the cost of those markers has been shown to be negligible (Gonzalez et al., 2018). The three strains were cryo-preserved in 30% (v/v) glycerol at -80 °C. To reactivate the bacteria,

cells were first plated on the LB agar plates (10g/L Tryptone, Oxoid; 5 g/L NaCl, Sigma-Aldrich; 5 g/L Yeast Extract, Oxoid; 15 g/L Agar, Carl Roth) through polygonal spreading and grown overnight at 37 °C in darkness. We then prepared bacteria suspension from the overnight culture; the three strains were inoculated into liquid LB medium and grew at 37 °C under constant rotation (300 rpm) for 16 hours. After that, the bacterial suspension was centrifuged (5 minutes at 3000G) and then resuspended in physiological water (9 g/L NaCl, Sigma-Aldrich). The bacterial suspension of each strain was adjusted to an optical density (at 600 nm) of 1.0.

1.3 Culturing media

We prepared three culturing media with different proportions of nutrients by supplementing the minimal *E. coli* medium M63-salts (Ausubel et al., 2003) with different amounts of Casamino acids (Sigma-Aldrich) and D-glucose (Carl Roth). Casamino acids are hydrolyzed casein, which contains a complex mixture of protein subunits ready for bacteria to transform into cellular building blocks. The media with high, intermediate, and low Casamino acids-to-glucose (CA:G) ratios contained 10 g/L, 3 g/L, and 1 g/L of Casamino acids and 0 g/L, 7 g/L, and 9 g/L of D-glucose, respectively. Growing in the medium with low Casamino acids requires extensive anabolism to lead to protein and lipid biosynthesis. To minimize the potentially deleterious effects of the colicin resistance mutation in poor media, we also added 1.25 mg/L of cobalamin (Fluka) to each medium.

1.4 Quantification of the strain-specific growth rates under different conditions

Cultures of the three genotypes were diluted in the three different culturing media to an optical density of 0.01. The growth of eight 200 µL replicates was monitored in a 96-well-plates incubated at 37 °C with constant agitation for 48 hours in a Bio-Tek Synergy HT microplate reader. The optical density (600 nm) was measured once an hour. The growth rates were calculated based on data recorded during the exponential growth phase.

1.5 Experimental conditions and continuous culturing of the bacterial communities

We implemented a factorial design of three different culturing media and two dilution speeds for a total of six different experimental conditions. Five replicates of the bacterial communities (each in a separate mini-bioreactor) were prepared for each experimental condition. We used two multi-channel peristaltic pumps (Longer, LP-BT100-1L) to control the inflow and outflow of the media into and out of each mini-bioreactor. The inflow rate was set to either 250 µL/h (high flow rate) or 100 µL/h (low flow rate); the outflow was kept at a constant pumping speed of 1 mL/h. Because the outlet of the mini-bioreactor was placed higher than the inlet, having a higher pumping speed at the outlet ensures sufficient air exchange and a constant volume of 1 mL in the mini-bioreactors. After connecting the mini-bioreactors, we flushed them with 100 mL fresh medium at maximum pumping speed to prevent contamination. Finally, we mixed the cell suspensions of

each strain in equal proportions and pipetted 50 µl of the mixed bacterial suspensions into each mini-bioreactor by shortly removing the air filter. The mini-bioreactors were kept at 37 °C in the darkness for 14 days.

1.6 Quantification of the bacterial community composition

The relative abundances of the three *E. coli* strains in each mini-bioreactor were quantified each weekday during the two weeks of experiments. A 150 µL sample was taken using a sterile syringe (1 mL, Codan) with a needle (Ø0.6 × 60 mm, Sterican) through the rubber stopper on the sampling window of each mini-bioreactor. The sample was centrifuged for 5 minutes at 2000 x g and 145 µL of the supernatant was removed. The cells were then resuspended in the rest 5 µL of the medium and placed on an agar pad. We then took pictures of the agar pad under a microscope (Leica DM4 B) in sets of three — a phase contrast picture, a picture with the GFP settings, and a picture with the RFP settings. For each sample, we took at least two pictures at different random positions on the agar pad with at least 60 cells in each picture. The pictures were then analyzed using the FIJI software (version 2.3.0, (Schindelin et al., 2012)) with the StarDist 2D plugin (Schmidt et al., 2018) to count cells of different colors. We also manually checked the results of the automatic cell detection and corrected possible detection errors in each picture.

2. The simulation model

2.1 Model overview

To help better understand the experimental results, we designed a spatially explicit, individual-based simulation model. Our model was based on a 200×200 lattice with periodic boundaries, where each position contained information about the toxin concentration and its spatial occupation by at most one bacterial cell (Figure 3). We considered three bacterial cell types, corresponding to the colicin-producing, resistant, and sensitive strains of *E. coli* we used in the experiments. To initiate the simulation, we populated 1% of the positions in the lattice with a bacterium chosen at random among the three strains. The toxin concentration was set to zero everywhere. In each of the subsequent time points, we updated every position of the lattice following the order of (i) cell death and removal, (ii) toxin concentration dynamics (including the production, diffusion, and removal of colicin), and (iii) colonization of the empty positions by cell growth. The simulations were stopped either when coexistence was lost (i.e., only one cell type was left) or when they reached 300’000 steps. We implemented the model using the *Julia* programing language. The simulation codes are available from the corresponding authors upon request.

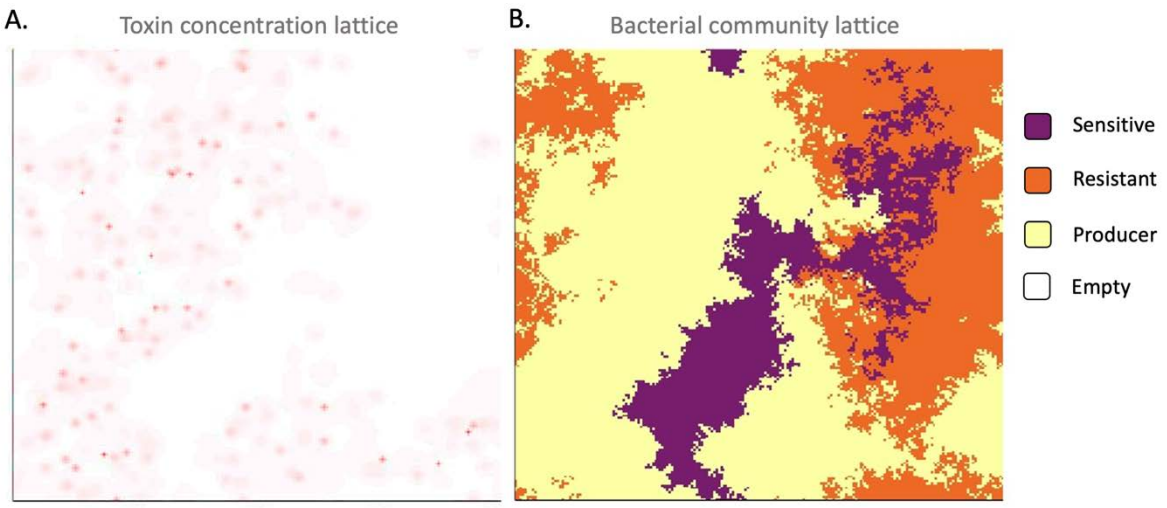

Figure 3. An illustration of the simulation model. Panels A and B show the toxin concentration and spatial occupation of bacterial cells in the lattice, respectively. The state of the simulation corresponds to timepoint t3 in Figure 1CD.

2.2 Simulation of cell death

Cells of different types can die due to different causes. Besides a baseline death probability (d_0) that we assumed to be identical for all cell types, the colicin-producing cells can also die from spontaneous lysis to release colicin, and the sensitive cells may be killed by colicin in the local environment. Because the resistant strain neither produces, nor can be killed by, colicin, its death probability $d_R = d_0$. The death probability of the colicin-producing strain $d_P = d_0 + d_l$, where d_l denotes the spontaneous lysis probability that was set to a positive constant. In contrast to the constant death probabilities of colicin-producing and resistant cells, the death probabilities of sensitive cells are spatially and temporally heterogeneous and depend on the local colicin concentration. We denote the death probability of a sensitive cell at location (i,j) as $d_{S_{i,j}} = d_0 + kc(x_{i,j},t)$, where k is a positive constant. The death probability $d_{S_{i,j}}$ is a linearly increasing function of the local colicin concentration c at the position $x_{i,j}$ at time step t. At each time step, all bacterial cells on the lattice may die at their corresponding strain- and location-specific probabilities. The death events occurred in random order, and the dead cells were removed to leave an empty space on the lattice.

2.3 Simulation of toxin concentration dynamics

The lysis of every colicin-producing cell releases an equal amount of colicin into the environment. The concentration dynamics of colicin are controlled by a set of partial differential equations

$$\frac{\partial c(x_{i,j},t)}{\partial t} = P(x_{i,j},t) - uc(x_{i,j},t) + D\nabla^2 c(x_{i,j},t), \quad \text{(Eq. 1)}$$

where $P(x_{i,j}, t)$ is the production rate of colicin, which equals a positive constant, p, if a colicin-producing cell was located at $x_{i,j}$ and just died at the current time step t; otherwise, it equals 0. The second term on the right-hand side of Eq. 1 describes the removal of colicin due to the bulk flow of culturing medium. Different values of the colicin removal rate u correspond to different medium flow rates that we implemented in the experiments. We assume that the spontaneous degradation rate of colicin is negligible relative to its removal by medium flow. The diffusion rate D in the last term of Eq. 1 controls the diffusion of colicin between close-by positions in the lattice. The value of D could be affected by factors such as the molecular mass of different colicin molecules and the pore size distribution in the biofilm where the cells are located. Assuming that colicin diffusion occurs at much faster rates than the death and division rates of bacterial cells, we can calculate the quasi-steady-state colicin distribution at time t by setting Eq. 1 to zero and solve for $c(x_{i,j}, t)$. We took the two-dimensional finite difference approximation of Eq. 1 and solved the 200×200 linear system using Fourier transformations following the methods in (Doekes et al., 2019). In the simulation model, the diffusion rate D is scaled so that it equals the fraction of colicin that diffused from one position to any of the four direct neighboring positions in the lattice at each time step. When $D = 1$, the colicin concentration is averaged over all positions at every time step.

2.4 Simulation of cell growth by colonizing empty spaces

A distinct feature of our model in contrast to typical existing lattice models of "rock-paper-scissors" games (reviewed in (Szolnoki et al., 2014)) is the way that we modeled growth. We did not allow cells of one type to replace any other type directly; instead, the growth of cells was space-limited, corresponding to exploitative competition where space is the limiting resource, such as in typical biofilms. To grow, a cell has to have access to an empty position among the eight positions in its direct neighborhood (i.e., the Moore neighborhood (Durrett & Levin, 1994)). Its probability of reproduction is a function of its own growth rate and the occupancy of the cells surrounding the position it attempts to divide into. Practically, for each empty position surrounded by at least one cell, the probability of this position becoming occupied by a colicin-producing, resistant, or sensitive cell was determined by the fraction of the strain's summed growth rates over the summed growth rates of all bacterial cells in the Moore neighborhood of the empty space. The strain-specific growth rate of sensitive cells was set to $r_S = 1$. Because toxin production and resistance cost resources that can be used otherwise for growth, we assumed that the growth rate of the resistant strain $r_R = r_S - v_R$ and the growth rate of the toxin-producing strain $r_P = r_S - v_R - v_P$, where v_R and v_P represent the cost of colicin resistance and production, respectively. A cell cannot reproduce twice during the same timestep.

Table 1. Parameters implemented in the simulation model.

d_0	Baseline per time step death probability of cells
d_l	Spontaneous lysis probability of the toxin-producing cells per time step
D	Diffusion rate of colicin
u	Removal rate of colicin by the flow of culturing medium
r_S	Growth rate of colicin sensitive cells
v_R	Cost on growth rate for colicin resistance
v_P	Cost on growth rate for colicin production
k	Killing rate of sensitive cells by colicin-induced cell lysis
p	Amount of toxin released when a producer cell lyses

Results

1. Experimental results

1.1 Growth rates of the three E. coli strains in different culturing media

Before studying the competition dynamics between the three *E. coli* strains, we first confirmed that their growth rates in monoculture fitted the requirements of a "rock-paper-scissors" game in the three different media used ("high CA:G," "intermediate CA:G," and "low CA:G"). We found that in all nutrient conditions, the sensitive strain had the highest growth rate, followed by the resistant strain, and by the colicin-producing strain. All pairwise comparisons between the growth rate distributions were still significant ($p < 0.001$) after using the Bonferroni correction for multiple comparisons (Figure 4). The average cell doubling times of the *E. coli* strains are shown in Appendix Figure S1. Because of the relatively low nutrient availability in all the culturing media, the doubling times were longer than the typical 20 minutes in rich medium but probably shorter than in the wild (Gibson et al., 2018). While strains grew faster with higher CA:G ratio, the numerical growth rate difference between the strains was relatively consistent across different nutrient conditions, with a growth rate increment of 0.020 ± 0.005 from the colicin-producing strain to the resistant strain, and an increment of 0.018 ± 0.009 from the resistant strain to the sensitive strain. The relative growth rate difference between the toxin-producing and sensitive strains, however, decreased as the CA:G ratio increased in the medium. The growth rate of the colicin producer strain was 22.0% less than the sensitive strain in the medium with the lowest CA:G ratio, and it was only 14.5% less in the medium with the highest CA:G ratio. This result is consistent with a reduction of colicin-producing cost in richer media, suggesting that the fraction of colicin-producing strains that lyse to release toxin might have decreased as the CA:G ratio increased in the medium. [34]

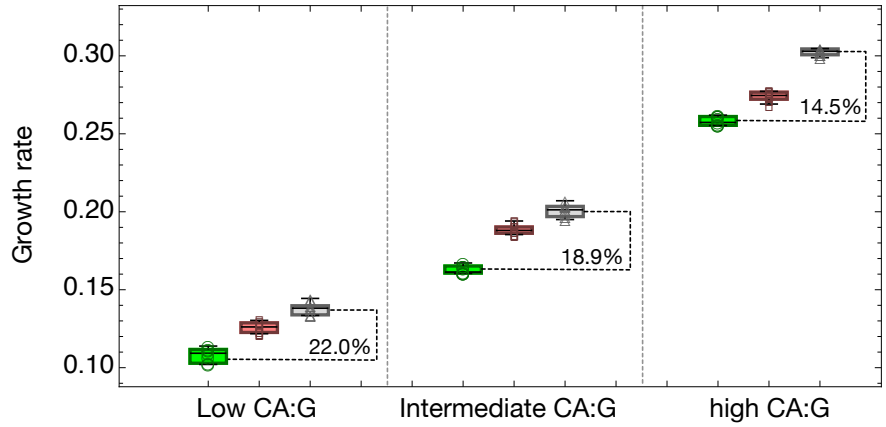

Figure 4. The growth rates of three *E. coli* strains under different nutrient conditions. The box-whisker charts filled with green, red, and gray colors and marked with circle, square, and triangle markers represent the toxin-producer, the resistant, and the sensitive strains, respectively. The boxplot center lines show the mean, box limits show upper and lower quartiles, whiskers show the 1.5x interquartile range, and each marker corresponds to the result of an independent replicate. We have eight replicates for each bacterial strain and culturing medium combination.

1.2 Effects of nutrient and flow regime on the competition dynamics of E. coli strains

We next followed the population dynamics of the three *E. coli* strains in the three different media and under two different flow regimes (slow and fast) for two weeks in the 3D-printed mini-bioreactors. We found consistent effects of the nutrient condition and the flow regime on the community composition trajectories (Figure 5). In the high CA:G ratio medium, the producer dominated the competition, making up more than 80% of the bacterial population over the entire duration of the experiments after the first day, but neither the resistant nor the sensitive strain became extinct. In contrast, the resistant and sensitive strains appeared more competitive in the medium with low CA:G ratio, where the producer never reached more than 10% of the population. In the medium with intermediate CA:G ratio, the competition outcomes were variable among the replicates, suggesting that the overall competitivities of the three strains were closer in this nutrient environment.

Besides the marked effect of the nutrient environment, the effect of the medium flow rate on the competition dynamics was also noteworthy. In the medium with low CA:G ratio, the flow rate determined which between the resistant and sensitive strain dominated the competition in the time window of our experiments: while a higher flow rate favored the sensitive strain, a lower flow rate favored the resistant strain. This result could be caused by different colicin removal rates. A higher flow rate would give an advantage to the sensitive cells by removing the toxin more quickly. The competition dynamics under low flow rate in the medium with intermediate CA:G ratio were most interesting: all replicates followed a consistent community composition trajectory over time, but the trajectories of different replicates strongly diverged from one another. This

suggests that the slightly different initial community composition caused by stochasticity in the inoculation or during the first hours of the experiments may have strongly impacted the subsequent evolutionary trajectories. This could happen if the overall competitiveness of the three strains were in a much closer range under this experimental condition than in the other conditions we tested.

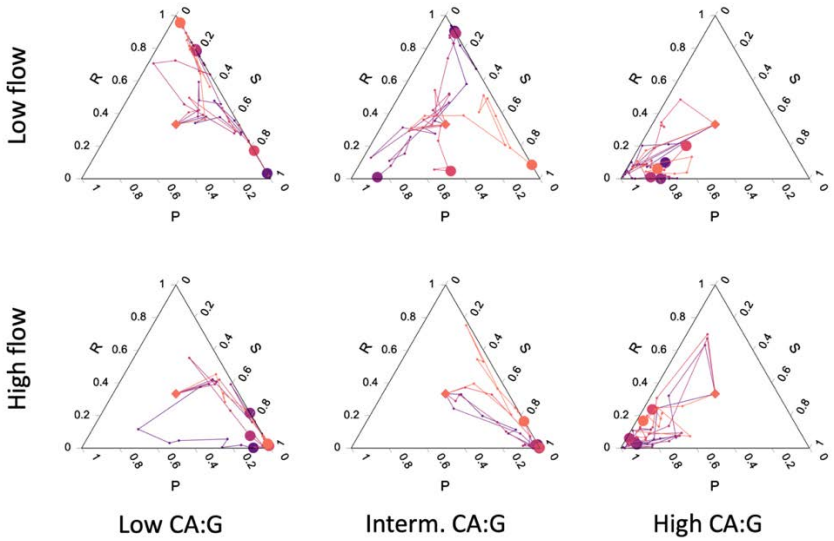

Figure 5. Ternary plots of the community composition of three *E. coli* strains over two weeks in three different media and under two different flow regimes. The frequency of each strain at each time point can be read on the respective side of the ternary plot. Five independent trajectories were plotted in different colors under each condition. The starting point of all trajectories is marked by a diamond; the end point of each trajectory is marked with a circle.

2. Simulation results

2.1 *Slower toxin diffusion tends to promote strain coexistence, but up to a limit*

To explore in more detail the impact of diffusion, flow, and growth rate on the population dynamics of the three *E. coli* strains, we designed and implemented a spatially explicit model of bacterial toxin-based cyclic competition. We first assessed the impact of toxin diffusion on the coexistence of the three competing strains. The simulations tended to produce longer coexistence times when slower toxin diffusion rates were used (Figure 6; Figure S2). Very short coexistence and no cyclic dominance were characteristic of the instantaneous toxin diffusion case, which is equivalent, when it comes to the toxin concentration, to a well-mixed environment (Figure 6, $D = 1.0$). Because, in this case, sensitive cells are killed at random over the entire lattice, the toxin gives the same advantage to the resistant as to the producer cells; since the resistant cells grow faster than the producer, the resistant wins whenever the toxin reaches concentrations sufficient to eradicate the sensitive and the sensitive wins whenever they do not. With slower diffusion rates, the sensitive population becomes less affected overall by the same amount of released toxin because it takes more time for it to reach patches of sensitive cells; however, in this case, the dying sensitive cells are more

often located at the interface with producer patches, which helps the latter strain conquer new space and gives it a colonization advantage. Nevertheless, below a certain toxin diffusion threshold, coexistence breaks down again: the toxin does not diffuse fast enough to free space around the growing producer patch and to help its population increase in frequency. Coexistence is therefore only possible at intermediate toxin diffusion rates.

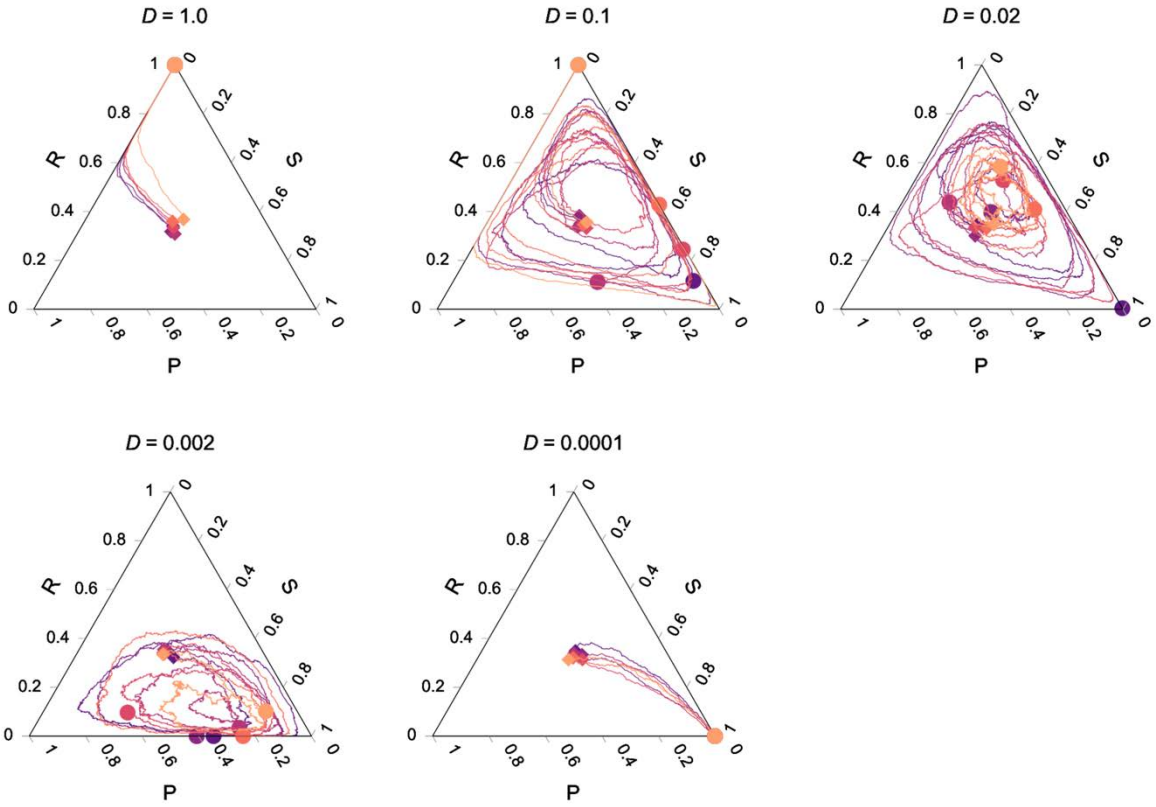

Figure 6. Competition dynamics between the three *E. coli* strains at different toxin diffusion rates (D). Very high ($D = 1.0$) and very low ($D = 0.0001$) toxin diffusion rates were detrimental to the colicin-producing strain. At intermediate diffusion rates, the frequencies of the three *E. coli* strains fluctuate in cycles that can be more or less favorable to one of the three strains. The spontaneous lysis rate of the colicin producers and the removal rate of colicin were set to intermediate values: $d_l = 10^{-4}$, and u =0.015. Six independent simulation trajectories were plotted in different colors under each condition. The start point and end point of each trajectory are marked with a diamond and a circle of the same color as the trajectory, respectively.

2.2 Strain coexistence is favored at intermediate toxin accumulation

The levels of toxin in the system are controlled by the producer lysis rate (d_l), which correlates with toxin release, and by the toxin removal rate (u) through medium flow. Both parameters can impact the concentration of toxin in the system, as can be observed in a community consisting of the colicin producer strain only (Figure 7A; Supplementary Figure S3): decreasing d_l and increasing u both lead to lower toxin levels in the system. Although toxin does not reach a steady state in populations comprising all three strains

because the producer frequency fluctuates over time, the amount of the toxin contributed by each producer cell which is retained in the system (or "toxin retention"), $pd_l(1-u)$, hereafter denoted as c^*, nonetheless controls toxin accumulation in the system. Our simulations showed that long-term coexistence is favored at intermediate c^* levels. When the values of c^* were too high, like in the cases of low or medium flow rates ($u = 0.0075$ or $u = 0.015$) in combination with high toxin release rates (d_l=3e-4) (Figure 7B), most of the sensitive cells were killed at the very beginning of the simulations runs, and the producer was subsequently outcompeted by the resistant strain. In such cases, coexistence broke down quickly, with either the resistant or the sensitive strain (if some sensitive cells happen to survive the initial colicin wave) dominating the entire population while the other two strains went extinct. In contrast, when the values of c^* were too low, like in the cases of high or medium flow rates ($u = 0.015$ or $u = 0.03$) in combination with low toxin release rate (d_l = 3e-5) (Figure 7B), the colicin producers were not able to maintain a toxin level that was high enough to kill sensitive cells. Consequently, the sensitive strain, which has the highest growth rate, excluded the other two strains. Only when c^* was kept within an intermediate range, cyclic population dynamics could emerge, and the coexistence of the strains could be maintained for a relatively long duration.

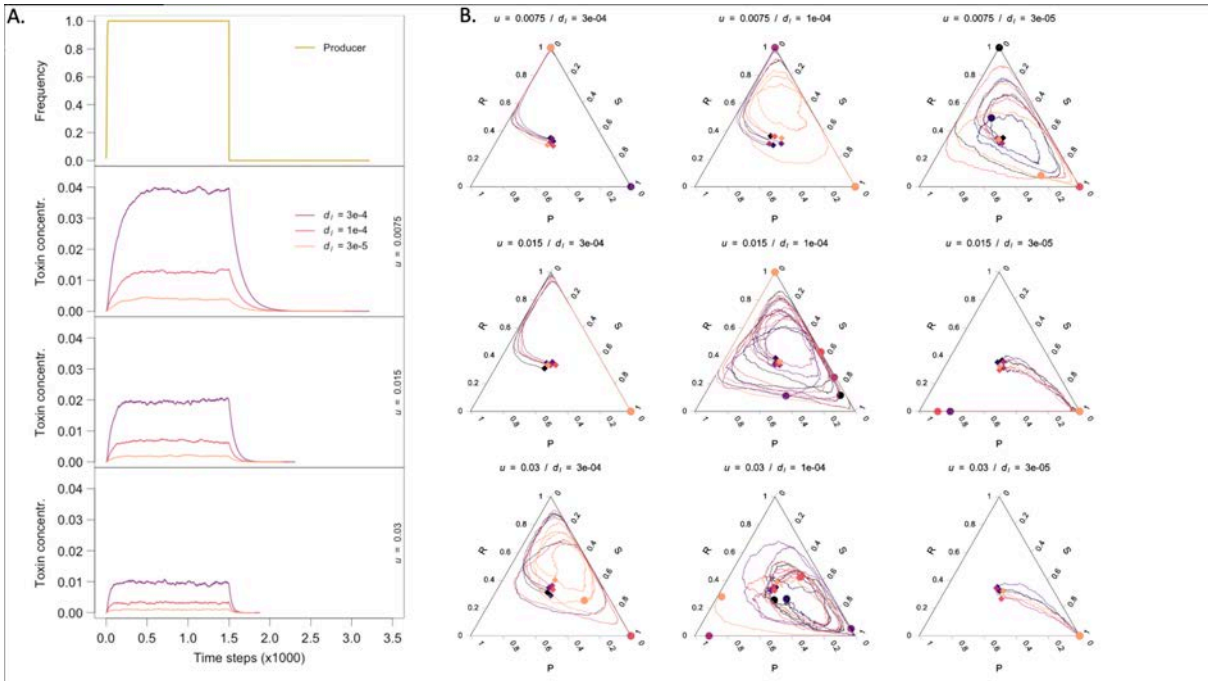

Figure 7. The impact of toxin accumulation on population dynamics. A. Toxin accumulation and toxin removal in a producer population at different toxin production and removal rates. A producer population was left to occupy the entire space for 1500 time steps and then eliminated; toxin increase and decrease (until it reaches the 1e-7 threshold) is observed. Three elements emerge that could affect the strain population dynamics: (1) the toxin steady-state level (plateau), which is the resultant of both production and removal rates and seems to have the highest impact on coexistence, (2) the toxin accumulation rate when the producer population is growing, mainly impacted by the toxin production rate, and (3) the toxin concentration decrease

rate when the producer population plummets, mainly impacted by the toxin removal rate. B. Population trajectory for the nine combinations of toxin production and removal rates we used in panel A. The toxin diffusion rate is set to fast (D=0.1); the plots for instantaneous (D=1.0) and slow (D=0.02) diffusion rates can be found in Supplementary Figure S4 for comparison. There are six independent simulation trajectories under each condition, indicated by lines of different colors. The start point and end point of each trajectory are marked with a diamond and a circle of the same color as the trajectory, respectively. Toxin production rate d_l=3e-5, 1e-4, 3e-4; toxin removal rate u=0.0075, 0.015, 0.03.

2.3 Extreme toxin fluxes can lead to population fluctuations that break down coexistence

Although the lysis rate of the colicin producers d_l and the removal rate of toxin u can both influence the accumulation of colicin in the system, their effects on the competition dynamics between the bacterial strains are not entirely interchangeable. The former controls how fast colicin can accumulate in the system (Figure 7A, colicin concentration rose faster at higher d_l values); the latter controls how fast colicin can be flushed out (Figure 7A, colicin concentration returned to zero faster at higher u values). At the bacterial population level, d_l determines the speed of the sensitive strain collapse when the producer frequency starts to increase, whereas u determines if and when the sensitive strain can bounce back from a toxin wave after the producer's frequency has declined. To show the effects of d_l and u without confounding effects, we adjusted these two parameters correlatively while maintaining the toxin retention, c^*, constant (Figure 8; Supplementary Figure S5). At too low and too high d_l and u values, long-term coexistence between the strains was compromised. In the former case, the toxin was not removed fast enough at the onset of the competition and the sensitive strain was heavily hit by the initial toxin wave leading to the dominance of the resistant strain (or rarely, after a bounce-back, the sensitive strain) over the producer. At too high d_l and u values, the toxin could not be accumulated to a high enough concentration to threaten the sensitive population at the onset of the competition, which then favored the sensitive strain (or sometimes the producer) at the expense of the resistant strain. Such extreme toxin fluxes, through their effect on the sensitive population, increase the probability for one of the three strains to be outcompeted at the very beginning of the competition and for coexistence to break down. Under intermediate toxin production and removal rates, by contrast, the fluctuations of toxin levels were damped, which limited the amplitude of changes in the sensitive and producer populations density and the risk of global disbalance that it entails. Both toxin accumulation and toxin flux need therefore to be within an intermediate range to support long-term strain coexistence.

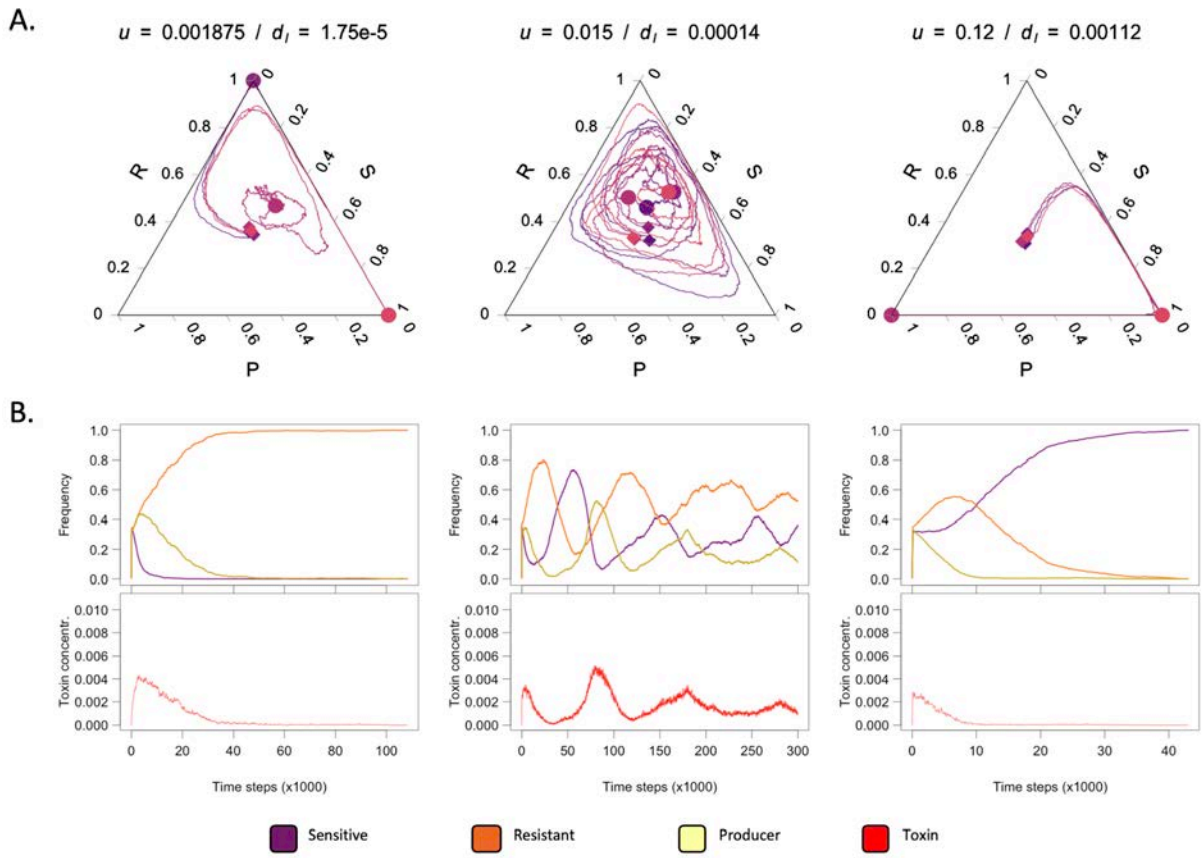

Figure 8. The impact of toxin flux on population dynamics. A. Impact of increasing flow and toxin production on cyclic competition patterns with the toxin retension, c^*, kept constant. There are four independent simulation trajectories under each condition, indicated by lines of different colors. The start point and end point of each trajectory are marked with a diamond and a circle of the same color as the trajectory, respectively. B. Dynamics over time of the three strains and the toxin levels for one of the four replicates. Diffusion rate D = 0.02.

2.4 The individual and population components of toxin production cost affect competition dynamics in similar ways

In the colicin system, the toxin production cost has two components: the cost, paid by all cells, of carrying the toxin producing gene (v_P), which lowers the growth rate, and the cost of random cell lysis (d_l) that is needed for toxin release. While the first type of cost slows down the growth and affects competition primarily at the edge of growing patches, the second type of cost increases the death rate randomly over the entire population and multiplies foci of toxin release. To test how these two types of cost affected the system, we ran the model in two ways while keeping c^* constant: 1. by varying the cost of carrying the toxin gene (v_P), while maintaining the growth rates of the sensitive and the resistant strains unchanged; 2. by varying the lysis rate of the toxin-producing strain (d_l) together with the amount of toxin released per lysis event (p). Increasing any of the two types of toxin production cost had similar effects: the center of the population

trajectories shifted towards the corner of the sensitive strain in the ternary plots, making it more likely for the sensitive than for the resistant to win the competition (Figure S6). However, modifications of the second type of cost had a much stronger effect on population dynamics than the first when the overall cost ($v_P + d_l$) were considered. This is because increasing the lysis frequency and decreasing the amount of toxin released, even when keeping the value of c^* identical, changes the toxin distribution over the lattice and thereby profoundly affects the capacity of the producer to interfere with the sensitive strain.

2.5 Varying the relative growth rates between competing strains can influence the competition outcome

Finally, we used our simulation model to test the potential consequences of differences in growth rates between strains in the range of the ones we observed in the experimental part (Figure 4). We ran simulations with the same parameters as in Figure 7B, but with smaller or larger differences in relative growth rates between the three strains by changing the cost of resistance (v_R) and of toxin production (v_P). To support lasting coexistence, lower growth rate differences needed to be compensated by a decrease in the expected retention of toxin contributed by each producer cell, c^*; on the contrary, with higher growth rate differences between the strains, coexistence would generally require higher c^* (Figure S7). This indicates that ecology-driven changes in the relative growth rates between strains, like the ones we observed between the three media in our experimental system, could lead to differences in competition outcome and population dynamics.

Discussion

In this work, we use lab experiments and individual-based simulations to study how relevant ecological factors affect the competition dynamics and coexistence between toxin-producing, toxin-resistant, and sensitive *E. coli* strains. This experimental system is used as a model for cyclic dominance in the "rock-paper-scissors" evolutionary game. The main ecological factors and processes we considered are the impact of resources (i.e., amino acids and glucose) on growth and the accumulation, diffusion, and removal of toxin, which are known to be key variables in *E. coli's* natural environment. The different nutrient conditions we tested by changing the CA:G ratio could emulate aspects of E. coli's biphasic lifestyle inside and outside hosts (Ihssen & Egli, 2005; van Elsas et al., 2011) or mimic a commensal vs pathogenic adaptation (Alteri et al., 2009; Chang et al., 2004). In complex environments like the mammalian gut, diffusion and flow greatly vary depending on growth conditions, especially on whether cells are in a planktonic or in a sessile state within a biofilm (Flemming & Wingender, 2010; Maunders & Welch, 2017). Viscosity is known to promote the maintenance of high levels of toxin production in colicinogenic strains because it ensures producer cell assortment (le Gac & Doebeli, 2010), but most likely also because it slows down diffusion and increases the benefit of toxin production as our model shows (Figure 6).

In our experiments, the most dramatic difference in competition outcome was due to the nutrients: while the toxin producer dominated under high CA:G, it was largely outcompeted under lower CA:G. To understand this result, it is important to observe that the *E. coli* system of cyclic dominance is fueled by two different types of competition: 1. exploitative competition, which is competition for a shared resource (e.g. nutrients) and plays a major role in the interactions between sensitive and resistant and between resistant and producer strains; 2. interference competition, which occurs when one competitor directly harms another, like when the producer secretes toxins to kill the sensitive strain. These two types of competition present very different dynamics and respond very differently to ecological factors (Cornforth & Foster, 2013; Lang & Benbow, 2013). The timescale of competition is typically long for exploitative competition, whose effect, in our system, requires several generations, while it is short for interference competition, since sensitive cells can be decimated within minutes once a toxin concentration threshold is reached. In the high CA:G medium, the density of all strains, including toxin producers, are higher, leading to higher overall toxin concentrations. Moreover, the relative growth rate differences between the colicin producer and the resistant strains are also smaller in this condition. The combined effect likely helped the colicin producer strain to outcompete the sensitive strain more easily in the medium with high CA:G ratio. Nevertheless, we expect that the resistant cells remaining in communities in the high CA:G medium would eventually take over the dominance if we followed the competition dynamics for a longer duration.

A feature of our work is to focus on the biological relevance of our experimental system and model design. Instead of implementing serial transfers of colonies like in previous experimental studies of the "rock-paper-scissors" dynamics (Kerr et al., 2002b; Liao et al., 2020), we designed and 3D-printed mini-bioreactors where we can keep the competing community in continuous culture. This, for example, allowed us to observe the effect of the toxin remaining in the system on the competition dynamics after the producer population had disappeared (Figure 5, low CA:G, low flow). By catching the "ghost of the colicin producers", we were able to explain the counterintuitive result that the resistant strain increased in frequency in competition with the sensitive strain for several days under low medium flow rate after the population of the producer strain had crashed. In previous simulation models, because toxin was rarely modeled explicitly, mobility of individuals was often introduced to allow cells at some distance to interact with each other. The models have produced interesting results, such as intermediate mobility promotes coexistence (Reichenbach et al., 2007, 2008), and long-distance mobility tends to cause coexistence to break down (Rulquin & Arenzon, 2014; G.-Y. Zhang et al., 2009). The way mobility was modeled was often by swapping the position of two cells or swapping the position of a cell and an empty space. It is still controversial whether those types of movement may occur in microbial biofilms, where the extracellular polymeric substances build up a matrix-like structure that limits the free movement of cells. In our model, we did not allow the cells to move, and all interactions were through the diffusion of toxin. Our finding that intermediate toxin diffusion rate promotes coexistence draws an analogy to the previous finding that intermediate mobility of individuals promotes coexistence, but

is more biologically relevant and has important implications. For example, while we know that spatial structure promotes coexistence in the *E. coli* system (Hol et al., 2014a; Kerr et al., 2002; Liao et al., 2020), the fact that population structure without restricted toxin diffusion does not support coexistence has not been sufficiently emphasized.

It is often challenging to predict the competition dynamics and outcome between multiple interacting species in complex environments where ecological factors and processes can influence the relative competitiveness between organisms. Recently, it has been found that fairly accurate predictions of the behavior of such complex systems can be achieved by some simple rules (Friedman et al., 2017). In our work, we found that what we called toxin retention (c^*), which is determined by the balance between toxin release and removal, is a useful simple indicator of the propensity of long-term coexistence between the *E. coli* strains. We found that intermediate c^* generally promotes coexistence, although extreme toxin fluxes caused by extreme toxin release and removal rates can lead to strong population fluctuations and premature collapse of coexistence. Such simple indicators, if widely applicable, can be very useful in predicting the behavior of cyclic competition dynamics in complex natural environments. We therefore encourage empirical tests in other communities where species interact in "rock-paper-scissors" games.

Evolutionary game theory, through its development in the last 50 years since the seminal work of Maynard Smith and Price (Maynard Smith & Price, 1973) that opened up this field, has provided great convenience for modeling and helping us understand complex evolutionary scenarios. Classic evolutionary game models, however, often rely on simple assumptions that ignore the mechanisms underlying the strategies, and do not consider how they might be influenced by ecological factors and processes. Because theoretical studies of evolution have been more advanced than their empirical counterpart in the early days of evolutionary game theory, simple assumptions such as the "phenotypic gambit" (Grafen, 1984) were often necessary. However, we should not forget that ecology sets up the theatre for the evolutionary play (Hutchinson, 1965; Post & Palkovacs, 2009), and evolutionary game models should not ignore ecological details. Nowadays, empirical studies of ecology and evolution are much more advanced, thanks to new technological developments like the sequencing and manipulation of genetic materials, convenient analysis of biochemical molecules and their properties, as well as 3D printing that allows us to build customized devices quickly at low costs. Theoreticians also have gained access to new analytical tools and unprecedented computational power. Equipped with these new tools and accumulating knowledge in both the empirical and theoretical studies of ecology and evolution, it should be our new goal to integrate mechanisms underlying evolutionary strategies into the models for the development of evolutionary game theory in the future.

Acknowledgement

We would like to thank Camille Tinguely and Valentin Voegeli for helpful discussions, and Céline Terrettaz for support with the experiments. The study is funded by the Swiss National Science Foundation grant PZ00P3_180142 to D.G. and grant PZ00P3_180145 to X-Y.L.R, and the Novartis Foundation for medical-biological Research grant 19A023 to D.G.

References

1. Czárán TL, Hoekstra RF, Pagie L. 2002 Chemical warfare between microbes promotes biodiversity. *Proceedings of the National Academy of Sciences* **99**, 786–790.
2. Kerr B, Riley MA, Feldman MW, Bohannan BJM. 2002 Local dispersal promotes biodiversity in a real-life game of rock–paper–scissors. *Nature* **418**, 171–174.
3. Kirkup BC, Riley MA. 2004 Antibiotic-mediated antagonism leads to a bacterial game of rock–paper–scissors in vivo. *Nature* **428**, 412–414.
4. Reichenbach T, Mobilia M, Frey E. 2007 Mobility promotes and jeopardizes biodiversity in rock-paper-scissors games. *Nature* **448**, 1046–1049.
5. Sinervo B, Lively CM. 1996 The rock–paper–scissors game and the evolution of alternative male strategies. *Nature* **380**, 240–243.
6. Taylor DR, Aarssen LW. 1990 Complex competitive relationships among genotypes of three perennial grasses: implications for species coexistence. *The American Naturalist* **136**, 305–327.
7. Cameron DD, White A, Antonovics J. 2009 Parasite–grass–forb interactions and rock–paper–scissor dynamics: predicting the effects of the parasitic plant *Rhinanthus minor* on host plant communities. *Journal of Ecology* **97**, 1311–1319.
8. Soliveres S *et al.* 2015 Intransitive competition is widespread in plant communities and maintains their species richness. *Ecology Letters* **18**, 790–798.
9. Stubbendieck RM, Straight PD. 2016 Multifaceted interfaces of bacterial competition. *Journal of Bacteriology* **198**, 2145–2155.
10. Granato ET, Meiller-Legrand TA, Foster KR. 2019 The evolution and ecology of bacterial warfare. *Current Biology* **29**, R521–R537.
11. Liao MJ, Miano A, Nguyen CB, Chao L, Hasty J. 2020 Survival of the weakest in non-transitive asymmetric interactions among strains of E. coli. *Nature Communications* **11**, 6055.
12. Gordon DM, Riley MA, Pinou T. 1998 Temporal changes in the frequency of colicinogeny in *Escherichia coli* from house mice. *Microbiology (N Y)* **144**, 2233–2240.
13. Riley MA, Gordon DM. 1999 The ecological role of bacteriocins in bacterial competition. *Trends in Microbiology* **7**, 129–133.
14. Schreiber SJ, Killingback TP. 2013 Spatial heterogeneity promotes coexistence of rock-paper-scissors metacommunities. *Theoretical Population Biology* **86**, 1–11.
15. Müller APO, Gallas JAC. 2010 How community size affects survival chances in cyclic competition games that microorganisms play. *Physical Review E* **82**, 52901.
16. Frean M, Abraham ER. 2001 Rock–scissors–paper and the survival of the weakest. *Proceedings of the Royal Society B* **268**, 1323–1327.
17. Neumann G, Schuster S. 2007 Continuous model for the rock–scissors–paper game between bacteriocin producing bacteria. *Journal of Mathematical Biology* **54**, 815–846.
18. Nahum JR, Harding BN, Kerr B. 2011 Evolution of restraint in a structured rock–paper–scissors community. *Proceedings of the National Academy of Sciences* **108**, 10831–10838.
19. Miller BM, Liou MJ, Lee J-Y, Bäumler AJ. 2021 The longitudinal and cross-sectional heterogeneity of the intestinal microbiota. *Current Opinion in Microbiology* **63**, 221–230.
20. Cascales E, Buchanan SK, Duché D, Kleanthous C, Lloubes R, Postle K, Riley M, Slatin S, Cavard D. 2007 Colicin biology. *Microbiology and Molecular Biology Reviews* **71**, 158–229.

21. Götz A, Lechner M, Mader A, von Bronk B, Frey E, Opitz M. 2018 CsrA and its regulators control the time-point of ColicinE2 release in *Escherichia coli*. *Scientific Reports* **8**, 6537.
22. Yang T-Y, Sung Y-M, Lei G-S, Romeo T, Chak K-F. 2010 Posttranscriptional repression of the cel gene of the ColE7 operon by the RNA-binding protein CsrA of *Escherichia coli*. *Nucleic Acids Research* **38**, 3936–3951.
23. Ghazaryan L, Tonoyan L, Ashhab A al, Soares MIM, Gillor O. 2014 The role of stress in colicin regulation. *Arch Microbiol* **196**, 753–764.
24. Sandrin D *et al.* 2016 Diffusion of macromolecules in a polymer hydrogel: from microscopic to macroscopic scales. *Physical Chemistry Chemical Physics* **18**, 12860–12876.
25. Cornforth DM, Foster KR. 2013 Competition sensing: the social side of bacterial stress responses. *Nature Reviews Microbiology* **11**, 285–293.
26. Lang JM, Benbow ME. 2013 Species interactions and competition. *Nature Education Knowledge* **4**, 8.
27. Gonzalez D, Sabnis A, Foster KR, Mavridou DAI. 2018 Costs and benefits of provocation in bacterial warfare. *Proceedings of the National Academy of Sciences* **115**, 7593 – 7598.
28. Ausubel FM, Brent R, Kingston RE, Moore DD, Seidman JG, Smith JA, Struhl K, editors. 2003 *Current Protocols in Molecular Biology*. John Wiley & Sons, Inc.
29. Schindelin J *et al.* 2012 Fiji: an open-source platform for biological-image analysis. *Nature Methods* **9**, 676–682.
30. Schmidt U, Weigert M, Broaddus C, Myers G. 2018 Cell Detection with Star-Convex Polygons. *Medical Image Computing and Computer Assisted Intervention - MICCAI 2018 - 21st International Conference, Granada, Spain, September 16-20, 2018, Proceedings, Part II* , 265–273.
31. Doekes HM, de Boer RJ, Hermsen R. 2019 Toxin production spontaneously becomes regulated by local cell density in evolving bacterial populations. *PLoS Computational Biology* **15**, e1007333.
32. Szolnoki A, Mobilia M, Jiang L-L, Szczesny B, Rucklidge AM, Perc M. 2014 Cyclic dominance in evolutionary games: a review. *Journal of the Royal Society Interface* **11**, 20140735.
33. Durrett R, Levin SA. 1994 Stochastic spatial models: a user's guide to ecological applications. *Philosophical Transactions of the Royal Society B* **343**, 329–350.
34. Gibson B, Wilson DJ, Feil E, Eyre-Walker A. 2018 The distribution of bacterial doubling times in the wild. *Proceedings of the Royal Society B* **285**, 20180789.
35. van Elsas JD, Semenov A v, Costa R, Trevors JT. 2011 Survival of *Escherichia coli* in the environment: fundamental and public health aspects. *The ISME Journal* **5**, 173–183.
36. Ihssen J, Egli T. 2005 Global physiological analysis of carbon-and energy-limited growing Escherichia coli confirms a high degree of catabolic flexibility and preparedness for mixed substrate utilization. *Environmental Microbiology* **7**, 1568–1581.
37. Chang D-E *et al.* 2004 Carbon nutrition of *Escherichia coli* in the mouse intestine. *Proceedings of the National Academy of Sciences* **101**, 7427–7432.
38. Alteri CJ, Smith SN, Mobley HLT. 2009 Fitness of *Escherichia coli* during urinary tract infection requires gluconeogenesis and the TCA cycle. *PLoS Pathogens* **5**, e1000448.
39. Flemming H-C, Wingender J. 2010 The biofilm matrix. *Nature Reviews Microbiology* **8**, 623–633.
40. Maunders E, Welch M. 2017 Matrix exopolysaccharides; the sticky side of biofilm formation. *FEMS Microbiology Letters* **364**, fnx120.
41. le Gac M, Doebeli M. 2010 Environmental viscosity does not affect the evolution of cooperation during experimental evolution of colicigenic bacteria. *Evolution (N Y)* **64**, 522–533.
42. Reichenbach T, Mobilia M, Frey E. 2008 Self-organization of mobile populations in cyclic competition. *Journal of Theoretical Biology* **254**, 368–383.
43. Rulquin C, Arenzon JJ. 2014 Globally synchronized oscillations in complex cyclic games. *Physical Review E* **89**, 32133.
44. Zhang G-Y, Chen Y, Qi W-K, Qing S-M. 2009 Four-state rock-paper-scissors games in constrained Newman-Watts networks. *Physical Review E* **79**, 62901.
45. Hol FJH, Voges MJ, Dekker C, Keymer JE. 2014 Nutrient-responsive regulation determines biodiversity in a colicin-mediated bacterial community. *BMC Biology* **12**, 68.
46. Friedman J, Higgins LM, Gore J. 2017 Community structure follows simple assembly rules in microbial microcosms. *Nature Ecology & Evolution* **1**, 109.

47. Holdridge EM, Cuellar-Gempeler C, terHorst CP. 2016 A shift from exploitation to interference competition with increasing density affects population and community dynamics. *Ecology and Evolution* **6**, 5333–5341.
48. Jensen AL. 1987 Simple models for exploitative and interference competition. *Ecological Modelling* **35**, 113–121.
49. Maynard Smith J, Price GR. 1973 The logic of animal conflict. *Nature* **246**, 15–18.
50. Grafen A. 1984 Natural selection, kin selection and group selection. In *Behavioural Ecology: An Evolutionary Approach* (eds JR Krebs, NB Davies), pp. 62–84. Blackwell Scientific.
51. Hutchinson GE. 1965 *The Ecological Theater and the Evolutionary Play*. Yale University Press.
52. Post DM, Palkovacs EP. 2009 Eco-evolutionary feedbacks in community and ecosystem ecology: interactions between the ecological theatre and the evolutionary play. *Philosophical Transactions of the Royal Society B* **364**, 1629–164

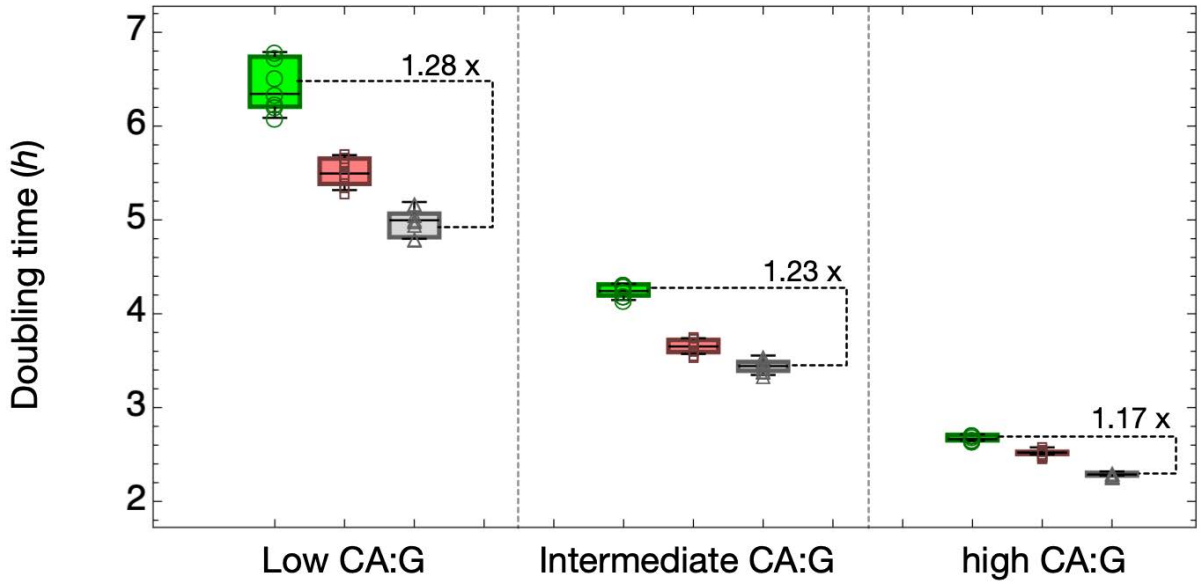

Figure S1. The doubling of three *E. coli* strains under different nutrient availability conditions. The box-whisker charts filled with green, red, and gray colors and marked with circle, square, and triangle markers represent the toxin-producer, the resistant, and the sensitive strains, respectively. The boxplot center lines show the mean, box limits show upper and lower quartiles, whiskers show the 1.5x interquartile range, and each marker corresponds to the result of an independent replicate. We have eight replicates for each bacterial strain and culturing medium combination.

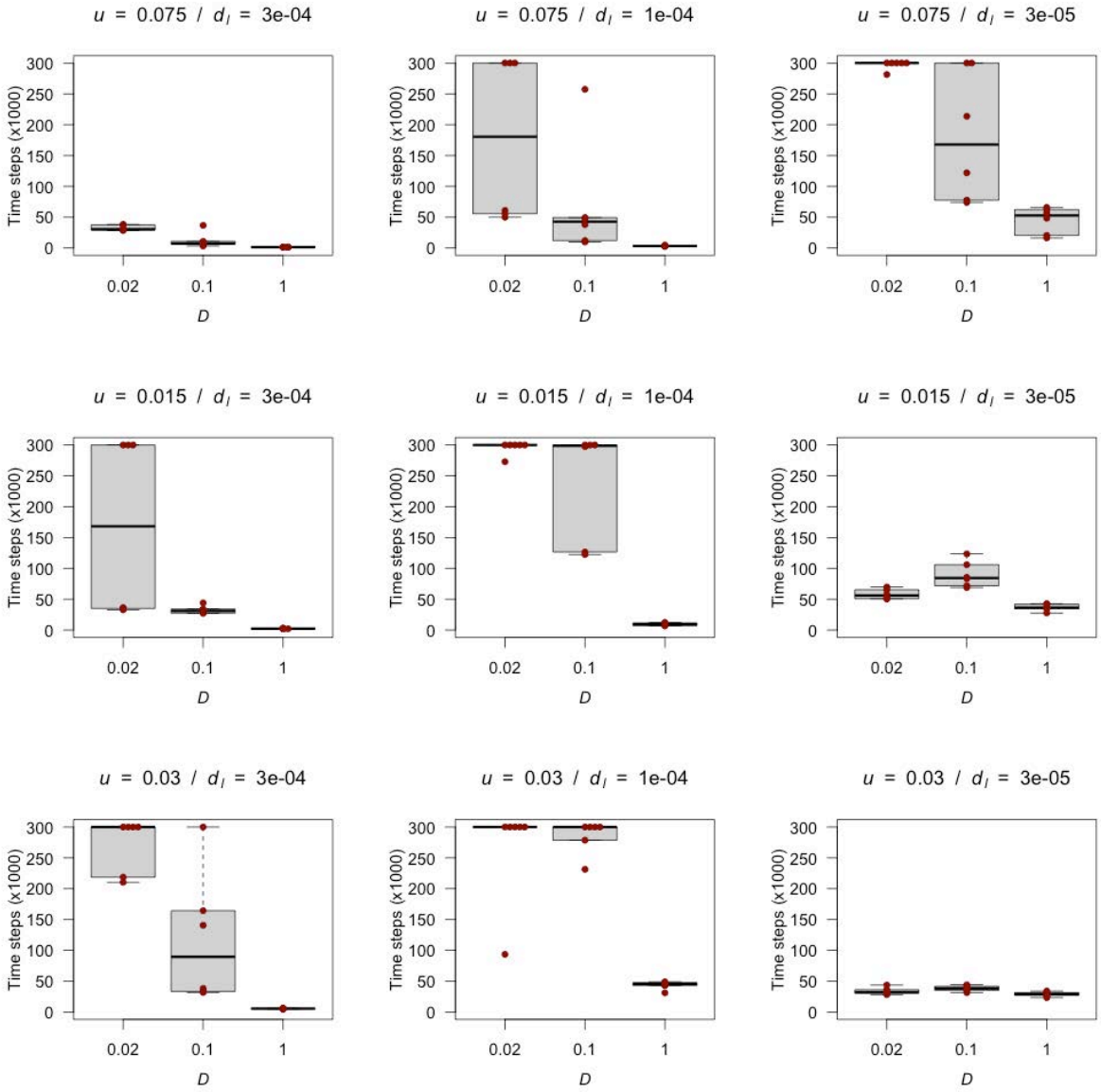

Figure S2: Coexistence times of the three strains for different toxin production and toxin removal rates with slow (D=0.02), fast (D=0.1), and instantaneous (D=1) toxin diffusion rates.

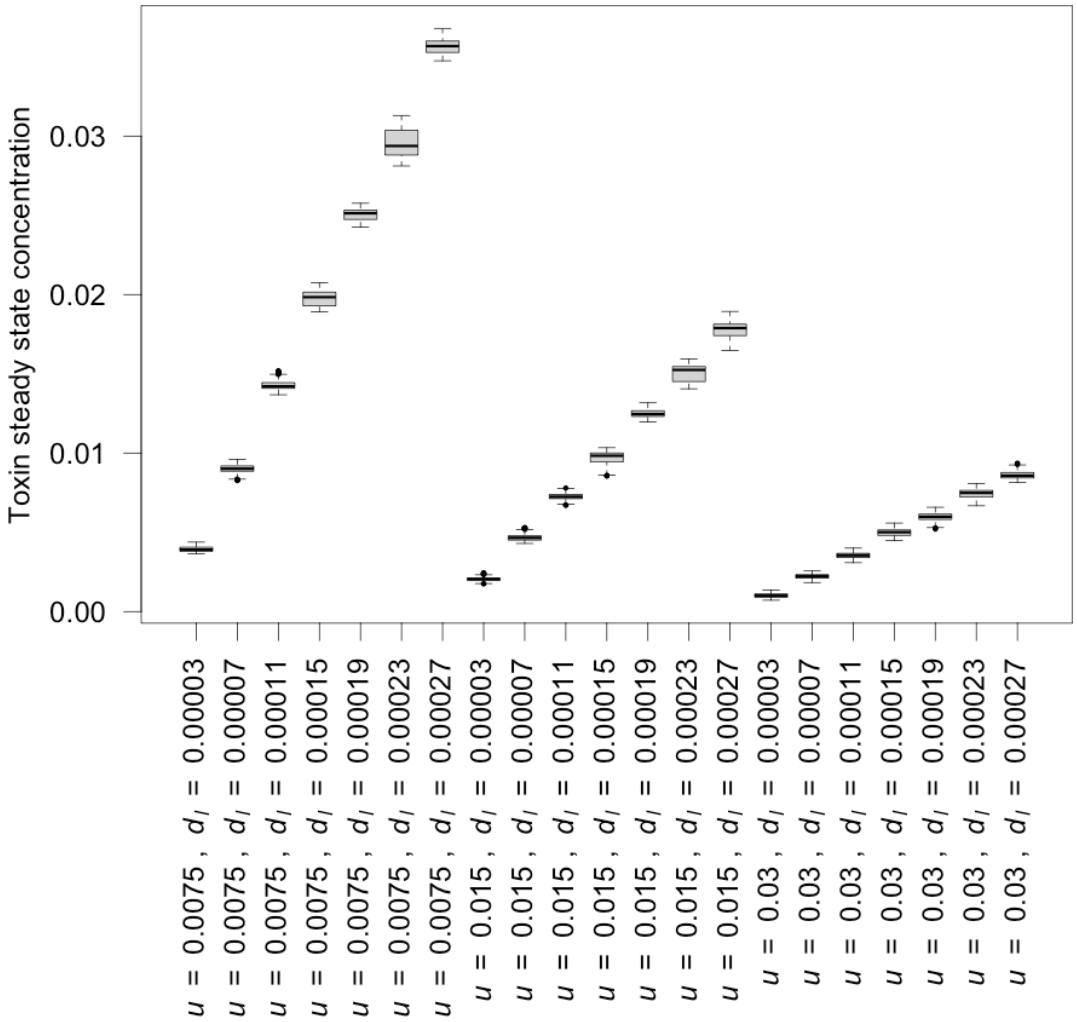

Figure S3. Steady-state toxin concentrations (between generations 700 and 1200) for different toxin production (d_l) and toxin removal (u) rates.

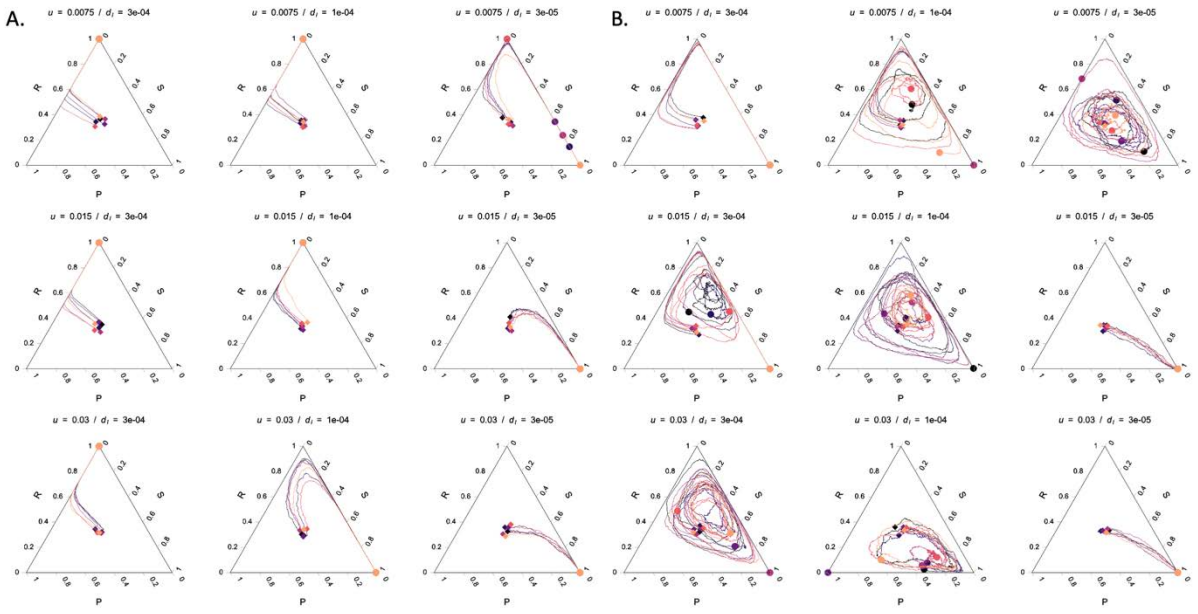

Figure S4. Population trajectory at instantaneous (panel A, $D = 1.0$) and slow diffusion (panel B, $D = 0.02$) for nine combinations of toxin production and removal rates, to be compared with the trajectories for fast diffusion shown in Figure 7B. There are six independent simulation trajectories under each condition, indicated by lines of different colors. The start point and end point of each trajectory are marked with a diamond and a circle of the same color as the trajectory, respectively. The lysis rate of toxin-producer cells, d_l=3e-5, 1e-4, 3e-4; toxin removal rate, u=0.0075, 0.015, 0.03.

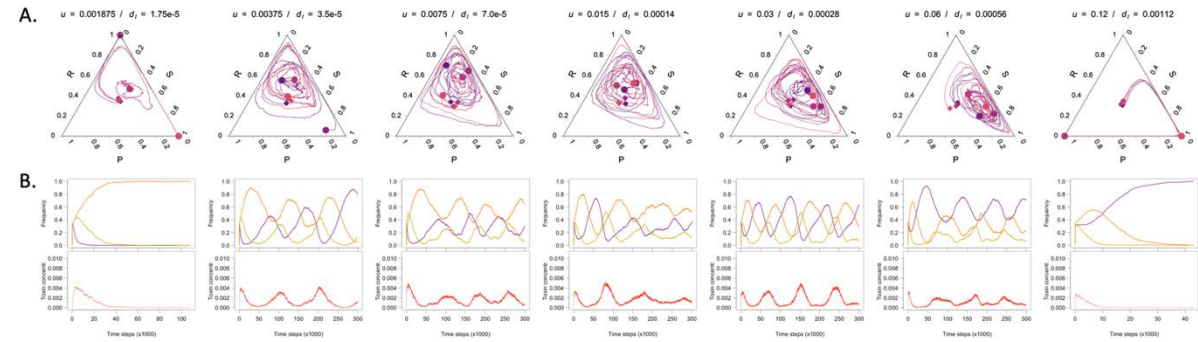

Figure S5. Impact of increasing flow and decreasing toxin production on cyclic competition patterns with toxin retention, c^*, kept constant. A. The values displayed above the ternary plots are the toxin removal rate (u) and the lysis rate of toxin-producer cells (d_l). B. Dynamics over time of the three strains and the toxin for one of the four replicates. Diffusion rate (D) is set at 0.02.

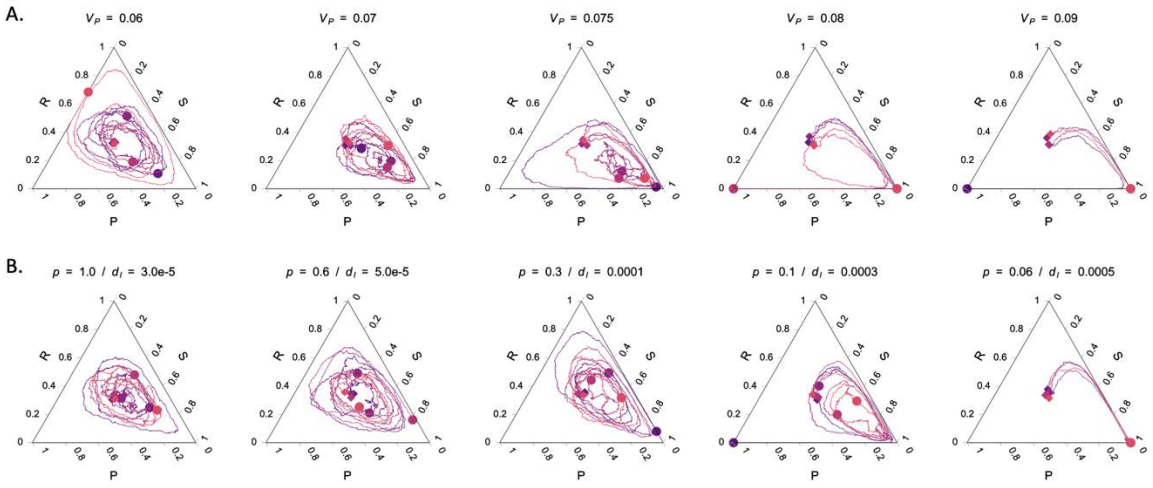

Figure S6. Impact of toxin production cost on the population trajectories. A. Trajectories for increasing toxin production costs (v_P), while keeping the lysis rate of producer cells (d_l) and toxin release per lysis event (p) constant. The values of d_l and p are set to 3e-5 and 1.0, respectively. B. Trajectories for increasing toxin-induced lysis rate (d_l), and correlatively adjusted toxin release per lysis event (p), the maximal toxin accumulation remaining the same; v_P is set to 0.06. The overall toxin production cost equals $d_l + v_P$. Diffusion rate (D) is set at 0.1 for both panels.

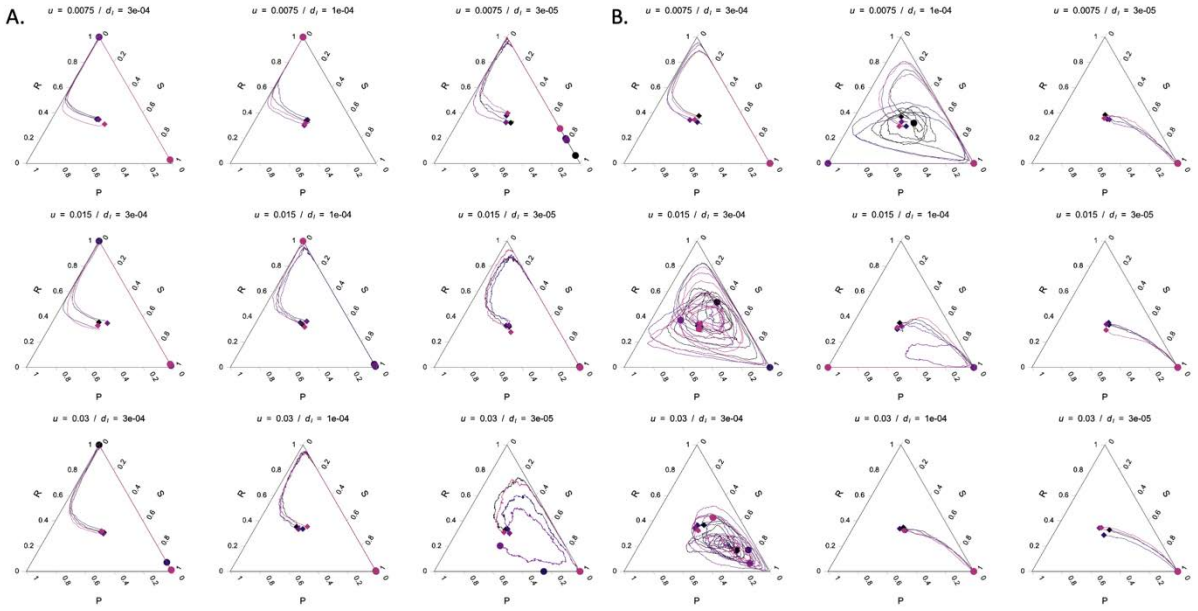

Figure S7. Population dynamics for low (A) and high (B) resistance and production costs. Simulations have been carried out with the same parameters as in Figure 7B except for $v_R = 0.01$ and $v_P = 0.02$ (panel A) or $v_R = 0.1$ and $v_P = 0.15$ (panel B). In comparison to the run presented in Figure 7B ($v_R = 0.04$ and $v_P = 0.06$), cyclic patterns tend to emerge at lower toxin concentrations in the first and at higher toxin concentrations in the second case.

General Discussion

Overview

This thesis examined two mechanisms that have been proposed to contribute to the coexistence of closely related species with overlapping niches.

The first mechanism investigated was spatial avoidance, and more specifically, the exploration-exploitation trade-off, in which a motile strain with higher motility uses dispersal to avoid competition with a more competitive strain on a local scale (de Martino et al., 2019; Gude et al., 2020). In the scope of this thesis, fungal highways were used to allow spatial avoidance. Two closely related *Pseudomonas putida* strains were used to investigate whether fungal highways support the maintenance of biodiversity of closely related strains sharing a similar niche. Our experiments showed that competition at the local scale led to competitive exclusion while regional competition promoted coexistence. When competing in the presence of dispersal networks, the growth-motility trade-off promoted coexistence only when the strains were inoculated in separate droplets. Furthermore, in order to investigate the mechanisms behind the exploration-exploitation trade-off in more detail and in a more controlled way, two devices mimicking different states of water saturation in soil were developed using 3D-printing technology. The trail device mimics fully saturated soil with thick liquid layers. The bridge device represents semi-saturated soil with a liquid layer allowing only active dispersal except for hitchhikers. The development and production of the two devices allow the study of dispersal in a liquid layer in a controlled abiotic system and it represents a showcase of the potential of 3D-printing in microbiology.

The second mechanism investigated here was non-transitive competition, in which non-hierarchical competition leads to cyclic dominance (Kerr et al., 2002). We used three *Escherichia coli* strains to study the population dynamics using a system akin to the rock-paper-scissors (RPS) game. New mini bioreactors were developed to investigate the impact of different nutrient compositions on the RPS dynamics. The different nutrient compositions in the bioreactors changed the dynamics dramatically, favouring in all but one treatment a single dominant *E. coli* strain. Moreover, by changing the production, removal and diffusion rate of a toxin in a computer model, the role of non-transitive competition on the population dynamic was also investigated. We showed that the amount of released toxin retained in the system predicts possible coexistence across broad parameter space.

Spatial avoidance

In the first chapter, we showed that when the competing species are involved in an exploration-exploitation trade-off, a dispersal network can help the species to coexist (Cohen et al., 2007; de Martino et al., 2019). When the two *P. putida* strains were inoculated on the local scale (combined inoculation in one drop) without a dispersal network, the strain UWC1 (fast-growing) outcompeted the KT2440 (motile) strain. In the presence of the fungal highway, the higher motility of the slow-growing strain (KT2440) only conferred an advantage on the

network on the regional scale when the two strains were inoculated in separated droplets. Otherwise, the fast-growing strain (UWC1) quickly outgrows the more motile strain, constraining the latter to the interior of the mixed colony and thus preventing it from dispersing. The competitive advantage of the KT2440 strain when dispersal is possible suggests that the exploration-exploitation trade-off plays a role in promoting the coexistence of these two bacterial strains, with the UWC1 strain growing faster under direct competition, while the KT2440 performing better at dispersing and exploring empty habitats.

When competing species are regulated by a trade-off between reproduction rate and dispersal, theory predicts that there are intermediate conditions in which coexistence is possible (Levins & Culver, 1971; Livingston et al., 2012; D. W. Yu & Wilson, 2001). In my experiments, I found coexistence on the regional scale but not on the local scale. On the regional scale, the competition pressure was most likely lower than on the local scale, which means we had an intermediate competition pressure between the two strains.

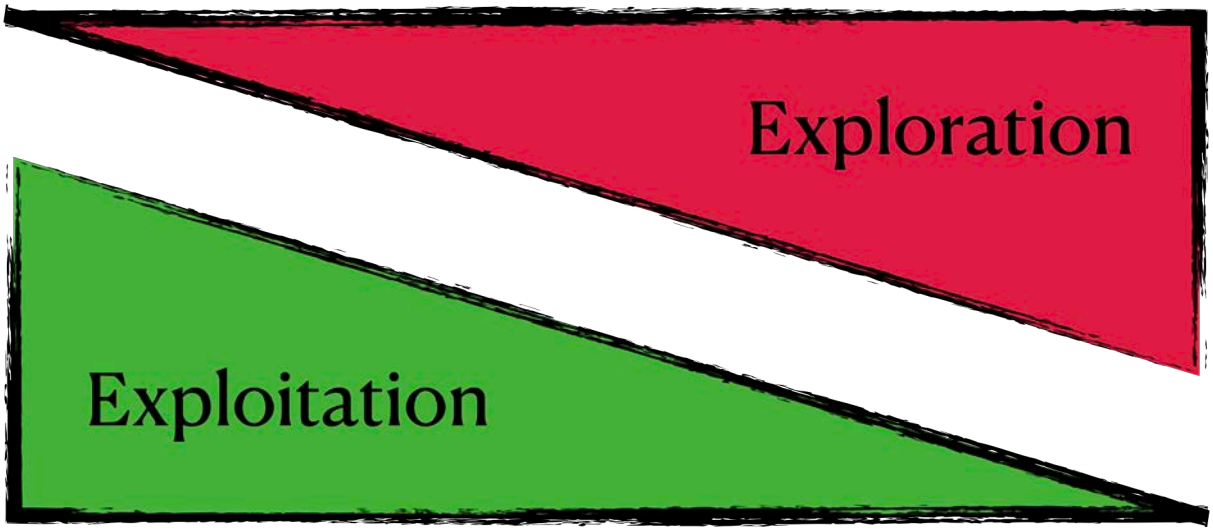

Figure 5 This figure represents the exploration-exploitation trade-off. The strain is either competitive or motile, but it cannot be good at both.

In the experiment described above, the spatial network was created by co-culturing with fungi and generating a so-called fungal highway. Along the fungal hyphae, there is a liquid film in which bacteria can disperse (Kohlmeier et al., 2005). This network is a biotic system which interacts with the bacteria and changes over time (Deveau et al., 2018; Warmink et al., 2011; Warmink & van Elsas, 2009). These interspecific interactions will certainly influence the experiment's outcome if one of the two strains is better adapted to live with the fungus (Thrall et al., 2007). However, to distinguish the fitness of the bacteria along the fungal highway, one should need to know, for instance, the growth rates of the strains while dispersing, but measuring this is currently extremely challenging. Moreover, apart from the interaction with the bacteria, the fungal network is variable over time (Morel et al., 2013). The experiment performed with fungi of different ages (see supplementary material in chapter one) showed differences in how the fungus interacted with the bacteria. While the young fungus (2 days post inoculation -dpi) could not penetrate the bacterial colonies, the older fungus (5 dpi)

could. Thereby the age of the fungus had an impact on the availability of the fungal highway to the bacteria. When the fungus grew around the colony, only cells at the border had access to the highway. However, when the fungus penetrated the colony, bacteria in the middle of the colony could enter the highway as well. Since the colonies were structured (UWC1 on the border and KT2440 on the inside) and the strains' abundance was different, this impacted the dynamics of co-existence between the strains. In summary, as the fungal highway is a hard-to-control system and its changes impact bacterial population dynamics, an abiotic control was needed to further the understanding of the exploration-exploitation trade-off in the experimental system used here.

Glass fibres have been used in the past as an abiotic controlled network mimicking the fungus (Pion, Bshary, et al., 2013). Glass fibres create spatial structures without adding an organism, thus preventing interspecific interactions and network changes over time. However, as shown in the first chapter, glass fibres have two significant disadvantages. First, it was not easy to recreate the same network multiple times, and therefore, considerable variability in the networks' topology persisted. Although one can argue that the fungal highways are intrinsically variable because of changes in the growth pattern of the fungus, still the goal of the abiotic system is to control part of the variability, and the impossibility of replication defeats this goal. The second problem occurred during the inoculation of the bacteria, during which a suction force passively distributed the cells along the network. Both bacteria strains were equally distributed along the entire network, which impacted the exploration-exploitation trade-off by removing the benefit of being the better disperser (Fronhofer & Altermatt, 2015). These limitations of the abiotic system and the need for reliable abiotic controls led to the creation of the trail and the bridge devices using 3D-printing technology.

The bridge device was designed to investigate the exploration-exploitation trade-off in a controlled environment without passive dispersal (Livingston et al., 2012). The bridge device presented in this thesis allows the connection of two wells. Thereby, a consistent network might be constructed, mimicking a fungal network. From a technical standpoint, the initial design connected two wells in a 24-well plate. However, with some minor adjustments to the foot of the bridge, connecting multiple wells of a 24-well plate with bridges are possible, thus expanding the possibilities to develop multiple network topologies. This would allow further investigations of the mechanisms of the exploration-exploitation trade-off without the biotic effect of the fungus or the passive dispersal along the glass fibres. Similar to the experiments in the first chapters, the inoculation of the bacteria can happen on the local scale (in the same well) or on the regional scale (in different wells) (Gude et al., 2020). Because the bridge system is a liquid-based system and not an agar-based system (as in chapter one), the competitive strain most likely will not be able to block the highway for the more motile strain. This should change the dynamic if the two strains get locally inoculated because the fast-growing strain cannot block the motile strain from excessing the dispersal network and the motile strain can avoid competition and use its motility advantage. I would assume that the dynamics in the locally inoculated experiment on a bridge network thus are closer to the one observed on the regional scale on an agar plate with the fungal highway.

The effect of heterogeneity

In my first two chapters I looked at the effect of the exploration-exploitation trade-off on biodiversity. To allow this trade-off to function, a heterogeneous environment with a dispersal network is needed (Martino et al., 2018; Wang & Or, 2012). The coexistence index shows the connection between coexistence of multiple species and the heterogeneous environment (Wang & Or, 2012). If the environment is too water saturated, and thereby in a well mix and homogeneous state, different strains and or species with overlapping niches cannot coexist. However, if the soil is semi-saturated and therefore patchy and heterogeneous the different strains and or species can coexist.

It is important to keep in mind, that these prediction on coexistence are at relative short time scales. These simulations or my experiments are only run for a few days. However, if the simulations or experiments would go on for longer, a more competitive strain would take over and out compete an explorative strain. The heterogeneity of the system would then only define the duration till one of the strains takes over. The big difference between natural system and the experimental/simulation set up is that in nature, there is no long-term stable environment and there are more entities involved like fungi, phages, plants, bacteria, and many more.

Changes in the environment free up new unpopulated habitats that allow explorative species to avoid the competition and to colonize these empty spots (Levins, 1979). These chaotic changes and the creation of new empty habitats do not happen in an experimental setting. Thereby, the coexistence between the strains is limited to a certain amount of time. This does not mean that the experiments lose their power. These experiments do show how the population behaves in the first stages of colonization and thereby allow to study the mechanisms involved in the early stages of coexistence. To investigate the short term and the long-term factors together, experiments which allow for chaotic events and the creation of new habitats should be run.

The other factors, which are not considered in most of the experiments is, that in nature coexistence and competition does not happen between two strains or species, but between multiple different entities like bacteria, fungi, phages and many more. These other players get involved into the competition game and might help one or the other strain to persist or colonize habitats (Ping et al., 2020; Z. Yu et al., 2021). For example, the growth of the fungus allows bacteria to conquer new habitats or the spread of a phage, that can result on the eradication of the host strains.

The experiments I run in my thesis give a small insight in many different inter- and intraspecific interactions, which occur in a natural system. By better understanding each of these interactions, a better understanding of how biodiversity is maintained is reached. This is the case even though; the experiments do not allow to study coexistence at all the different stages at the same time. But like a puzzle every experiment adds another piece.

Development of abiotic controls to study bacterial dispersal

The bridge device, which was briefly discussed in the previous part, was not the only abiotic device I designed during my work. Prototyping of devices to mimic the fungal network led me to development of multiple systems to study the dispersal of bacteria in liquid films. Two of these designs were fully developed and tested in this thesis: the trail and bridge devices.

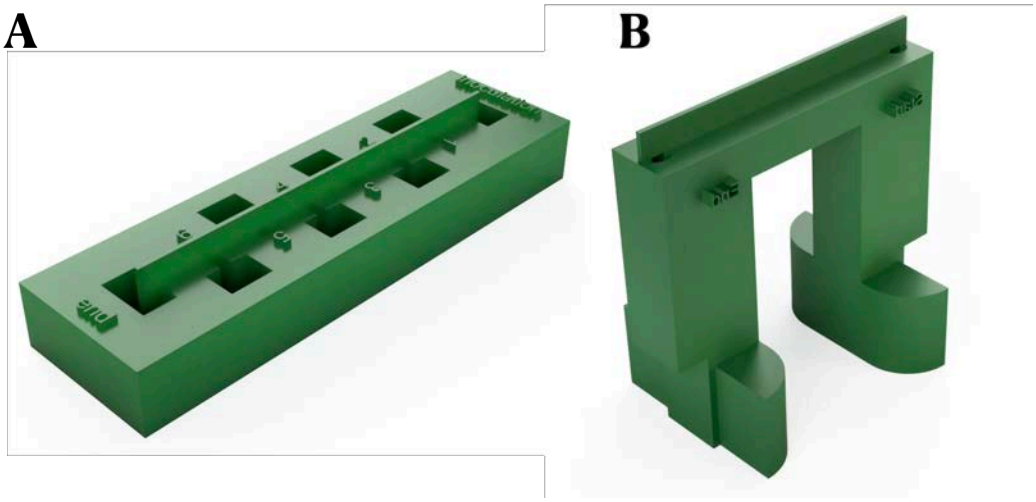

Figure 6 Panel A shows the trail device. Panel B shows the bridge device.

The key design component of these devices was the formation of a continuous liquid film (trail device 1.35 mm, bridge device 0.14 mm thick) connecting two or multiple discrete reservoirs. To check how faithfully the liquid films generated represent those formed along fungi, the liquid film widths generated in the devices were compared to previously calculated liquid films expected to be formed along fungi (Kohlmeier et al., 2005). Kohlmeier *et al.* 2005 calculated the liquid layer width using water potential and contact angle. The two matric potentials that are comparable to our devices are -0.5 kPa (almost saturated) for the trail device and -5 kPa (semi-saturated) for the bridge device. According to their calculation, in an almost water-saturated system, the liquid layer width formed around hyphae is around 0.3 mm. Thus the 1.35 mm width liquid layer in the trail device is thicker than the liquid layer expected in a natural system. Because of the huge difference of the liquid film size between the trail device and the fungus, the trail device does not represent the fungal highway. Even though there is a difference in the size of the liquid layers of the trail device and the fungal highway, fully saturated soil and the trail device should share core properties like passive dispersal of bacterial cells, as structures like pores (soil) or wells (trail device) are completely flooded with water (Tecon & Or, 2016, 2017b). Therefore, the trail device can be used to mimic fully saturated soil.

For investigating the exploration-exploitation trade-off, the trail device is not ideal because bacteria can passively disperse (Burgess et al., 2016). Thus, the trail device has the same limitation in investigating the exploration-exploitation trade-off as the glass fibres (Fronhofer & Altermatt, 2015). However, the trail device allows to study how microbes passively disperse

in fully saturated soil. Thereby, passive dispersal dynamics during a wetting event can be investigated.

Compared to the trail device, the bridge device mimics the situation in which bacteria cannot disperse passively in soils. The liquid layer width of the bridge device is ten times smaller than the one of the trail devices. However, it is still wider than the calculated liquid layers on the surface of fungal hyphae. The liquid layer along fungi in soil with a matric potential of -5 kPa was calculated to be between 0.04 mm and 0.01 mm (Kohlmeier et al., 2005), which is 20 times thinner than the one measured on the bridge device. However, the liquid layer of the bridge device is smaller than the calculated one for semi-saturated conditions, suggesting that the bridge device would be representative of a matric potential between -0.5 and -5 kPa in soil (Ebrahimi & Or, 2014; Krüger et al., 2019; Tecon & Or, 2016). More importantly, the bridge's design hinders passive dispersal, albeit in a thicker liquid layer, and this opens up the possibility of investigating other aspects related to the active dispersal of microorganisms in soils.

Microbial hitchhiking

By locally inoculating two strains on the bridge device, one of which was motile and the second one that was non-motile, we were surprised by the detection of both strains in the target well. This was surprising because when the two strains were inoculated separately, only the motile strain managed to cross the bride. Therefore, the only way for the non-motile strain to cross the bridge was to exploit the motile strain for its own dispersal. This behaviour, when a non-motile microbe uses a motile one two disperse, is called hitchhiking (Muok et al., 2021; Ping et al., 2020; Uppal et al., 2020; Warmink et al., 2011; Z. Yu et al., 2021).

The mechanism involved in bacterial hitchhiking along the bridges is not clear yet. There are multiple different possible mechanisms. It has been described that bacteria can either attach to the flagella or the cell wall of motile cells (Muok et al., 2021; Uppal et al., 2020). However, to my knowledge, attachment to the flagella was only described for fungal and bacterial spores, which are reduced in size as compared to their vegetative cells' counterparts.

Uppal and colleagues described 2020 a mechanism in which non-motile bacteria attach themself to a motile bacteria cell. This behaviour was also observed between motile cells to reduce water resistance and increase travelling speed. In my microscopical observation of the two bacteria strains, I was not able to observe any cells attached to each other. Even though this does not eliminate the possibility that our strains attach in a similar way, it makes it unlikely. A further hint that the bacteria do not attach is given by an additional experiment I performed. I inoculated the bacteria with flow cytometry beads and observed the recovery of a small fraction of the beads in the target well of the motile strain. The beads have a size of 3 μm and are around three times as big as the bacterial cells. I highly doubt that these beads can attach to the bacteria, especially since they were not found attached to any bacterial cells. I assume that the non-motile bacteria and beads were transported by the same mechanism. Either by being pushed in front of a group of motile cells or by being dragged behind a group

and getting transported by a "water shadow". In the second case the non-motile bacteria would be sucked behind the group and would stay in this protected area, similar to a wind shadow. The transportation of large cargo by bacteria (i.e., larger than their own cell size) was described in 2012 by Shklarsh and colleagues (Shklarsh et al., 2012). They found that swarming bacteria can transport particles up to a size of 20 μm. To determine the mechanisms by which bacteria hitchhike along the fungal highway, further investigations are needed. In the future, it might be possible to use the drop system developed by Matteo Buffi to image the process (Buffi et al., n.d.). However, if hitchhiking is extremely rare, it might be too hard and time-consuming to observe it directly.

Despite the unknown mechanism, potentially hitchhiking is a strategy for the exploitation specialist to close their motility gap. Hitchhiking allows the strain to move between the patches potentially with minimal energetical costs (Uppal et al., 2020). By creating a dispersal network with the adjusted bridge device (allowing multiple connections), the impact of bacterial hitchhiking on the exploration-exploitation trade-off could be investigated. Therefore, the motile and non-motile bacteria would get inoculated either locally (in the same well) or regionally (in different wells). In the locally inoculated setups, hitchhiking would be possible from the beginning. The non-motile cell could spread with the motile and possibly outcompete the motile one. On the regional scale, the non-motile strain could not spread till the motile strain arrives. From this point on, I could imagine two scenarios. First, the non-motile strain has already used up all the nutrients in the well, so that the motile strain could not establish a sufficiently large population to transport the non-motile cells. Or second, the motile strain arrives and starts transporting the non-motile cells, which then start taking over the wells it arrives in. If so, bacterial hitchhiking could represent a cheating strategy for less motile or non-motile strains in the exploration-exploitation trade-off, which might limit its effectiveness in maintaining biodiversity (Uppal et al., 2020).

It has previously shown that not only bacteria can hitchhike but also phages and fungal spores (Ben-Jacob et al., 2016; Inghama et al., 2011; Muok et al., 2021; Muok & Briegel, 2021). Experiments performed with the bridge devices showed that bacteria can transport phages. Thereby, non-susceptible bacteria strains function as carriers which spread the phage without getting infected (Périat et al., n.d.). The carrier bacteria can transport phages to their host, and the host bacteria get eradicated, creating a huge advantage for the competing carrier bacteria. The removal of the host impacts the population dynamics and allows for easier invasions of the transporting bacteria (Ping et al., 2020; Z. Yu et al., 2021). This might be one mechanism which allows the motile strain to invade patches occupied by a more competitive strain. To test this hypothesis, the bridge device could be used. If the two strains get inoculated in separate wells, and the phages are only inoculated with the carrier bacteria, it could be tested what the advantage of the phage transportation for the carrier bacteria is. Furthermore, the impact of the phages on the population dynamics could be studied.

In addition to bacteria and phages, fungal spores can hitchhike as well. By transporting spores along the fungal highway or in liquid films in the soil, bacteria can potentially seed or place the start of their new fungal highway. This would lead to an interesting exploration concept in which bacteria disperse along the fungal highway or liquid films transporting a spore. At the

end of the accessible area, the spore would get placed, and a new fungus would grow to create a new fungal highway. The fungi and the bacteria together would open new habitats, the bacteria by moving along the existing liquid films, and the fungus providing them (Inghama et al., 2011). A first step in investigating these exploring dynamics would be to investigate which type of spores can be transported by which type of bacteria. In a simple experiment, the bacteria and the spore would get inoculated in the same well of the bridge device and then the number of spores on the other side would be counted. Furthermore, the transport efficiency of this system could get investigated by calculating the percentage of transported spores.

Modelling the exploration-exploitation trade-off

In my thesis, I planned to investigate the exploration-exploitation trade-off not only with experiments but also with the help of a computer model. The big advantage of modelling is that it allows for testing the effect of multiple parameters in a resource-efficient way. Thereby, computer models allow us to conceptualize the experimental findings and help to understand the context of experiments. In my computer model, I wanted to explore the exploration-exploitation trade-off along the fungal highway. Therefore, I created a virtual fungal network. I used an algorithm designed to mimic the growth of trees to create the network because the fungus shows a similar apical growth pattern as the tree (Runions et al., 2007; Wessels, 2003). However, many parameters of bacterial behaviour were missing, like the bacteria's speed along the fungal highway, how many bacteria move simultaneously and how the two strains compete on a network. To measure these parameters, new methods had to be established. I used the drop system developed by a colleague in the lab to measure the speed and the dispersal pattern of the bacteria along the fungal highways (Buffi et al., n.d.). This data was collected, and I started analysing it. However, I did not have the time to finish the analyses and integrate the measured parameters into the existing model.

To investigate the competition of the two strains along the fungal highway, I developed the bridge device. However, to establish a complex network with multiple connections, some changes on the foot of the bridge device have to be made. I already redesigned the bridge this way, but I did not have time to test the system again as soon as the functionality of the new design would have been established. I wanted to inoculate the two strains on a bridge network connecting different wells. By sampling the different wells, I could monitor the dynamics of the competition between the two strains. Parameters like how much earlier the motile strain arrives and how long it takes for the competitive strain to outcompete the other strain can then be included in the computer model. With the measured parameters, bigger networks can be simulated, allowing an advanced understanding of the mechanisms behind the population dynamics of the two strains. To increase the realism of the simulation, mechanisms like hitchhiking or other bacteria strains and phages should be integrated. Even though the model never represents reality, it can be useful for understanding natural mechanisms and by using realistic parameters, its results should get more reliable.

Non-transitive competition

In the third chapter, I used small 3D-printed bioreactors and an Individual-based-model (IBM) to investigate the non-transitive competition between three *E. coli* strains. The focus of the experiments was on the impact of nutrient composition and toxin production, removal and diffusion rates on the coexistence of the three strains. Three different casamino acid (CA) to glucose (G) ratios and two different nutrient flow rates were used. The IBM was used to investigate the toxin's role further. In contrast to previous models, where the dispersal of cells led to the distribution and killing of the sensitive, in this model, the cells themselves cannot disperse (Kerr et al., 2002; Reichenbach et al., 2007; Schreiber & Killingback, 2013; Szolnoki et al., 2014). However, the toxin is explicitly modelled and diffuses.

In our experiments, nutrients significantly impacted the outcome: while the toxin producer dominated under the high CA: G ratio, it was largely outcompeted under the low CA: G ratio. Even though the producing strain dominated in these setups, the resistant strain did not become extinct and, due to its fitness benefit over the producer, would probably take over in the long term. Because exploitation competition takes a long time to induce changes, I could not detect the shift during the experiments (Holdridge et al., 2016). However, I would assume that in an experiment longer than two weeks, the change from producer to resistant strain should be observable (Kerr et al., 2002; Kirkup & Riley, 2004).

The dominance of the toxin producer in the high CA treatments comes from a higher toxin production rate than in the high G treatment (Cascales, Buchanan, Duché, Kleanthous, Lloubès, et al., 2007). In this CA-based treatment, the producing strain's reproduction rate is higher, leading to more SOS events and, thereby, to higher lysis frequency and a higher toxin concentration (Cascales, Buchanan, Duché, Kleanthous, Lloubès, et al., 2007). The SOS response of the bacteria is the coordinated gene expression after the DNA of the bacterium gets damaged (Erill et al., 2007).

The higher growth rate in the CA-based treatment compensates for the increased lysis rate and thereby reduces the cost of the toxin-producing plasmid. This allows for a higher growth despite the higher lysis frequency. This shift is also supported by the growth rates measured in growth rates experiments. The difference between toxin-producer and sensitive strain´s growth rate is the smallest in the high CA medium.

In the setups with a low Ca: G ratio, the sensitive strain was dominant. This was caused by the lower toxin production rate due to the high glucose concentration. When the toxin production is too low to kill the sensitive strain, the sensitive dominates the other strains. Similar to the high CA: G ratio, none of the other strains were out-competed, and the producer and resistant strains were still abundant in lower numbers.

Compared to the nutrient composition, the flow rate had a smaller influence on the population dynamics in the experiments. Differently from the previous rock-paper-scissor (RPS) experiments, in our experimental setup, the medium was under constant change. Thereby toxin was removed at a constant rate, while in previous studies, the toxin was

completely removed by a transfer (Kerr et al., 2002). The different setting allowed us to observe the "ghost of the colicin producers". This means that even though the toxin producer was less abundant, the sensitive strain struggled for a while to take over because the toxin produced previously remained in the system for a while.

In the simulations, I found what I call toxin retention (c^*), which is determined by the balance between toxin release and removal. It is a useful simple indicator of the propensity of long-term coexistence between the *E. coli* strains. An intermediate c^* generally promotes coexistence. However, extreme toxin fluxes caused by extreme toxin release and removal rates can lead to strong population fluctuations and premature collapse of coexistence. The computer model also allowed for an in-depth view of the effect of toxin diffusion and its effect on the *E. coli* community. Differently from previous models, the toxin is explicitly modelled and can diffuse (Kerr et al., 2002; Reichenbach et al., 2007). Like in the bioreactors, the toxin gets produced and removed at different rates.

Our finding that the intermediate toxin diffusion rate promotes coexistence draws an analogy to the previous finding that the intermediate mobility of individuals promotes coexistence but is more biologically relevant and has important implications (Hol et al., 2014; Reichenbach et al., 2007; Szolnoki et al., 2014). We assume that *E. coli* form biofilm on the bottom of the bioreactors. It is unclear if bacteria can disperse in biofilms, but molecules like colicin can diffuse. Thus, modelling diffusion of the toxin might be more accurate than the dispersal of the cells. Additionally, we know that spatial structure promotes coexistence in the *E. coli* system; the fact that population structure without restricted toxin diffusion does not support coexistence has not been sufficiently emphasised (Kerr et al., 2002; Liao et al., 2020).

Even though the toxin was explicitly modelled, there are some major differences between the model and the experimental setup. First, while in the simulations, 300'000 generations were observed, in the experimental setup, it was only possible to look at a couple of hundred generations. These relatively few generations in the experimental setup did not allow for studying extinction dynamics in any setup. However, most of the time, two strains were at low numbers. Second, in the computer model, the cell numbers, toxin concentration, etc., of every generation were recorded. Such a high sampling frequency was not possible to maintain in the experiments. The samples were taken every 24 hours and, therefore, not every generation. Thereby, the resolution of the results is much higher in the model than in the experiment. The third important difference between the model and the experiments is that in the model, only one cell layer got created on a 200 x 200 grid. In the bioreactors, however, there was a biofilm. However, we had another life state than the cells in biofilm as some of them were also in the planktonic phase. The cell numbers in the bioreactors, therefore, should be much higher than the 40'000 cells in the simulation.

Even though the model cannot represent reality, it is still useful. It allows insight into mechanisms, like toxin diffusion, which would be extremely hard to measure in an experimental setup. The experiments combined with the model allow for a more detailed understanding of how non-transitive competition helps maintain biodiversity in closely related species.

Non-transitive competition in a spatial background

In this thesis, I focus on two different mechanisms which maintain biodiversity. In the first two chapters, I focus on spatial avoidance and in the third chapter on the non-transitive competition. However, I did not manage to combine the two concepts and study their interactions. Nevertheless, the devices I have developed in this thesis would allow for combining spatial avoidance and non-transitive competition.

The bridge device allows for connecting multiple wells, and the bacteria can disperse between them. However, the bridge device is not ideal for investigating a RPS system with a spatial background. The limitation is that removing the toxin from the system is impossible. By pumping in and out the media, there would be too much disturbance, and the cells would get flushed from one well to the other. A way around this limitation would be to transfer the *E. coli* cells to a new network daily, similar to Kerr's experiment in 2002 (Kerr et al., 2002). However, this would remove the "ghost of the colicin producers", and thereby, it might change the population dynamics. A better workaround would be to use another non-transitive system in which no toxin is released. The bacteria could use, for example, Type VI secretion system or contact-dependent growth inhibition (CDI) systems to prey on each other and thereby form the RPS dynamics (Mattick, 2002).

Nevertheless, for cases with the "ghost of the colicin producers" effect, experiments over multiple weeks will not be possible in the bridge system because there will not be new nutrients coming into the network as soon as all the nutrients are consumed, and all the bacteria will enter the stationary phase. I doubt that the non-transitive competition would go on. Furthermore, the waste products of bacterial growth would accumulate in the wells like the toxin does. The bridge system has many areas of application, but exploring non-transitive competition on a spatial scale is likely not one of those.

The bioreactor does not have the limitation of toxin removal or nutrient flux, but the design does not allow for active dispersal between the different bioreactors. However, the bioreactors can get connected by transferring some of the reactor's liquid into another reactor with a syringe. These transfers would allow connecting the different reactors (Nagatani et al., 2018). There are two different transfer setups that would be interesting to investigate in the future. The first one would be to inject always a given strain (the same one or alternating between different strains) in the bioreactors. The second option is to take a sample from one bioreactor and inject it into another reactor. The first setup would allow studying the invasion rate of the three different *E. coli* strains during the ongoing experiment. Depending on the state of the dynamics in the reactor, the injection of the strain could have different impacts: it can have no effect, for example, if the resistant strain gets added to a system where only resistant bacteria are left or it would have a minimal impact if it gets injected when its opponent is dominant. For example, if the sensitive strain gets injected into a toxin-producer-dominated reactor, the added sensitive cells will be killed by the toxin. However, it could change the transition speed between toxin–resistant and resistant-sensitive strains. If the added strain belongs to the next strain up (to the resistance in the toxin-resistant transition), the transition should take less time. The transition would get delayed if the toxin producer

gets added. The biggest impact will get achieved if a strain gets reintroduced. This could either restart the cycles or, if only one strain is left, change the outcome to the reintroduced strain.

In the second scenario, a network with multiple connected reactors gets built. The setup would be similar to Kirkup and Riley's mice experiment in 2004 (Kirkup & Riley, 2004). In these experiments, they studied the population dynamics of *E. coli* in the gut of mice. For this, they sampled the faeces and counted the different strains. They found that biodiversity first got lost in an individual, then in a cage and last over all cages. With the bioreactors, sampling would be facilitated and could be done at any time. Compared to mice, each reactor could have defined properties like temperature, flow rate or nutrient composition, and these properties can be different between the reactors and can be changed during the experiment if needed. Furthermore, the arrangement and connection between the different reactors can be controlled and would not be random as in a mice population. Thereby, the network could have different shapes, like circular or dendritic (Carrara et al., 2012).

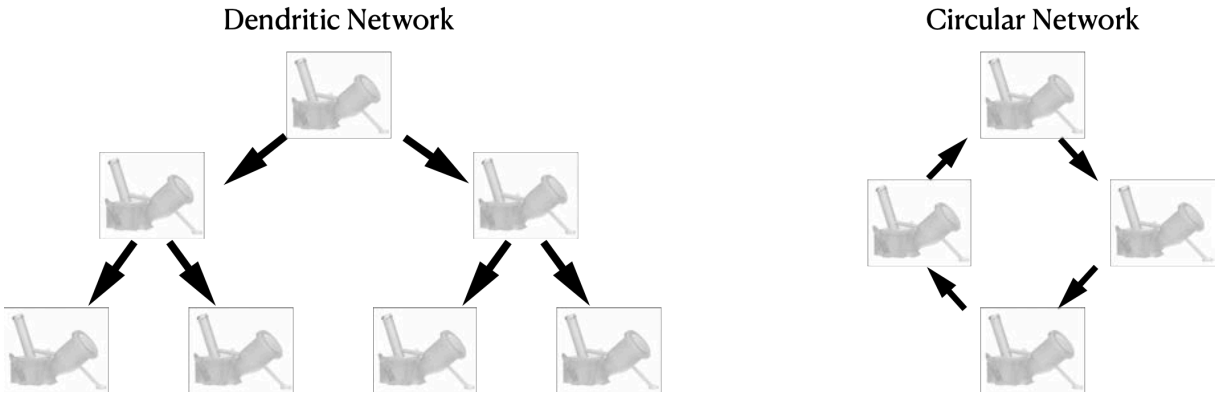

Figure 7 To perform the non-transitive competition in a spatial background, there are different network types. In this figure, two possible organizations of the mini bioreactor are represented.

The experiments executed in the bioreactors would allow studying the dynamics of each reactor in detail and how the dynamics get impacted by the transfers. The strain under the strongest competition could escape to a reactor at a more feasible state. Depending on the organisation of the reactor network, the outcome of the dynamics could be different. In a circular arranged network, extinct strains can get reintroduced multiple times, and the different reactors could synchronise. Such as that, the dynamics in the reactors are the same, just with a time difference between the reactors. In a dendritic system, the transfers would have a direction and only would go downstream (Carrara et al., 2012). Thereby a reintroduction of strains in higher-up reactors would not be possible. I would assume that it is more likely to end up with one strain dominating the entire network in a dendritic system than in a circular system.

Combining spatial avoidance and non-transitive competition would allow the investigation of the mechanistic interaction between the two concepts. Thereby, it would give further insight into how the biodiversity of closely related species sharing a similar niche can be maintained.

Biological implications

In my thesis I studied the effect of two different mechanisms on biodiversity maintenance. I showed that spatial avoidance allows for coexistence on the regional scale but not on the local scale. Furthermore, I used computer simulations and experiments to investigate the effect of non-transitive competition. My results show that intermediate toxin concentration and diffusion allow for coexistence of the three *E. coli* strains and the impact of nutrient composition on the population dynamics.

In these experiments I studied the mechanisms for some days and in a simplified environment. Therefore, it leaves the question if the results of the experiments are applicable in nature. Even though in nature there are more species, interacting in a longer time frame and in a more complex environmental structure than in my experiments, I would argue that the general rules I detected are applicable to a natural system. In the case of the spatial avoidance, I was able to proof the concept on the regional scale and showed that if the two strains were able to access the fungal highway, they were able to coexist. I look at this result as a pattern that is not correct for every community in every ecosystem, but might be correct for those populations, which are exploring a not colonized fungal highway system. Furthermore, the sampling resolution in the experiments must be considered. I counted all the cells on a Petri dish and thereby did not consider the structure of the populations. If the less competitive strain was able to survive somewhere on the Petri dish in small numbers, this would not have impacted the outcome of the experiment, because of the low spatial sampling resolution. These two factors led to the former conclusion that the results of these experiments do represent trends or a certain part of the population dynamics but do not draw a precise picture of what is going on in nature.

In my third chapter I look at the at the non-transitive competition between, three *E. coli* strains. We used different nutrient compositions to investigate their effect on the population dynamics. I showed that the nutrient composition has a considerable impact on the population dynamics. These results are applicable into a natural system highlighting the importance of nutrient composition on the population dynamics. The same is true for the toxin diffusion and concentration. I showed that an intermediate diffusion rate and toxin concentration favours coexistence. These patterns are applicable in natural systems. Especially, for the diffusion rate, because this pattern has been found in many other experiments and simulations (Kerr et al., 2002; Reichenbach et al., 2007).

To conclude the implications of my work on the understanding of biodiversity maintenance in nature are that my results provide elements to understand how the investigated mechanisms act. However, the findings cannot be generalized, and one must considered that every biological system has its own precise rules, depending on the involved species and the environment. To understand these rules in greater details more *in-vivo*, *in-vitro* and *in-silico* work is needed.

3D printing

This thesis demonstrates the potential of 3D-printing technology in microbiology. Additive manufacturing allows for the fast development and production of new devices. In-house production increases the development speed because of multiple reasons; the person needing the device can design and print them on his own. Thus, the pieces get produced when they are needed and have the design he has in mind. The devices do not have to get shipped, which saves time and minimises the risk of damage.

The high versatility of 3D-printers allows to produce a wide range of prototypes simultaneously with the same machine. Compared to casting or banking, the production of prototypes or a small number of devices is cheaper (C. Zhang et al., 2016).

Another advantage of having access to a 3D-printer is the ability to produce spare or missing parts for machines (Song & Zhang, 2019). Some companies already provide the STL file for the needed spare parts, which reduces the waiting time. This is especially useful for damaged supply chains due to Covid or other crises.

Furthermore, additive manufacturing allows the production of the same part anytime, anywhere on the globe. A simple STL file allows for reproducing the same devices. This can help us democratise science and enable poorer countries to participate more in today's science community, independently run the same experiments in different labs, or provide the same material to students at various universities (Ravindran, 2020).

As with every technology, additive manufacturing has limitations; for example, due to its layer-by-layer build, surfaces not parallel to the printing bed are not perfectly flat. They often have a stair-like shape. Compared to photolithography, the resolution of SLA 3D-printers is low. The resolution depends on the material, printer and design of the device. In the best case, the resolution is around 50 μm. Light blending makes building narrow structures like capillaries or small channels more difficult and inhibits printing them with a diameter smaller than 0.5-1 mm. Furthermore, it takes more time to post-cure these structures because the leftover resin must be washed manually.

Like capillaries, hollow structures are challenging to build. While printing, the prototypes are physically supported by structures. These structures help keep the prototype in shape and allow the devices to be designed more freely. However, the support structures should get manually removed after the print. Removing structures in closed hollow objects is often impossible. Optimised orientations on the printing bed and adjusted designs are the only solutions for this problem.

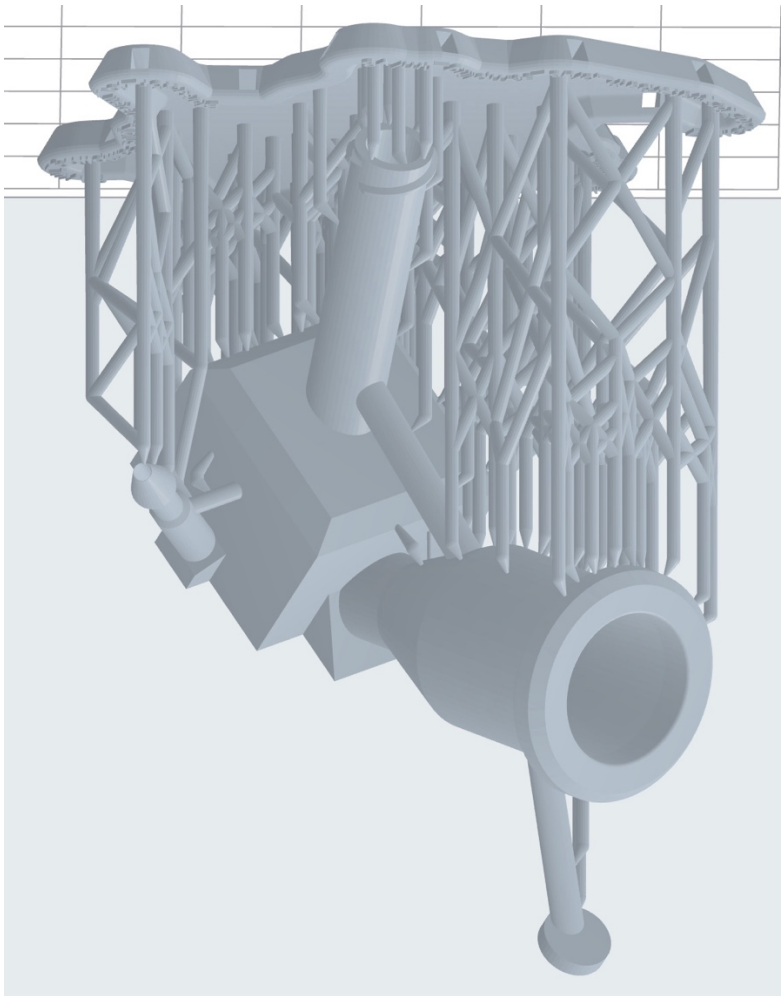

Figure 8 To print the mini bioreactor, some supports were needed. The supports ensure that the bioreactor stays in place and the shape is maintained during the print.

Additive manufacturing allows the in-house production of a wide range of devices with the same machine in a short time. However, due to its layer-by-layer build, not all surfaces are perfectly flat, and the resolution of the 3D-printer is low compared to other methods.
Despite these restrictions, our work shows the potential of 3D-printing in microbiology, and due to the dropping cost, the wide variety of printable structures and the rapid development of new materials, 3D-printing has a huge potential in the future.

References

Ben-Jacob, E., Finkelshtein, A., Ariel, G., & Ingham, C. (2016). Multispecies Swarms of Social Microorganisms as Moving Ecosystems. *Trends in Microbiology*, *24*(4), 257–269. https://doi.org/10.1016/J.TIM.2015.12.008

Buffi, M., Cailleau, G., Kuhn, T., Li Richter, X.-Y., Stanley, C., Wick, L., Chain, P. S., Bindschedler, S., & Junier, P. (n.d.). Fungal drops: a novel method for the observation of fungal modularity and coordination. *In Preparation*.

Carrara, F., Altermatt, F., Rodriguez-Iturbe, I., & Rinaldo, A. (2012). Dendritic connectivity controls biodiversity patterns in experimental metacommunities. *Proceedings of the National Academy of Sciences of the United States of America*, *109*(15), 5761–5766. https://doi.org/10.1073/PNAS.1119651109/SUPPL_FILE/PNAS.201119651SI.PDF

Cascales, E., Buchanan, S. K., Duché, D., Kleanthous, C., Lloubès, R., Postle, K., Riley, M., Slatin, S., & Cavard, D. (2007). Colicin Biology. *Microbiology and Molecular Biology Reviews*, *71*(1), 158–229. https://doi.org/10.1128/MMBR.00036-06/FORMAT/EPUB

Cohen, J. D., McClure, S. M., & Yu, A. J. (2007). Should I stay or should I go? How the human brain manages the trade-off between exploitation and exploration. *Philosophical Transactions of the Royal Society B: Biological Sciences*, *362*(1481), 933–942. https://doi.org/10.1098/RSTB.2007.2098

de Martino, A., Gueudré, T., & Miotto, M. (2019). Exploration-exploitation tradeoffs dictate the optimal distributions of phenotypes for populations subject to fitness fluctuations. *Physical Review E*, *99*(1), 012417. https://doi.org/10.1103/PHYSREVE.99.012417/FIGURES/5/MEDIUM

Deveau, A., Bonito, G., Uehling, J., Paoletti, M., Becker, M., Bindschedler, S., Hacquard, S., Hervé, V., Labbé, J., Lastovetsky, O. A., & others. (2018). Bacterial--fungal interactions: ecology, mechanisms and challenges. *FEMS Microbiology Reviews*, *42*, 335–352.

Ebrahimi, A. N., & Or, D. (2014). Microbial dispersal in unsaturated porous media: Characteristics of motile bacterial cell motions in unsaturated angular pore networks. *Water Resources Research*, *50*(9), 7406–7429. https://doi.org/10.1002/2014WR015897

Erill, I., Campoy, S., Barbébarb´barbé, J., Barbé, J., & Barbé, B. (2007). Aeons of distress: an evolutionary perspective on the bacterial SOS response. *FEMS Microbiology Reviews*, *31*(6), 637–656. https://doi.org/10.1111/J.1574-6976.2007.00082.X

Fronhofer, E. A., & Altermatt, F. (2015). Eco-evolutionary feedbacks during experimental range expansions. *Nature Communications 2015 6:1*, *6*(1), 1–9. https://doi.org/10.1038/ncomms7844

Gude, S., Pinçe, E., Taute, K. M., Seinen, A.-B., Shimizu, T. S., & Tans, S. J. (2020). Bacterial coexistence driven by motility and spatial competition. *Nature*, *578*, 588–592. https://doi.org/10.1038/s41586-020-2033-2

Hol, F. J. H., Voges, M. J., Dekker, C., & Keymer, J. E. (2014). Nutrient-responsive regulation determines biodiversity in a colicin-mediated bacterial community. *BMC Biology*, *12*(1), 1–14. https://doi.org/10.1186/S12915-014-0068-2/FIGURES/6

Holdridge, E. M., Cuellar-Gempeler, C., & terHorst, C. P. (2016). A shift from exploitation to interference competition with increasing density affects population and community dynamics. *Ecology and Evolution*, *6*(15), 5333–5341. https://doi.org/10.1002/ECE3.2284

Inghama, C. J., Kalismand, O., Finkelshteind, A., & Ben-Jacob, E. (2011). Mutually facilitated dispersal between the nonmotile fungus Aspergillus fumigatus and the swarming bacterium

Paenibacillus vortex. *Proceedings of the National Academy of Sciences of the United States of America*, *108*(49), 19731–19736. https://doi.org/10.1073/PNAS.1102097108/SUPPL_FILE/SM03.AVI

Kerr, B., Riley, M. A., Feldman, M. W., & Bohannan, B. J. M. (2002). Local dispersal promotes biodiversity in a real-life game of rock–paper–scissors. *Nature 2002 418:6894*, *418*(6894), 171–174. https://doi.org/10.1038/nature00823

Kirkup, B. C., & Riley, M. A. (2004). Antibiotic-mediated antagonism leads to a bacterial game of rock–paper–scissors in vivo. *Nature 2004 428:6981*, *428*(6981), 412–414. https://doi.org/10.1038/nature02429

Kohlmeier, S., Smits, T. H. M., Ford, R. M., Keel, C., Harms, H., & Wick, L. Y. (2005). Taking the fungal highway: Mobilization of pollutant-degrading bacteria by fungi. *Environmental Science and Technology*, *39*(12), 4640–4646. https://doi.org/10.1021/es047979z

Krüger, U. S., Dechesne, A., Bak, F., Badawi, N., Nybroe, O., & Aamand, J. (2019). Bacterial dispersers along preferential flow paths of a clay till depth profile. *Applied and Environmental Microbiology*, *85*(6). https://doi.org/10.1128/AEM.02658-18/SUPPL_FILE/AEM.02658-18-S0001.PDF

Levins, R. (1979). Coexistence in a Variable Environment. *Https://Doi.Org/10.1086/283527*, *114*(6), 765–783. https://doi.org/10.1086/283527

Levins, R., & Culver, D. (1971). Regional Coexistence of Species and Competition between Rare Species. *Proceedings of the National Academy of Sciences*, *68*(6), 1246–1248. https://doi.org/10.1073/PNAS.68.6.1246

Liao, M. J., Miano, A., Nguyen, C. B., Chao, L., & Hasty, J. (2020). Survival of the weakest in non-transitive asymmetric interactions among strains of E. coli. *Nature Communications 2020 11:1*, *11*(1), 1–8. https://doi.org/10.1038/s41467-020-19963-8

Livingston, G., Matias, M., Calcagno, V., Barbera, C., Combe, M., Leibold, M. A., & Mouquet, N. (2012). Competition–colonization dynamics in experimental bacterial metacommunities. *Nature Communications 2012 3:1*, *3*(1), 1–8. https://doi.org/10.1038/ncomms2239

Martino, A., Gueudré, T., Miotto, M., & de Martino, A. (2018). *An exploration-exploitation tradeoff dictates the optimal distribution of phenotypes for populations in presence of fitness fluctuations*. https://www.researchgate.net/publication/327979593

Mattick, J. S. (2002). Type IV Pili and Twitching Motility. *Annu. Rev. Microbiol*, *56*, 289–314. https://doi.org/10.1146/annurev.micro.56.012302.160938

Morel, M., Meux, E., Mathieu, Y., Thuillier, A., Chibani, K., Harvengt, L., Jacquot, J. P., & Gelhaye, E. (2013). Xenomic networks variability and adaptation traits in wood decaying fungi. *Microbial Biotechnology*, *6*(3), 248–263. https://doi.org/10.1111/1751-7915.12015

Muok, A. R., & Briegel, A. (2021). Intermicrobial Hitchhiking: How Nonmotile Microbes Leverage Communal Motility. *Trends in Microbiology*, *29*(6), 542–550. https://doi.org/10.1016/J.TIM.2020.10.005

Muok, A. R., Claessen, D., & Briegel, A. (2021). Microbial hitchhiking: how Streptomyces spores are transported by motile soil bacteria. *The ISME Journal 2021 15:9*, *15*(9), 2591–2600. https://doi.org/10.1038/s41396-021-00952-8

Nagatani, T., Ichinose, G., & Tainaka, K. I. (2018). Heterogeneous network promotes species coexistence: metapopulation model for rock-paper-scissors game. *Scientific Reports 2018 8:1*, *8*(1), 1–9. https://doi.org/10.1038/s41598-018-25353-4

Périat, C., Kuhn, T., Buffi, M., Corona-Ramirez, A., Fatton., M., Cailleau, G., Chain, P. S., Stanley, C., Wick, L., Bindschedler, S., Gonzalez, D., Li Richter, X.-Y., & Junier, P. (n.d.). Evaluating Passive Dispersal and Active Transport of Bacteriophages Along Fungal Highways. *In Preparation*.

Ping, D., Wang, T., Fraebel, D. T., Maslov, S., Sneppen, K., & Kuehn, S. (2020). Hitchhiking, collapse, and contingency in phage infections of migrating bacterial populations. *The ISME Journal 2020 14:8*, *14*(8), 2007–2018. https://doi.org/10.1038/s41396-020-0664-9

Pion, M., Bshary, R., Bindschedler, S., Filippidou, S., Wick, L. Y., Job, D., & Junier, P. (2013). Gains of bacterial flagellar motility in a fungal world. *Applied and Environmental Microbiology*, *79*, 6862–6867.

Ravindran, S. (2020). How DIY technologies are democratizing science. *Nature*, *587*(7834), 509–512. https://go.gale.com/ps/i.do?p=HRCA&sw=w&issn=00280836&v=2.1&it=r&id=GALE%7CA642124280&sid=googleScholar&linkaccess=fulltext

Reichenbach, T., Mobilia, M., & Frey, E. (2007). Mobility promotes and jeopardizes biodiversity in rock–paper–scissors games. *Nature 2007 448:7157*, *448*(7157), 1046–1049. https://doi.org/10.1038/nature06095

Runions, A., Lane, B., & Prusinkiewicz, P. (2007). Modeling Trees with a Space Colonization Algorithm. *Eurographics Workshop on Natural Phenomena*.

Schreiber, S. J., & Killingback, T. P. (2013). Spatial heterogeneity promotes coexistence of rock–paper–scissors metacommunities. *Theoretical Population Biology*, *86*, 1–11. https://doi.org/10.1016/J.TPB.2013.02.004

Shklarsh, A., Finkelshtein, A., Ariel, G., Kalisman, O., Ingham, C., & Ben-Jacob, E. (2012). Collective navigation of cargo-carrying swarms. *Interface Focus*, *2*(6), 786–798. https://doi.org/10.1098/RSFS.2012.0029

Song, J. S., & Zhang, Y. (2019). Stock or Print? Impact of 3-D Printing on Spare Parts Logistics. *Https://Doi.Org/10.1287/Mnsc.2019.3409*, *66*(9), 3860–3878. https://doi.org/10.1287/MNSC.2019.3409

Szolnoki, A., Mobilia, M., Jiang, L. L., Szczesny, B., Rucklidge, A. M., & Perc, M. (2014). Cyclic dominance in evolutionary games: a review. *Journal of The Royal Society Interface*, *11*(100). https://doi.org/10.1098/RSIF.2014.0735

Tecon, R., & Or, D. (2016). Bacterial flagellar motility on hydrated rough surfaces controlled by aqueous film thickness and connectedness. *Scientific Reports*, *6*, 1–11.

Tecon, R., & Or, D. (2017). Biophysical processes supporting the diversity of microbial life in soil. *FEMS Microbiology Reviews*, *41*(5), 599–623. https://doi.org/10.1093/FEMSRE/FUX039

Thrall, P. H., Hochberg, M. E., Burdon, J. J., & Bever, J. D. (2007). Coevolution of symbiotic mutualists and parasites in a community context. *Trends in Ecology & Evolution*, *22*(3), 120–126. https://doi.org/10.1016/J.TREE.2006.11.007

Uppal, G., Hu, W., & Vural, D. C. (2020). Evolution of chemotactic hitchhiking. *Journal of Evolutionary Biology*, *33*(11), 1593–1605. https://doi.org/10.1111/JEB.13695

Wang, G., & Or, D. (2012). A Hydration-Based Biophysical Index for the Onset of Soil Microbial Coexistence. *Scientific Reports 2012 2:1*, *2*(1), 1–5. https://doi.org/10.1038/srep00881

Warmink, J. A., Nazir, R., Corten, B., & van Elsas ., J. D. (2011). Hitchhikers on the fungal highway: The helper effect for bacterial migration via fungal hyphae. *Soil Biology and Biochemistry*, *43*(4), 760–765. https://doi.org/10.1016/J.SOILBIO.2010.12.009

Warmink, J. A., & van Elsas, J. D. (2009). Migratory response of soil bacteria to Lyophyllum sp. strain Karsten In soil microcosms. *Applied and Environmental Microbiology*, *75*(9), 2820–2830. https://doi.org/10.1128/AEM.02110-08/ASSET/AAE5C6EB-8DEC-4E79-A2B4-CDF7ABCC1EDD/ASSETS/GRAPHIC/ZAM0090998910006.JPEG

Wessels, J. G. H. (2003). DEVELOPMENTAL REGULATION OF FUNGAL CELL WALL FORMATION. *Https://Doi.Org/10.1146/Annurev.Py.32.090194.002213*, *32*, 413–437. https://doi.org/10.1146/ANNUREV.PY.32.090194.002213

Yu, D. W., & Wilson, H. B. (2001). The Competition-Colonization Trade-off Is Dead; Long Live the Competition-Colonization Trade-off. *Https://Doi.Org/10.1086/320865*, *158*(1), 49–63. https://doi.org/10.1086/320865

Yu, Z., Schwarz, C., Zhu, L., Chen, L., Shen, Y., & Yu, P. (2021). Hitchhiking behavior in bacteriophages facilitates phage infection and enhances carrier bacteria colonization. *Environmental Science and Technology*, *55*(4), 2462–2472. https://doi.org/10.1021/ACS.EST.0C06969/ASSET/IMAGES/LARGE/ES0C06969_0007.JPEG

Zhang, C., Wijnen, B., & Pearce, J. M. (2016). Open-Source 3-D Platform for Low-Cost Scientific Instrument Ecosystem. *Journal of Laboratory Automation*, *21*(4), 517–525. https://doi.org/10.1177/2211068215624406/ASSET/IMAGES/LARGE/10.1177_2211068215624406-FIG3.JPEG

Conference presentations

A 3D-printed open microfluidic “bridge” device for active dispersal of flagellated bacteria

Thierry Kuhn

University of Neuchatel

3D-printing a microfluidic artificial fungal highway

Thierry Kuhn

University of Neuchatel

Zürich Mycology Symposium 2022

3D-printing a microfluidic artificial fungal highway

Thierry Kuhn

University of Neuchatel

CV

Thierry Kuhn

Höhenstrasse West 35
4600 Olten

+41 76 424 78 93

thierry.kuhn@unine.ch

07.08.1993

Profile

Professional competence
- Experience in a microbiological laboratory
- Prototype development
- Expertise in Biology
- Advanced knowledge of Statistics
- Experience in Programming
- Experienced group leader
- Advanced knowledge in analyze biological systems

Methodological Skills
- Quick comprehension
- Recognize essentials
- Set priorities
- Solution-oriented
- Independent
- Resilient
- Innovative
- Interconnected thinking

Professional activities

2019 – 2022
PhD in Microbiology • Universität of Neruchatel

2012 - 2013
Military service as a servant in the medical school 42 • **Bedrina Airolo**

Publications

2022

In review:
Spatial scales of competition and a growth-motility tradeoff interact to determine bacterial coexistence
https://doi.org/10.1101/2022.01.05.474435

In review:
Ecology shapes the cyclic dominance games between *Escherichia coli* strains
https://doi.org/10.1101/2022.08.15.504033

Design and construction of 3D printed devices to investigate active and passive bacterial dispersal on hydrated surfaces
https://doi.org/10.1186/s12915-022-01406-z

2018

Comparative effects of the parasiticide ivermectin on survival and reproduction of adult sepsid flies
https://doi.org/10.1016/j.ecoenv.2018.07.029

Education

2017 -2019
Master of Science in Systematics and Evolutionary Biology • University of Zürich • Title of the Master Thesis: „The influence of predation on prey adaptation and persistence in a changing environment. "

2013 - 2017
Bachelors of Science in Biology and Environmental Science (Minor)• University of Zürich

Others

Hobbies:

Floorball Referee (National Ligue) & Diving (Divemaster)

Volunteer Work:

2013
All out Africa Mozambique, Marine protection and teaching in sustainability

2014
Praktikawelten South Africa, Marine Protection

2015
Praktikawelten South Africa, Marine protection, organizing and leading of dives, teaching in Ecology

2016
OPWALL Cuba, Marine protection, organizing and leading of dives, teaching in Ecology

2019
OPWALL Indonesia, Marine protection, organizing and leading of dives, teaching in Ecology

Language

German: Native language
English: C2
French: B1

IT-Knowlege

MS-Office
- **Word** (+++)
- **Excel** (+++)
- **PowerPoint** (+++)

Programming languages
- **R** (+++)
- **Python** (+++)
- **Julia** (+++)
- **Java** (++)
- **C++** (++)

Additional Programs
- **Auto CAD** (++)
- **ImageJ** (++)

(+++) excellent skills, (++) Advance skills, (+) basic skills